2012

BIFUNCTIONAL BISPHOSPHONATES FOR DELIVERING BIOMOLECULES TO BONE

Jivan N. Yewle
University of Kentucky, yewlejivan@gmail.com

STUDENT AGREEMENT:

I represent that my thesis or dissertation and abstract are my original work. Proper attribution has been given to all outside sources. I understand that I am solely responsible for obtaining any needed copyright permissions. I have obtained and attached hereto needed written permission statements(s) from the owner(s) of each third-party copyrighted matter to be included in my work, allowing electronic distribution (if such use is not permitted by the fair use doctrine).

I hereby grant to The University of Kentucky and its agents the non-exclusive license to archive and make accessible my work in whole or in part in all forms of media, now or hereafter known. I agree that the document mentioned above may be made available immediately for worldwide access unless a preapproved embargo applies.

I retain all other ownership rights to the copyright of my work. I also retain the right to use in future works (such as articles or books) all or part of my work. I understand that I am free to register the copyright to my work.

REVIEW, APPROVAL AND ACCEPTANCE

The document mentioned above has been reviewed and accepted by the student's advisor, on behalf of the advisory committee, and by the Director of Graduate Studies (DGS), on behalf of the program; we verify that this is the final, approved version of the student's dissertation including all changes required by the advisory committee. The undersigned agree to abide by the statements above.

Jivan N. Yewle, Student

Dr. Leonidas Bachas, Major Professor

Dr. John Anthony, Director of Graduate Studies

BIFUNCTIONAL BISPHOSPHONATES FOR DELIVERING BIOMOLECULES TO BONE

DISSERTATION

A dissertation submitted in partial fulfillment of the
requirements for the degree of Doctor of Philosophy in the
College of Arts and Sciences
at the University of Kentucky

By
Jivan N. Yewle

Lexington, Kentucky

Director: Dr. Leonidas Bachas, Professor of Chemistry

Director: Dr. David Puleo, Professor of Biomedical Engineering

Lexington, Kentucky

2012

ABSTRACT OF DISSERTATION

BIFUNCTIONAL BISPHOSPHONATES FOR DELIVERING BIOMOLECULES TO BONE

Active targeting with controlled delivery of therapeutic agents to bone is an ideal approach for treatment of several bone diseases. Since bisphosphonates (BPs) are known to have high affinity to bone mineral and are being widely used in treatment of osteoporosis, they are well-suited for drug targeting to bone. For this purpose, bifunctional hydrazine-bisphosphonates (HBPs) with spacers of various lengths and lipophilicity were synthesized and studied. Crystal growth inhibition assays demonstrated that the HBPs with shorter spacers bound more strongly to bone mineral, hydroxyapatite (HA), than did alendronate. HBPs were also demonstrated to be non-toxic to MC3T3-E1 pre-osteoblasts. The targeted delivery of the HBP-conjugated model drug, 4-nitrobenzaldehyde, was demonstrated through hydrolysis of the hydrazone linkage at the low pH of bone resorption and wound healing sites.

In another series of experiments, a method to orient proteins on HA surfaces was developed to improve protein bioactivity. Enhanced green fluorescent protein (EGFP) and β-lactamase were used as model proteins. These proteins have a Ser or Thr at their N-terminus, which was oxidized to obtain a single aldehyde group that was subsequently used for bonding HBPs of various length and lipophilicity through formation of a hydrazone bond. The amount of protein immobilized through various HBPs was determined and found not to be exclusively dependent on the length of HBPs. The enzymatic activity of HBP-immobilized β-lactamase, measured with cefazolin as substrate, was found to be higher than β-lactamase that was simply adsorbed on HA.

In a third set of studies, HBPs were evaluated for delivering parathyroid hormone (PTH) to bone mineral to enhance cell responses for bone formation. PTH was oxidized and conjugated to HBPs, followed by targeting to bone wafers. *In vitro* bioassays demonstrated that HBP-targeted PTH stimulated greater synthesis of cAMP in pre-osteoblasts compared to surfaces with simply adsorbed PTH. HBPs were also found to have similar pro-apoptotic activity to widely used alendronate.

Overall, HBPs can be used for drug delivery to bone and oriented immobilization of proteins and peptides, with or without anti-osteoclastic action, for a variety of applications including bone tissue engineering.

KEYWORDS: Bisphosphonate, Bone Regeneration, Hydroxyapatite, Oriented Protein Immobilization, Targeted Drug Delivery

Jivan N. Yewle

01/13/2012

BIFUNCTIONAL BISPHOSPHONATES FOR DELIVERING BIOMOLECULES TO BONE

By

Jivan N. Yewle

Dr. Leonidas Bachas

Director of Dissertation

Dr. David Puleo

Director of Dissertation

Dr. John Anthony

Director of Graduate Studies

02/13/2012

Dedicated to my parents
Meera & Namdeo

ACKNOWLEDGMENTS

This dissertation would not have been completed without the support of a number of individuals. First of all, I would like to express my most sincere gratitude and appreciation to Dr. Leonidas Bachas, my Dissertation Chair, for the continued support, guidance, and freedom to grow into an independent researcher over the extent of my graduate career. I would like to thank Dr. David Puleo, my Dissertation co-Chair, for the constant support, guidance, encouragement, and always being there throughout my graduate career. I would like to thank Dr. Sylvia Daunert, my Dissertation co-Chair, for the guidance, encouragement, and motivation to attain best in me. Finally, I would like to thank a remaining member of my advisory committee, Dr. Mark Watson, for his time and inputs on the work.

I am grateful to Dr. Yinan Wei for her time, inputs, and introducing me to molecular biology world. I thank Dr. Vivek Rangnekar for his inputs and collaboration on the cancer project. I also thank to Dr. Arthur Cammers for resourceful insights and discussions. I am also grateful to past and present fellow members of Bachas, Daunert, and Puleo research groups, including Karthik, Amol, Anjali, Robin, Santosh, Smita, Nilesh, Sanja, Elsayed, Nitin, Emre, Xin, Ayca, Brad, Leslie, Megan, Ramesh, Adam, Sharath, Sandeep, Amanda, Matt, and Bryan for their support and friendship.

My family has always been a driving force in my success. I am extremely thankful to my parents, Meera and Namdeo, the reason for my existence. Without their sacrifice, blessings, encouragement, and unconditional love it would have been impossible to reach this stage. I would like to thank my beloved wife, Rashmi, for always

standing by me and supporting me no matter what we were going through. I also thank my sisters, Jyoti and Jwala, and my friends, Ajit, Manoj, and Sachin, who are like my brothers, for their constant support, care, and encouragement.

My special thanks to my friends Nitin, Sarita, Abhay, Kunal, Karthik, Amol, Sandeep, Vasu, Anjali, Hari, Gauri, Shriram, Smita, Nilesh, Shankar, Raghu, and Pramod for their supportive, warm and fun-filled company. Finally, I want to thank the University of Kentucky for a Research Challenge Trust Fund fellowship (RCTF), US Army Medical Research and Materiel Command (W81XWH-09-1-0461) and the National Institutes of Health (AR048700) for the financial support to this work.

TABLE OF CONTENTS

LIST OF TABLES

LIST OF FIGURES

LIST OF SCHEMES

CHAPTER ONE

INTRODUCTION

Skeletal System

The skeletal system is one of the most important organ systems of the human body. It is made up of many bones, cartilage, and joints. The adult human body has 206 bones, while a baby has 300. Bone tissue is an integral part of the body providing mechanical support, movement, protection, and various physiological functions. It is a dynamic tissue that maintains the mineral balance and facilitates hematopoiesis in bone marrow. It stores fatty acids and various growth factors (*1*, *2*). It helps maintain the systemic acid-base balance and provides a defense mechanism against acid-base disorders (*3*). Overall, bone is an active tissue with both mechanical and metabolic functions.

Bone is a rigid and dense connective tissue consisting of water, inorganic matter, and organic material. Inorganic matter mostly contains calcium phosphate in the form of hydroxyapatite (HA) ($Ca_{10}(PO_4)_6(OH)_2$). Bone tissue contains more than 99% of the calcium in the body. Organic material is composed of collagen, extracellular matrix, and cell protein. Collagen, which is the major component of the organic material of bone tissue, is composed of three strands of protein structured into left-handed helices. These helices are coiled together into a right-handed helix of procollagen. The procollagen strands aggregate further to form tropocollagen. Tropocollagen assembles in an orderly fashion to form fibrils, which further bundle to form collagen fibers. About 90% of total

protein in bone is type I collagen fibers, which interlink and orient in a preferential direction giving lamellar bone its shape, structure, and lightweight nature. Deposition of inorganic mineral in the empty spaces of the collagen network provides strength, rigidness, and density to bone tissue (*4*, *5*).

Other than biological apatite, bone enfolds bone marrow, nerves, blood vessels, endosteum, periosteum, cartilage, and cells. Bone contains of several types of cells, such as mesenchymal stem cells, hematopoietic stem cells, preosteoblasts, and mature cells of osseous tissue. Osteoblasts, osteoclasts, and osteocytes are three main types of mature osseous cells that maintain the dynamic nature of bone. Osteoblasts are mononucleate bone forming cells. They deposit a protein matrix for bone regeneration and/or bone growth. Osteoclasts are multinucleate bone resorbing cells. They are responsible for bone dissolution and function by secreting hydrogen ions and a variety of proteolytic enzymes. Osteoblasts migrate to the surface of bone where they can become entrapped through the deposition of bone matrix around them. In the formed lacunae, they mature into osteocytes. Osteoblasts and osteoclasts are very important cells in the bone remodeling cycle. They maintain bone health by balancing bone-formation and bone-resorption through the bone remodeling cycle (*4*-*7*).

Bone Remodeling

Bone tissue is constantly undergoing renewal called bone remodeling. It is a life-long and complex process, where bone formation via osteoblasts and bone resorption via osteoclasts are coupled. In general, osteoclasts release lysosomal enzymes through their ruffled border and cause matrix resorption. The pit formed by matrix resorption is called

the resorptive pit or Howship's lacuna. Bone resorption is followed by bone formation. Osteoblasts fill the resorptive pits by forming an osteoid, which subsequently mineralizes to form new bone matrix. Bone resorption followed by bone formation constitutes a bone remodeling unit (BMU). Figure 1.1 demonstrates a bone remodeling cycle showing one BMU. The balanced bone remodeling is essential for various bodily functions, such as blood-calcium level, acid-base balance, hematopoiesis or blood cell formation, repair of micro-damaged bones, etc. Any disturbance in the bone remodeling cycle (e.g., any change in the rate of bone resorption or formation) leads to net bone change (gain or loss) (*8*).

Bone remodeling can be altered by various parameters. Various factors, such as PTH, calcitonin, vitamin D, growth hormones, steroids, and cytokines, are also actively involved in bone remodeling. Imbalance in any of the above factors may cause a disturbance in bone remodeling and affect bone health (*9, 10*). As a result of disease, bone resorption could exceed bone formation and cause brittleness in bone (*11*). Postmenopausal estrogen depletion, transplantation surgeries, drug therapies such as glucocorticoids, and other unrelated diseases may interrupt the bone remodeling cycle. Usually, menopause is one of the major reasons behind disturbed bone remodeling. Typically, after the age of 60s, bone resorption becomes dominant over bone formation and leads to weaker bone, which could in turn lead to bone-related diseases, such as osteoporosis (*12*).

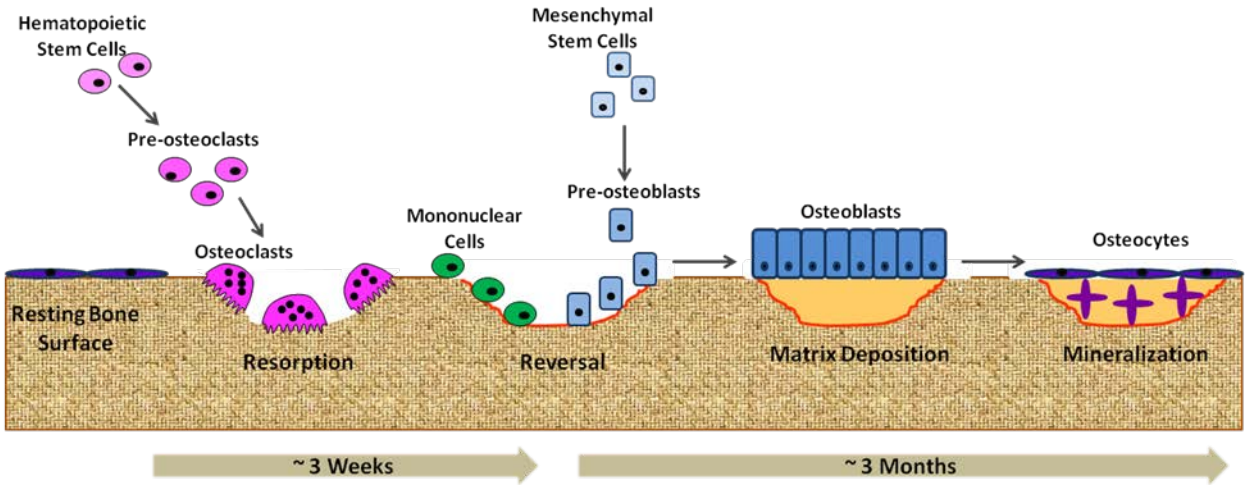

Figure 1.1. Bone remodeling cycle, showing sequential osteoclastic bone resorption, osteoblastic bone formation, followed by mineralization.

Bone Diseases

Osteoporosis is the most frequently diagnosed disease among bone diseases. In 2000, around 10 million people had been diagnosed with osteoporosis in the United States alone (*13*). It is a progressive disease in which the mineral density of bone decreases. Normally, when the person grows older, osteoblast activity decreases and osteoclast activity increases. Osteoporosis primarily affects women after menopause (*11*). In general, menopause limits estrogen, which has an anti-resorptive characteristic, in the body and causes increase in bone resorption (*14, 15*). Thus, increased age and menopause are both additive factors of osteoporosis. Since the longevity of the average person is increasing, osteoporosis has become more prevalent. Moreover, diseases such as rheumatic arthritis and spinal cord injuries, which alter the bone turnover, may lead to osteoporosis (*16*). Overall, increased bone resorption with decreased bone formation is the primary cause of osteoporosis.

Osteoporotic bone is characterized by high porosity and increased brittleness. It also becomes smaller and thinner. The total amount of protein decreases in osteoporotic bone and causes weakening of bone. Overall, bone mineral density decreases with disruption in bone micro-architecture compared to healthy normal bone. Therefore, osteoporotic bone becomes fragile and very prone to fracture. Fractures in hip, spine, wrist, and proximal humerus, as well as vertebral compressions, are more common in the osteoporotic patient. The actual bone strength and bone fractures depend on the quality as well as quantity of bone tissue, and it was observed that both, quality and quantity diminish in osteoporosis (*17*). Potential risk of osteoporosis can be reduced by promoting healthy life style with regular exercise, and calcium and vitamin D enriched diet (*18*).

Since hormonal deficiency could lead to osteoporosis, hormone replacement therapy is a well-known treatment for osteoporosis. BPs, small organic molecules with two phosphonates, are widely prescribed therapeutic agents for treatment of osteoporosis (*19*).

Bisphosphonates

BPs have been widely explored because of their clinical applications. BPs are chemical analogues of naturally occurring pyrophosphate. Pyrophosphate is an excellent complexing agent, and it is present throughout living organisms. The unstable P-O-P backbone of pyrophosphate has an affinity towards biological apatite, which is a carbonated form of stoichiometric HA. Therefore, pyrophosphate also acts as a poisoning agent to the growing crystal of HA. Conversely, pyrophosphate, coated on the HA surface, prevents the dissolution of HA crystal. Overall, pyrophosphate prevents aberrant calcification in the body and suppresses the dissolution of the calcified bodies. However, due to the unstable nature of P-O-P linkage in the pyrophosphate, it is unable to prevent dissolution of the biological apatite effectively (*20*). The shortcomings of pyrophosphate are overcome by BP, replacing the unstable P-O-P bond of pyrophosphate with the stable P-C-P bond of BP. Therefore, BPs are capable of preventing the dissolution of the biological apatite as well as preventing pathological aorta calcification.

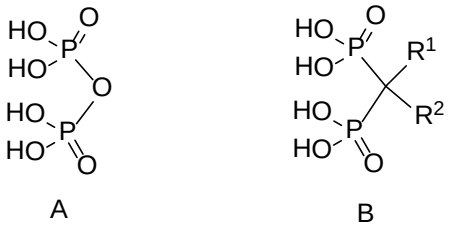

Figure 1.2. A) Structure of pyrophosphate. B) General structure of bisphosphonate.

BP has two phosphonates on its geminal carbon, which causes BP to have high affinity for HA or bone mineral. The distance between the two deprotonated hydroxyls of the two phosphonates in BP (2.9-3.1 Å) is similar to the distance between the two calcium-chelating oxygen atoms in HA. Therefore, BP could have an ideal situation for bidentate binding to the Ca^{2+} in HA, showing an affinity to HA. In addition to two phosphonates, BP has two substituents (R^1 and R^2) on its geminal carbon (Figure 1.2). The presence of -OH or $-NH_2$ groups at R^1 position provides an extra hand for chelation of the Ca^{2+} in HA. This extra hand offers tridentate binding over bidentate binding and shows enhanced affinity for HA (*21, 22*). Hydrophobicity or lipophilicity of the R^2 substituent affects the bone affinity of BP (*23-25*). In recent studies it was found that an R^2 substituent having pK_a greater than 7 shows higher binding affinity under physiological conditions (*20*). Overall, it can be stated that, along with the two phosphonates and R^1 substituent, the R^2substituent also contributes to the binding affinity of BP (*26-28*). Therefore, BP could be structurally modified to obtain higher affinity.

The structural variations of R^1 and R^2 allow a wide range of BP structures with varying degrees of drug potency (*29*). In general, there are three generations of BPs. Medronate, clodronate, and tiludronate are examples of first generation BPs. The first generation BPs mostly have hydrogen as R^1 substituent. They generally have a small and simple R^2 substituent, and are not very effective at inhibiting bone resorption (*27*). The second generation BPs generally have a hydroxyl group as R^1 substituent and a nitrogen containing group on their R^2 substituent. As a result they show improved affinity and anti-resorptive properties over the first generation BPs (*26-28, 30*).

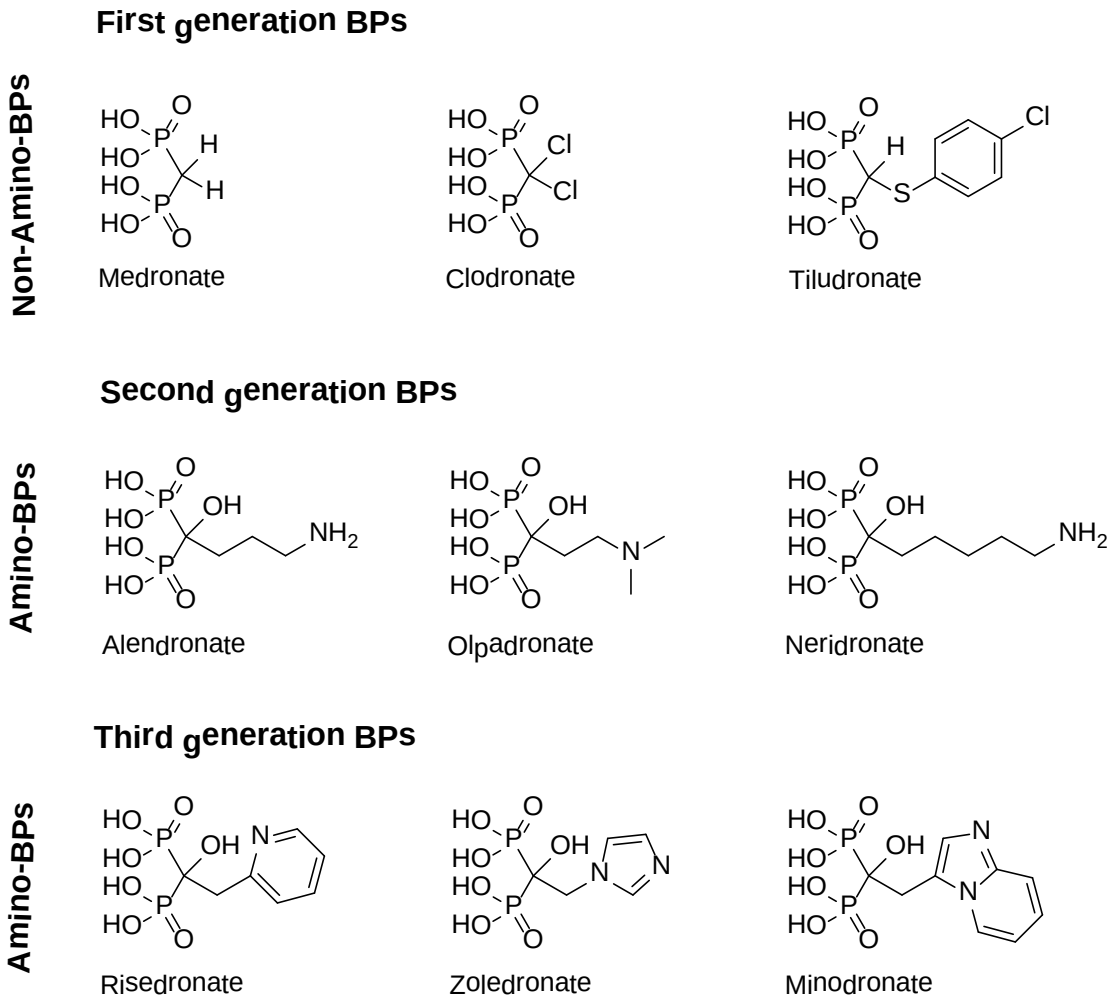

Figure 1.3. Classification of BPs showing representative structures for first, second, and third generation BPs.

The third generation BPs have a hydroxyl group as R^1 and nitrogen containing ring structures at R^2; these BPs show improved anti-resorptive function over second generation BPs. Some of these BPs have shown the highest anti-resorptive effects over any other BPs (*27*). BPs can also be classified into two classes: Amino-BPs (N-BPs) and non-amino-BPs. N-BPs have nitrogen in their structure, while non-amino-BPs are simple BPs without nitrogen. N-BPs generally posses higher drug potency than simple BPs. The first generation BPs belong mostly to the non-amino-BPs class, while second and third generation BPs are categorized into the amino-BPs class. The classification of BPs with their structures can be seen in Figure 1.3.

Several BPs show anti-resorptive properties and are prescribed in the treatment of various skeletal diseases (*31-33*). Alendronate, ibandronate, risendronate, and zoledronate are some of the currently prescribed BPs in the treatment of osteoporosis, and are marketed under the names of Fosamax, Boniva, Actonel, and zometa by Merck, Roche Pharmaceuticals, Procter & Gamble, and Novartis, respectively. Clodronate and pamidronate are also used in the treatment of Paget's disease, whereas zoledronate is being explored for the treatment of prostate cancer.

Mechanism of Action

The molecular mechanism of BPs vary with the structure of BPs. At the tissue level, BP controls bone dissolution and increases bone mineral density by decreasing bone resorption. At the cellular level, BP causes apoptosis of the bone resorbing cells, osteoclasts. The bone resorption by BPs has been detected by several methods, including the decrease in the secretion of bone resorption markers such as CTx (bone type I

collagen C-telopeptide). CTx is generally produced by osteoclasts in the bone degradation process and can be detected in blood or urine. BP treatment also reduces the osteocalcin or bone-specific alkaline phosphatase, which are bone formation biochemical markers. The reduction of bone formation is an ultimate effect of the reduction of bone resorption or bone turnover. In other words, reduction in bone formation is not a direct effect of BP treatment (*17*). A couple of mechanisms of apoptosis of osteoclasts by BP have been discovered. After administration, BPs are primarily attracted to bone and bind to the mineral surface. BPs on the bone surface get internalized into osteoclasts through the ruffled border and prevent their resorptive function (*34*). The general mechanism of BPs can be seen in Figure 1.4.

The first generation BPs, which are also non-amino-BPs, form methylene-containing (AppCp type) analogues of ATP in osteoclasts. The toxic analogues of ATPs accumulate in the cytosol of osteoclasts. Their accumulation in high concentration causes apoptosis of osteoclasts. Presumably, AppCp-type analogues inhibit ATP-dependent enzymes, such as the adenine nucleotide translocase (a component of the mitochondrial permeability transition pore) and cause cell apoptosis followed by inhibition of resorption. This is a primary mechanism of inhibition of bone resorption, generally shown by simple BPs, such as clodronate and etidronate, as shown in Figure 1.5 (*35-37*).

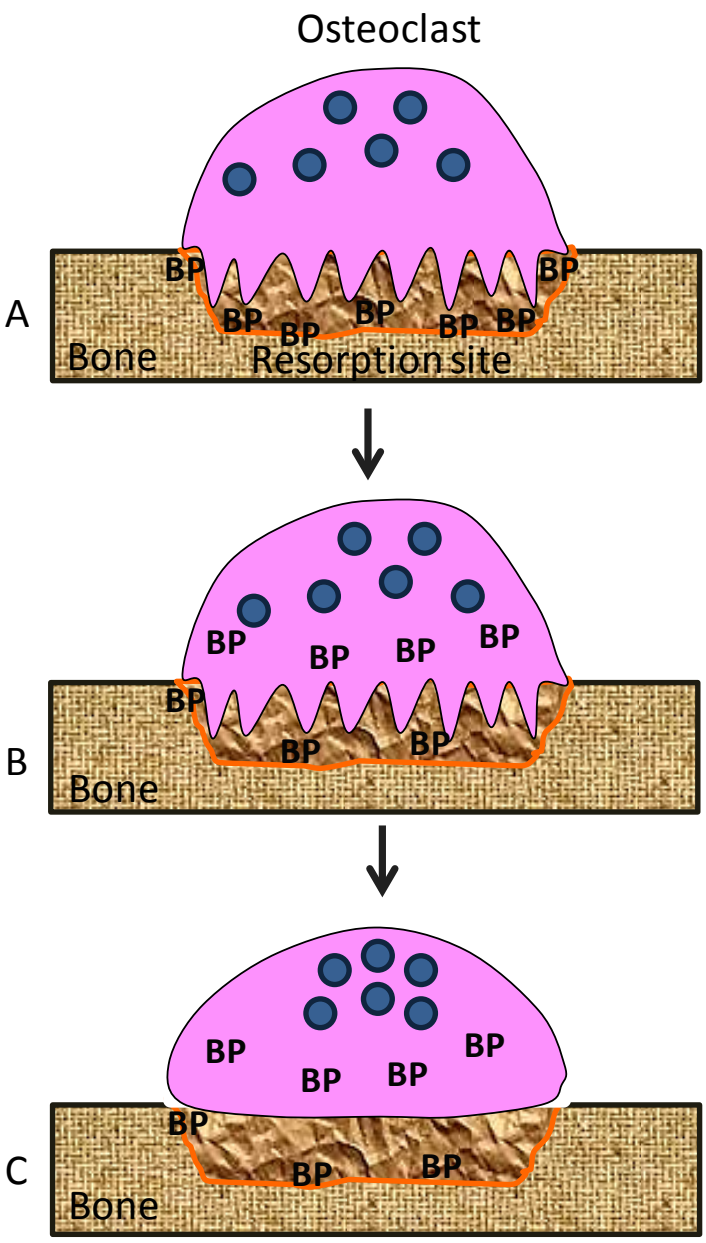

Figure 1.4. Mechanism of action of BP. A) BP binds to bone mineral in body and exposes to osteoclast at the resorption site. B) BP is taken up intracellularly by the osteoclast during bone resorption. C) Absorbed BP causes inhibition of osteoclast function and apoptosis.

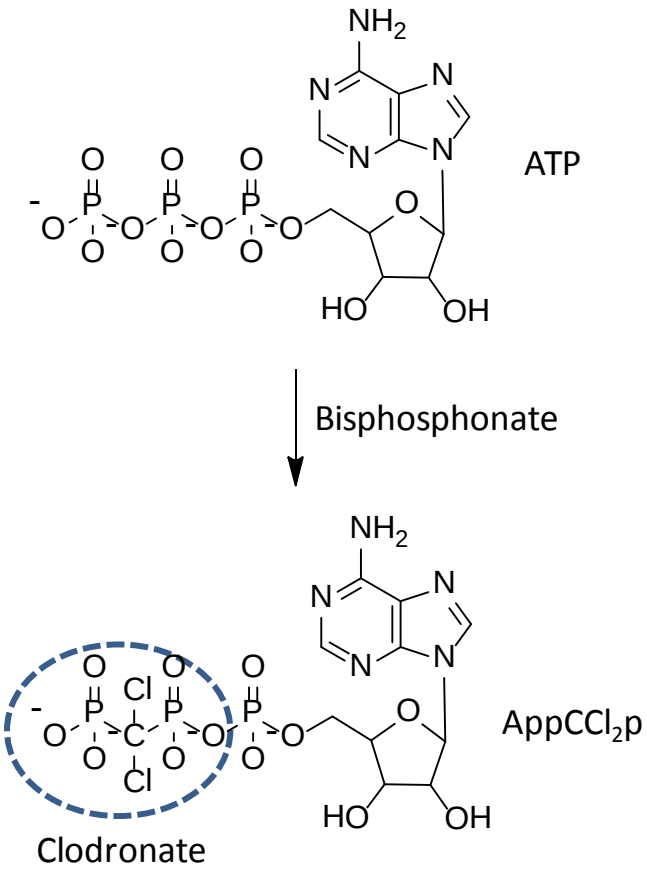

Figure 1.5. Primary mechanism of inhibition of bone resorption. Clodronate forms a methylene-containing ($AppCCl_2p$ type) analogues of ATP in osteoclasts and causes inhibition of bone resorption.

N-BPs are several orders of magnitude more potent at inhibiting bone resorption than the simple BPs (*38-41*). They interfere in the mavalonate pathway of osteoclasts by inhibiting fernesyl diphosphate (FPP) synthase (Figure 1.6). In particular, N-BPs bind in the geranyl diphosphate (GPP) binding site of the FPP synthase by forming a stable complex between the nitrogen moiety of the N-BP and conserved threonine and lysine residues in the FPP synthase. This prevents the synthesis of FPP and geranylgeranyl diphosphate (GGPP) that is required for protein prenylation. Overall, N-BPs stop the biosynthesis of isoprenoid lipids, which are necessary for the prenylation of small GTPase signaling proteins, and discontinue the cell signaling, causing apoptosis of osteoclasts (*35, 36, 38-41*). Thus, apoptosis of osteoclasts is necessary to control the bone resorption by first generation BPs. However, the second and third generation N-BPs are capable of stopping cell signaling/functions including bone resorption, and they do not need to induce apoptosis of osteoclasts to control bone resorption (*37, 42*). Therefore, N-BPs are more effective than simple BPs.

Since the molecular mechanism of inhibition of bone resorption by BP has been discovered, a variety of BPs have been studied for better drug potency. Moreover, because of the high mineral affinity, several BPs have been utilized for drug targeting and drug delivery to bone tissue. Basic strategies of the synthesis of BPs and synthesis of bifunctional BPs are discussed in Chapter Two.

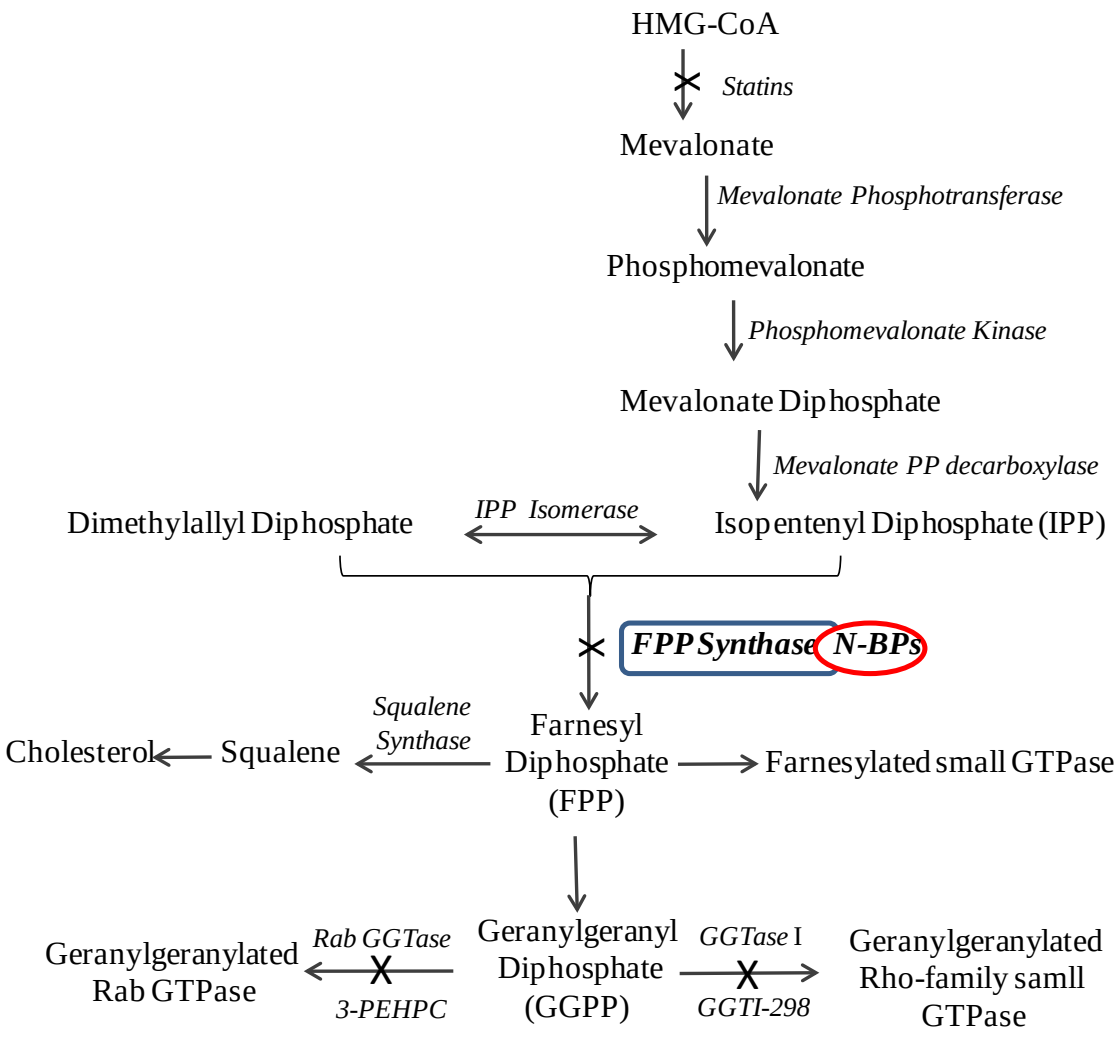

Figure 1.6. Inhibition of the mevalonate pathway by N-BPs. N-BPs inhibit FPP synthase and prevent the synthesis of FPP and geranylgeranyl diphosphate (GGPP) required for protein prenylation and causes inhibition of bone resorption.

BPs and Targeted Delivery of Therapeutic Agents to Bone

There are number of skeletal diseases, such as osteoporosis, bone metastasis, Paget's disease, hypercalcemia, osteoarthritis, etc. Similarly, there are many therapeutic agents and procedures known to treat these diseases, and the discovery process is continuous (*43*). However, there is no universal solution or drug treatment for all bone related diseases. Each disease or condition requires treatment with a specific therapeutic agent or a combination of several drugs (*31*). Several factors need to be considered when treating a particular disease, such as the type and amount of drug, mode of administration, time frame of treatment, etc. However, the main concern regarding the treatment of any disease is selecting the most appropriate type of drug administration that circumvents unwanted absorption of the drug at non-desired sites. Because of the uptake of drugs at non-desired sites of the body, treatments sometimes involve higher drug dosages than required, which may lead to toxic side effects (*11*). Therefore, most of the skeletal diseases require a targeted delivery of therapeutic agents to bone tissue or diseased tissue.

In general, targeted delivery of therapeutic agents to the desired site is an ideal approach for the treatment of any disease. It has enormous benefits and, therefore, it has been widely explored. It can deliver the drug at the desired site (diseased site) with prolonged drug action. Targeted drug delivery reduces the frequency of drug dosage and gives more uniform drug action compared to conventional drug delivery methods. It reduces the side effects of the drug and gives a localized drug effect at the diseased site. Therefore, it is also known as 'Smart drug delivery'. However, it requires a drug delivery vehicle which could direct the drug at the desired site. In the case of skeletal diseases, it

requires a vehicle that could direct and/or deliver the drug molecules to bone tissue. This can be achieved by using molecules that have a natural attraction or affinity to bone tissue.

There are several bone-seeking molecules, such as BPs, D-aspartic acid octapeptide (*44, 45*), polymalonic acid (*46*), tetracycline (*47, 48*), strontium, rhenium, lead, and fluoride (*10*). However, most of these molecules cannot be used for drug delivery because of several reasons, such as toxicity, heterogeneous distribution on the skeleton, sex dependency, inability to be conjugated to drugs, and poor affinity to bones. Among the above bone-seeking molecules, BPs are the most studied agents because of their bone affinity and anti-resorptive properties (*31-33*). Therefore, BPs could be the most suitable candidates for drug targeting and drug delivery applications for bone diseases.

BPs have been studied widely for drug delivery. Since BP has two substituents (R^1 and R^2), which can be modified to introduce a selective functional group for the attachment of a drug molecule, a variety of strategies of BP-drug conjugation have been explored by us and others (*16, 49-52*). Moreover, there are various linkers commercially available, which are being used for BP and drug conjugation. Overall, formation of the BP-drug conjugate has been a subject of prime importance for targeted drug delivery.

BP Conjugates for Drug Delivery

BPs have been conjugated to several types of therapeutic agents, such as radioisotopes, imaging agents, anti-neoplastic drugs, anti-inflammatory drugs, anti-resorptive drugs, and bone regenerative drugs. Zhang *et al*. have reviewed the recently

reported delivery of drugs through BP (*20*). A variety of conjugates with various bonds have been reported to link BPs with therapeutic agents. The conjugates can be designed to be labile or non-labile in nature and can be classified into two general classes: stable conjugates and unstable conjugates. Amide, ester, thioester, thioether, disulfide, and hydrazone bonds have been commonly used as linkages for BP conjugation. In stable conjugates, BPs are conjugated to drugs via stable linkages, such as C-C, C-N, amide, etc. The stable conjugation is crucial for applications such as bone imaging and radiotherapy of skeletal sites. Moreover, stable linkages are more valuable in the case of drugs that remain active in their conjugated form. For other applications, a link between BP and a therapeutic agent could be designed to be cleavable under certain conditions, such as temperature, pH, specific proteases, etc. Some drugs remain active in their BP conjugated form and, therefore, there is no need to release them from BPs. However, most drugs are not fully active in their conjugated form and need to be cleaved from BPs in order to maximize their pharmacological activity. For delivery of such drugs, a cleavable linkage between BP and the drug needs to be designed in a way so that it gets cleaved at the required site in the body; this should take place with a specific cleavage rate to deliver the required amount of drug in a sustained manner. We have developed a strategy to deliver drug molecules to the bone resorption and wound healing sites using bifunctional BPs, which is discussed in detail in Chapter Three.

Bone Fractures and Bone Loss

Apart from the effective treatment of skeletal diseases, efficient treatment of bone fractures and bone loss is crucial and requires serious attention. Other than osteoporotic

bone fractures, other bone diseases, such as osteosarcoma and osteoarthritis, also require a surgical replacement of bone. Osteosarcoma is a bone disease in which cancer cells are found in the bone. It is a frequently detected bone cancer. Osteosarcoma usually develops in growing bones and commonly in children of age of 10-25. Chemotherapy, radiation, and surgery are the common therapies for bone cancer. Although the mode of treatment depends on various factors, such as the age of the patient, location, stage of cancer, etc., surgery is often the main and most effective treatment for osteosarcoma.

Osteoarthritis, a degenerative joint disease, involves degradation of joints. Mechanical stress or heavy use of joints usually leads to a loss of synovial fluid, which lubricates the joints. It often damages the cartilage that lines the subchondral bone surface and exposes the bone surface. Since cartilage acts as a protective cushion and prevents wear and tear of the joints, the loss of cartilage causes pain and inflammation in the joints. It may lead to local joint destruction and systemic bone loss (*53*, *54*). The load bearing joints, such as hips and knees, suffer most with osteoarthritis. Osteoarthritis also occurs in the feet, spine, shoulders, and hands (*55*). Although several pharmaceutical therapies are being used in the treatment of osteoarthritis, joint replacement surgery remains the most effective option.

In the USA, around 10.8 million car accidents were reported in 2009 (according to US government 2010 census report). In addition, explosions by terrorist or military practices and wars around the world are persistently increasing and causing severe bone injuries or loss (*56*). The annual bone fracture rate in USA is about 6.5 million per year, and about 550,000 cases requires bone grafting (*5*). Furthermore, there are several causes, such as bone infections and bone defects, where the whole bone or part of the bone

requires bone replacement surgery. However, in the case of major bone loss or critical-size bone defects, the bone tissue is unable to bridge the defects on its own. Such cases are typically treated by bone implant surgery with various types of drug treatment. Therefore, various techniques and materials have been developed for successful bone implant surgeries (*56*).

Bone Implant Materials

The most useful technique to replace damaged bone or to fill a large section of lost bone is bone grafting. It is a surgical procedure in which missing bone is replaced by autografts, allografts, xenografts, or other bone graft substitutes. Autograft is an implantation of bone harvested from another part of the same patient, while allograft is an implantation of bone obtained from another individual. In xenografts, bone grafts are harvested from non-human species. The drawbacks in utilizing allografts, and xenografts include a risk of disease transmission, a limited number of donors, etc. (*57, 58*). Remaining techniques (such as bone graft substitutes) have been explored widely.

From an ancient age, various artificial materials have been explored as bone or tooth implants. Artificial tooth implants, made up of sea shells and iron, were used by Mayans and Europeans from ~600 A.D. and ~200 A.D., respectively (*59*). Currently, there are several types of materials used as implants including synthetic polymers, natural polymers, ceramics, metals, and their combinations. Polymeric material has limited applications for bone implants because of their low strength, high wear and tear, and poor bone attachment. Metals are preferred over polymeric material because of their high strength, low flexibility and low wear and tear. Currently, various types of metals and

their alloys, such as stainless steel, cobalt-chromium alloys, and titanium and its alloys, are being used for implant applications. Titanium and its alloys are strong, chemically stable and fairly biocompatible. Titanium is a reactive metal and forms oxides in the presence of air, water, and other electrolytes. Since titanium oxide is a good insulator, it acts as a protective layer on the implant surface, and no metal ion reaches the implant surface, whereas conductive materials could start redox reactions on the implant surface and denature the surrounding macromolecules (*60*).

On the contrary, ceramic materials, such as HA and tricalciumphosphate, are brittle and hard. They are bioactive and biodegradable. These materials have a similar composition as that of bone mineral, and they are not cytotoxic to the body. Moreover, they are very suitable for temporary mechanical support and fixation devices. Since ceramic materials are biodegradable, they are expected to degrade gradually and be replaced by new tissue. Because of all the above qualities, ceramic materials are advantageous over other types of material (*61*). Moreover, the chemical composition of a few ceramic materials, such as HA, is similar to bone mineral. HA has also been used as a coating material for other types of implants. Overall, ceramic materials have great potential for bone tissue engineering applications.

BPs and Bone Tissue Engineering

Although a variety of materials have been explored as bone implant materials (*62*), because of their similar composition to bone mineral a naturally occurring HA has been widely used for bone implants and as coating material for other implants. Several advances have been made in implant materials and devices; however, biocompatibility is

a major issue faced by the current medical society. In general, tissue engineering has become an interdisciplinary field for development of artificial smart material for biological substitutes. It is expected that these substitutes restore, maintain, or improve the tissue function of a whole organ (*63*). However, after implant surgery, the body identifies the implant as a foreign object and produces, among others, an inflammatory response. Therefore, the interactions between the implant material and the surrounding tissue play an important role.

There are several ways to overcome problems associated with the biocompatibility of the implants. The ultimate solution to overcome the biocompatibility issue is to achieve a good cell/tissue response. Since cells/tissue interact with the implant surface and their behavior changes with the physical and chemical properties of the implant surface, several advances have been made to improve implant surfaces. Implant surface can be improved physically by optimizing surface topography, as well as chemically, by incorporating bioactive material on the surface (*64-66*).

One of the effective ways to achieve a good cell response is to apply a bioactive protein on the surface of the implant. Protein immobilization could improve cell-implant interactions (*67-69*). Moreover, immobilization of proteins is an essential step in creating protein-based functional materials for various applications, such as protein microarrays, biosensors, biotechnology, chemical manufacturing, nanotechnology, single molecule enzymology, and drug discovery.

Immobilization of Proteins

Immobilization of proteins on surfaces enables the localization and retention of the proteins on the surface. Several methods have been explored for protein immobilization on solid surfaces (*70-73*). Protein immobilization can be classified into three main categories: coating or physical adsorption, random immobilization, and site-specific or oriented immobilization. Figure 1.7 is a pictorial representation of the general types of immobilization. Coating or physical adsorption is the most straightforward method of protein fixation on the surface. It can be simply accomplished by submerging the implant surface in the protein solution. In coating or physical adsorption methods, a protein is generally attached to the surface through non-covalent interactions. Therefore, the attached protein could be washed out or leached out easily from the surface. Since there is no linker between the protein and the surface, protein can be denatured because of surface interactions. Moreover, there is no direct control on the orientation and the amount of the protein attached on the surface and the active site of the protein may not be available for bioactivity (*74*). Therefore, coating or physical adsorption is not the best way of protein immobilization.

In random immobilization, a protein is attached to the surface through a strong linkage, such as a covalent bond. However, this immobilization method has limited control on the orientation of the protein on the surface. In general, proteins have several functionalities such as, amines, carboxylates, thiols or hydroxyls. These functional groups could be used for the fixation of the protein on the surface. However, there could be multiple numbers of the same functional group on a single molecule of a protein. This makes the protein fixation non-selective, which results in random immobilization of the

protein. In random immobilization, the active site of the protein may be blocked, which results in decrease in the bioactivity of the immobilized protein. Moreover, it is difficult to control the amount of bioactive protein on the surface in random immobilization (*75*).

Site-specific or oriented immobilization of proteins is advantageous over physical adsorption and random immobilization. This immobilization method utilizes a single functional group of the protein for fixation of the protein on the surface through a covalent linkage. Since it is rare to have a single functionality of one kind on a protein, a selective chemical reaction or protein engineering can be done to obtain a unique functional group on the protein (*75*). Bioaffinity between two biomolecules is frequently used for the oriented immobilization of proteins. A typical example of immobilization through affinity interactions is the immobilization of antibodies on a surface modified by protein A or G. In oriented immobilization, the orientation of the protein can be predetermined so that a reactive site of the protein could become available for specific action. Moreover, the amount of protein and bioactivity can also be controlled.

Overall, oriented immobilization has several benefits over coating, physical adsorption and random immobilization of protein; therefore, it has been explored for various applications (*75, 76*). However, oriented immobilization has only occasionally been investigated for bone implant modifications. Since, ceramic materials are widely used as implants or coating material, we have developed a novel approach of oriented immobilization of proteins through bifunctional BPs on ceramic material and discussed it in Chapter Four.

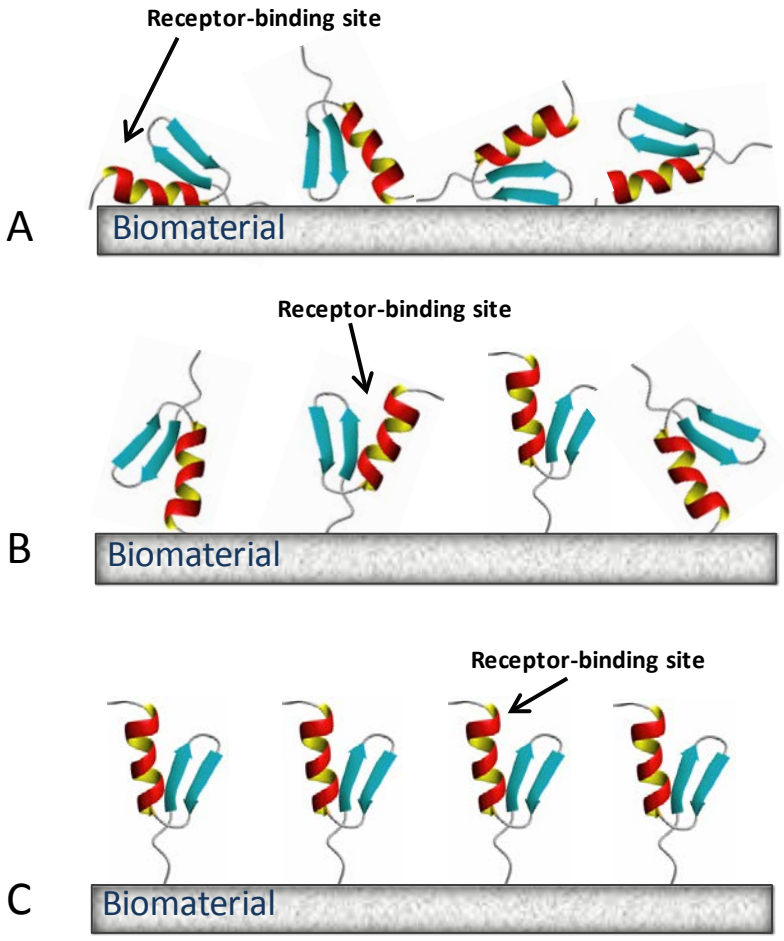

Figure 1.7. Types of protein immobilization. A) Coating or physical adsorption of protein; B) Random immobilization of protein; C) Oriented immobilization of protein.

On the whole, bone related diseases and bone surgeries have a large economical and health impact on society, which needs to be addressed at the bone level. Targeted delivery of therapeutic agents to bone tissue for treatment of skeletal diseases and surface modification of bone implants for tissue-engineering applications could provide solutions toward these needs. Tissue engineering is a multidisciplinary field that unites engineering and biology for replacement and/or regeneration of damaged tissues. In other words, polymeric, metallic, or ceramic engineering materials are combined with biological elements, such as proteins, cells, etc., to create a biological material. Since growth factors are responsible for growth and numerous functions of various systems in the body, they have great importance in tissue engineering. Therefore, for bone tissue engineering applications, localized treatment of bone forming molecules could regenerate bone tissue in a faster and selective manner. Similarly, for treatment of bone diseases such as osteoporosis, unlike several other treatments that focus on controlling bone resorption, delivery of bone forming molecules can be a more effective treatment.

In general, growth factors are protein, peptide, or hormone molecules made by the body. Growth factors can stimulate various cellular events, such as adhesion, migration, proliferation, differentiation, etc. They are used for intercellular or intracellular signaling by various cells in the body. There are several families and super-families of growth factors belonging to a number of molecules that are structurally or evolutionarily related. Bone morphogenetic proteins (BMP), fibroblast growth factors (FGF), insulin-like growth factors (IGF), vascular endothelial growth factors (VEGF), and platelet-derived growth factors (PDGF) are some of the growth factors present in the skeletal system and can be useful for bone regeneration.

Parathyroid hormone (PTH) is also an important peptide related to bone remodeling. It can have anabolic as well as catabolic effects, which depend on its concentration and mode of administration in the body. High and sustained doses of PTH lead to bone resorption, whereas, intermittent doses of higher amounts or infusion of low doses leads to bone formation (*77, 78*). Overall, growth factors related to the skeletal system and other molecules, such as PTH, are the most promising molecules for treating bone diseases or bone tissue engineering. Oriented immobilization on bone implants or targeted delivery at a bone site while maintaining intact the bioactivity of PTH is crucial for bone formation. We discuss a targeted delivery of PTH through a single molecule of bifunctional BPs for enhanced cell/tissue interactions in Chapter Five.

STATEMENT OF RESEARCH

The overall goal of this work was to develop a method of delivering therapeutic agents to sites of bone resorption and wound healing, and to develop a method of oriented immobilization of bioactive therapeutic proteins on mineralized surfaces. The presented work relates the varying aspects of bifunctional BPs and their applications towards bone tissue regeneration through the targeted delivery of drugs to bone and through the oriented immobilization of therapeutic proteins on bone implant surfaces. The advancement in the treatment of bone diseases and replacement of bone lost due to illness or injury are discussed.

Chapter Two discusses basic methods of synthesis of BPs, followed by synthesis of several bifunctional BPs such as, aldehyde-BPs, hydrazide-BPs, and hydrazine-BPs (HBPs). Synthesis and characterization of bifunctional HBPs of varying length and lipophilicity are discussed in detail. Moreover, the probable reasons of failure of synthesis of aldehyde-BPs and hydrazide-BPs are discussed herein.

BPs have high affinity to bone mineral and have been used for delivering therapeutic agents to bone for various purposes. The drug delivery through HBPs and its related aspects are discussed in Chapter Three. The binding affinities of HBPs were determined using crystal growth inhibition assays and compared with a widely used BP drug, alendronate. HBPs were also studied for their non-cytotoxicity towards pre-osteoblasts. Conjugation of a model drug, 4-nitrobenzaldehyde, to HBP and its *in vitro* targeted delivery to bone mineral were demonstrated.

Oriented or site-specific immobilization of a protein/peptide to the surface of

implantable-biomaterial has several benefits because of the importance to maintain the bioactivity of proteins during and after its immobilization for its specific action. A method for oriented immobilization of proteins was developed using HBPs. Genetically engineered EGFP and β-lactamase were used as model proteins. Oriented immobilization of proteins and their bioactivities are discussed in Chapter Four.

Targeted delivery of bone growth proteins is very difficult, but has many advantages in treatment of various bone diseases and in tissue engineering applications. Targeted delivery of bone stimulatory proteins, such as PTH, to bone mineral can facilitate bone regeneration and treat numerous skeletal diseases. PTH was selectively oxidized and conjugated to HBPs followed by delivery to bone mineral. The anti-resorptive properties of HBPs and HBP-PTH conjugates were demonstrated. The osteoblast interactions with the PTH delivered/immobilized to bone surface are discussed in Chapter Five.

The overall research presented in this dissertation concludes with a discussion on additional future research in Chapter Six.

RESEARCH HYPOTHESES

Hypothesis of Dissertation: Bifunctional BPs can be utilized for the targeted delivery of therapeutic agents to bone mineral and for oriented immobilization of proteins/peptides on bone implant surfaces for improved bioactivity of proteins/peptides towards bone formation.

Hypothesis One: Structural modifications of BP by introducing a hydrazine functionality at R^2 substituent can improve the drug potency of the BP.

Hypothesis Two: HBPs can be conjugated to therapeutic agents having aldehyde functionality through the hydrazone linkage, and the HBP-attached drug molecule can be released by hydrolysis of the hydrazone linkage at acidic environment.

Hypothesis Three: Proteins with N-terminal serine or threonine can be selectively oxidized to obtain a unique amino-terminal aldehyde functionality that can be used for site-directed immobilization of proteins through HBPs.

Hypothesis Four: A single molecule of HBP can be used to target the protein/peptide molecule to the bone mineral surface and improve the bioactivity of the targeted protein.

CHAPTER TWO

SYNTHESIS AND CHARACTERIZATION OF BIFUNCTIONAL BISPHOSPHONATES

Bisphosphonates (BPs) have been widely explored because of their various clinical applications. Several BPs show anti-resorptive properties and, therefore, used in the treatment of various skeletal diseases (*31-33*). BPs also show anti-scaling, anti-corrosive, and complexing characteristics. Therefore, they are used in oil, fertilizer, and textile industries.

In general, BPs are structurally similar to pyrophosphates, except the hydrolysis prone P-O-P moiety of pyrophosphate is replaced by the stable P-C-P. BPs have two phosphonates attached to the geminal (α) carbon (Figure 2.1), which are mainly responsible for the bone affinity of BPs by exhibiting bidentate binding to Ca^{2+} of the bone matrix. BPs could also have two more substituents, R^1 and R^2, which contribute to their bone affinity and pharmacological activity. BPs with R^1 substituents containing hydroxyl or amine groups show enhanced affinity to bone through tridentate binding to the bone matrix (31). Recent studies showed that the R^2 substituent may also influence the bone affinity of BP (32, 33). Overall, the anti-resorptive property and bone-seeking ability of BPs as well as their clearance from the body depend on the structure of BPs, and slight structural changes can significantly affect these properties (7). Because of their therapeutic importance in bone diseases, various BP analogues have been synthesized and studied in order to improve their anti-resorptive properties. However, limited research has

been focused on the synthesis of drug-carrying BPs. Overall, BPs show great affinity to bone and have been widely used in the treatment of various bone diseases; therefore, they are the most suitable candidates for drug targeting and drug delivery to bone.

BPs have been known for more than a century. In the past, they were called diphosphonates and were mainly used in textiles, fertilizers and oil industries as anti-scaling agents (*79*). The first biological characteristics of BPs were reported in 1968 by the Fleisch group (*80*). Since then, BPs have been explored widely for their synthesis and their applications in various fields. Several methods of synthesis of BPs have been reported to date. In what follows we describe some major methods for synthesis of 1-hydroxy-1,1-bisphosphonate. The direct method for synthesis of 1-hydroxy-1,1-bisphosphonate from carboxylic acid is shown in Scheme 2.1. The treatment of carboxylic acid with phosphorous trichloride and phosphorous acid, followed by hydrolysis gives 1-hydroxy-1,1-bisphosphonic acid. The reaction requires a solvent, which could dissolve all the starting materials, especially phosphorous acid. Most of the commonly used solvents are not suitable for this reaction. Ethereal solvents, such as ether, THF, and dioxane form a homogenous mixture. However, as the reaction proceeds, it separates into two layers, and the denser layer gets solidified. It was reported that the use of methanesulfonic acid as a solvent allows the reaction to remain in the fluid state. Moreover, the complete conversion of carboxylic acid into α-hydroxy bisphosphonic acid was possible with an excellent yield (*81, 82*).

Scheme 2.1. Synthesis of bisphosphonate I

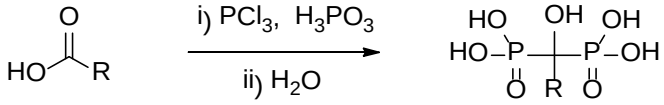

The first base catalyzed synthesis of 1-hydroxy-1,1-bisphosphonic acid was reported in 1956 (*82-84*). In this synthesis, an acyl halide reacts with trialkyl phosphate to give dialkyl acylphosphonate. Further addition of dialkyl phosphate in a neutral medium gives 1-hydroxy-1,1-bisphosphonate (Scheme 2.2). The first step of the synthesis is a Michaelis-Arbuzov reaction, where trialkyl phosphite reacts with acyl halide in SN^2 manner to give dialkyl acylphosphonate. Aryl and vinyl halides are less reactive in SN^2 reactions. In the second step, dialkyl acylphosphonate undergoes an addition reaction with dialkyl phosphite to give the 1-hydroxy-1,1-bisphosphonic ester. It was also reported that the yield of this reaction varies with the choice of the reaction solvent.

Scheme 2.2. Synthesis of bisphosphonate II

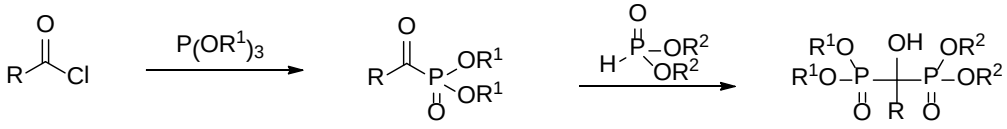

Another one-pot method for synthesis of the symmetrical 1-hydroxy-1,1-bisphosphonate ester without use of dialkyl phosphite was reported, in which an acyl halide reacts with trialkyl phosphite at -10 to 0 °C and gives dialkyl α-ketophosphonate. This is an exothermic and fast reaction. The use of 0.5 equivalents protic reagents, such

as MeOH, converts dialkyl α-ketophosphonate into dialkyl phosphite. Under the same reaction conditions, α-keto-phosphonate reacts with dialkyl phosphite to give 1-hydroxybisphosphonate ester (Scheme 2.3) (*85, 86*).

Scheme 2.3. Synthesis of bisphosphonate III

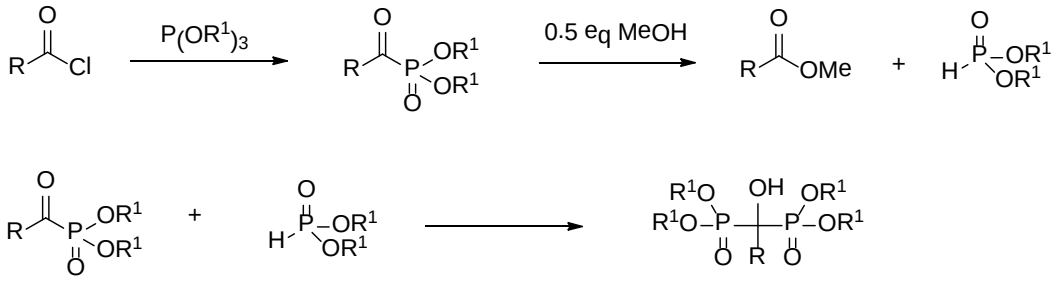

Scheme 2.4 shows a standard way of synthesis of α-hydroxybisphosphonate ester. This avoids the formation of an intermediate dialkyl α-ketophosphonate. This is also a one-pot synthesis, which can produce symmetrical as well as unsymmetrical esters in good yield. An acyl halide reacts with a mixture of trialkyl phosphite and dialkyl phosphite at 50-60 °C and gives 1-hydroxy-1,1-bisphosphonate. This method is also suitable for preparation of dihydroxy tetraphosphonates.

Scheme 2.4. Synthesis of bisphosphonate IV

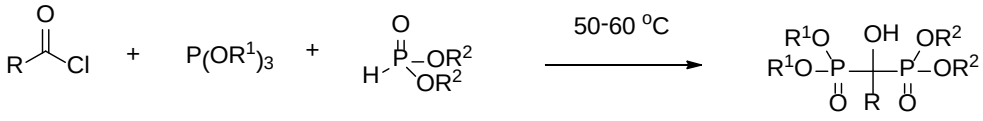

Acetyl chloride or benzyl chloride reacts with tris(trimethylsilyl) phosphate to give the corresponding silylated ester, which after alcoholysis gives acyl phosphonic acid

as shown in Scheme 2.5. Alcoholysis with a mixture of methanol and aniline gives the monoanilinium salt of acyl phosphonic acid with a good yield.

Scheme 2.5. Synthesis of bisphosphonate V

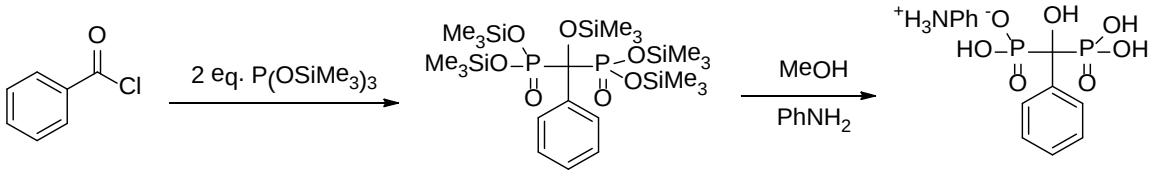

Bromotrimethyl silane or chlorotrimethyl silane on treatment with α-hydroxybisphosphonate ester, replaces the alkyl group of the ester with trimethyl silane to obtain tetrakis(trimethylsilyl) ester. These silylated esters on alcoholysis give 1-hydroxy-1,1-bisphosphonic acid (*87*, *88*). This is a gentle method of hydrolysis to obtain α-hydroxybisphosphonic acid as shown in Scheme 2.6. Several methods for hydrolysis of the esters are known including acid hydrolysis and base hydrolysis. However, the treatment of trimethylsilylbromide is an ideal method for hydrolysis of α-hydroxybisphosphonate ester.

Scheme 2.6. Synthesis of bisphosphonate VI

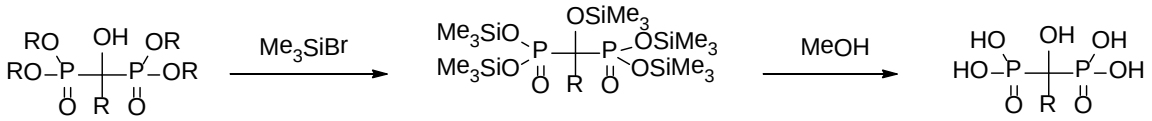

Overall, there are several synthetic methods for synthesis of BPs, however one-pot methods of synthesis have been widely used. The synthesis shown in Scheme 2.1 is a

one-pot synthesis that gives an excellent yield. Using the above synthetic methods, several derivatives of BPs have been synthesized for a wide range of applications, such as the treatment of bone diseases, drug targeting, and drug delivery to bone (*49, 89-93*). BPs are also synthesized and used in the administration of radiopharmaceuticals and imaging agents to bone for diagnostic applications (*50, 94-97*). Moreover, using various strategies, several BPs have been conjugated to therapeutic agents or targeting agents. However, the BPs, which were used for the targeted delivery of the attached drug to the bone, did not have a stable linkage, which could survive in systemic circulation, but gets cleaved at bone sites. Most of the reported BP conjugates for drug delivery applications are highly stable or too unstable. On the other hand, protein therapeutics and conjugation of proteins to BPs have also been explored, but the site-specific conjugation of BPs to protein has hardly been achieved. In most of the cases, BPs were attached to multiple sites of proteins, which lead to a random orientation of proteins on the surface (*51*). In this study, our objective was to synthesize bifunctional BPs which are capable to conjugate proteins in a site specific manner, and capable to conjugate therapeutic agents with labile linkage. Towards this goal, we synthesized and structurally characterized several bifunctional hydrazine bisphosphonates (HBPs) of varying length and hydrophobicity (Figure 2.1). Furthermore, other attempts of synthesis of bifunctional BPs, such as hydrazide bisphosphonates and aldehyde bisphosphonates, are also described.

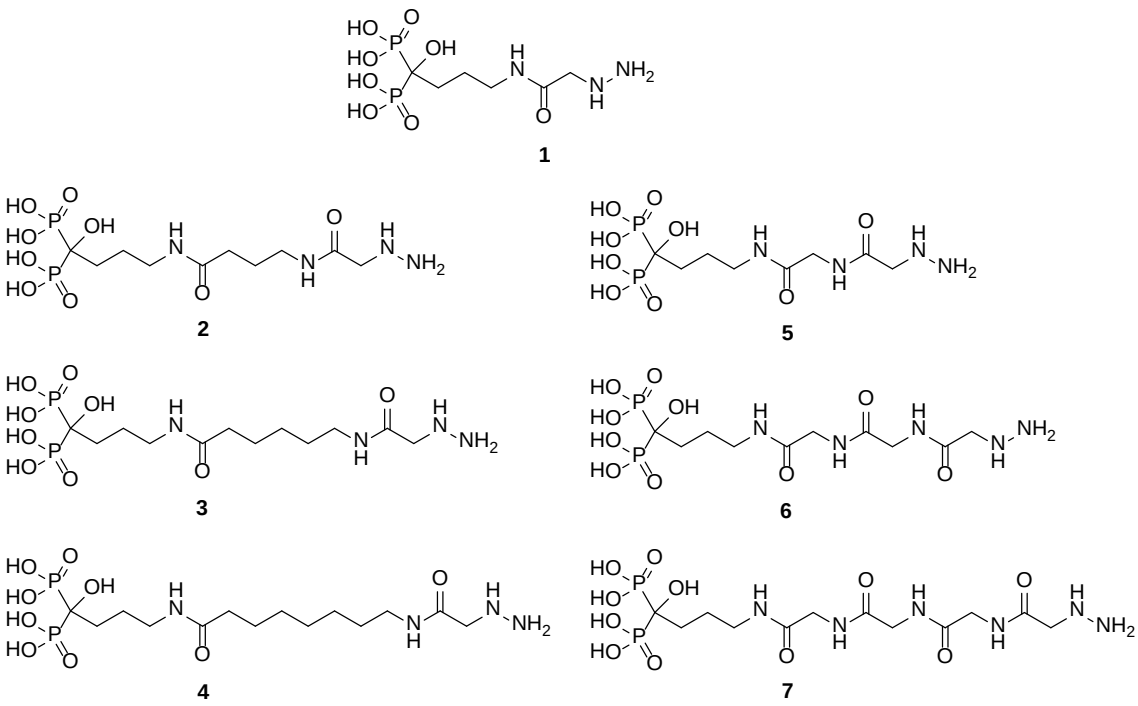

Figure 2.1. Structures of hydrazine-bisphosphonates (HBPs) (**1-7**)

EXPERIMENTAL SECTION

Reagents. 4-Aminobutanoic acid (**12a**), 6-aminohexanoic acid (**12b**), 8-aminooctanoic acid (**12c**), glycine (**12d**), glycylglycine (**12e**), glycylglycylglycine (**12f**), succinic anhydride (**19**), Ethyl chloroformate (**24**), methanesulfonic acid, phosphorous acid, phosphorous trichloride, and 3,5,6-tetrafluorophenol (TFP) were purchased from Alfa Aesar (Ward Hill, MA, USA). Triethylamine (TEA), tri-BOC-hydrazinoacetic acid (TBHA), 3-butenoic acid, 4-pentenoic acid, 6-heptenoic acid, 10-undecenoic acid, succinic anhydride, and sodium hydroxide, were purchased from Sigma-Aldrich (St. Louis, MO, USA). Hydrochloric acid, and potassium dihydrogen phosphate were obtained from EMD chemicals (Gibbstown, NJ, USA). Acetonitrile, chloroform, dichloromethane (DCM), diethyl ether, dimethyl sulfoxide (DMSO), hexane, and phosphoric acid were purchased from Mallinckrodt (Hazelwood, MO, USA). NMR solvents, deuterium oxide, and deuterated chloroform were purchased from Cambridge Isotope Laboratories (Andover, MA, USA).

Apparatus: ^{1}H NMR, ^{31}P NMR, and ^{13}C NMR spectra were obtained on a Varian INOVA 400 MHz spectrometer (Palo Alto, CA, USA). Electrospray ionization mass spectrometry was performed on a ThermoFinnigan LCQ mass spectrometer (Waltham, MA, USA). UV-vis spectroscopy was performed with an Agilent 8453 UV-visible spectrophotometer (Agilent Technologies, Santa Clara, CA, USA). Deionized water was produced using a Milli-Q water purification system (Millipore, Bedford, MA).

Scheme 2.7. Synthesis of monosodium alendronate (**8**)

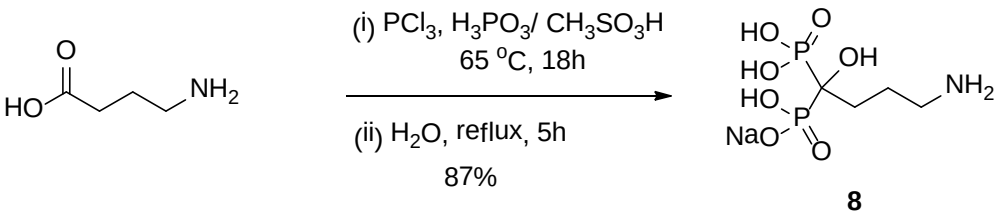

8

Synthesis of (4-Amino-1-hydroxybutylidene)bisphosphonic Acid Monosodium Salt (8)

A 25-mL flask was fitted with an addition funnel and a reflux condenser. Ice cold water was circulated through the condenser. The system was flushed with nitrogen and 4-aminobutyric acid (**12a**) (4.0 g, 38.7 mmol), phosphorous acid (3.18 g, 38.7 mmol), and methanesulfonic acid (16 mL) was added to the flask. The mixture was heated for 5 min at 65 °C. PCl_3 (9.0 mL, 85.3 mmol) was added over 20 min, and the mixture was stirred for 18 h at 65 °C. The solution was cooled to 25 °C and quenched into 0-5 °C water (40 mL) with vigorous stirring. The reaction flask was rinsed with additional 16 mL of water, and the combined solution was refluxed for 5 h at 110 °C. The solution was cooled to 23 °C, and the pH was adjusted to 4-4.5 with 50% (v/v) NaOH. The resulting mixture was let react for 10-12 h at 0-5 °C. The white solid obtained was filtered and washed with cold water (20 mL) and 95% ethanol (20 mL). The solid was dried under vacuum at room temperature (RT) to obtain compound **8** in yield 87.1% (9.22 g), as the monosodium salt. ^{1}H NMR (D_2O): δ 3.02 (t, 2H), δ 2.00 (m, 4H). ^{13}C NMR ($MeCN/D_2O$): δ 72.9 (t), δ 39.33 (s), δ 29.94 (s), δ 21.48 (t). ^{31}P NMR (H_3PO_4/D_2O): δ 18.53. MS (MALDI-TOFMS): $[M + H^+ + Na^+]$ calculated for $C_4H_{13}NO_7P_2Na^+$: 272, found 272.

Scheme 2.8. Synthesis of HBP **1**

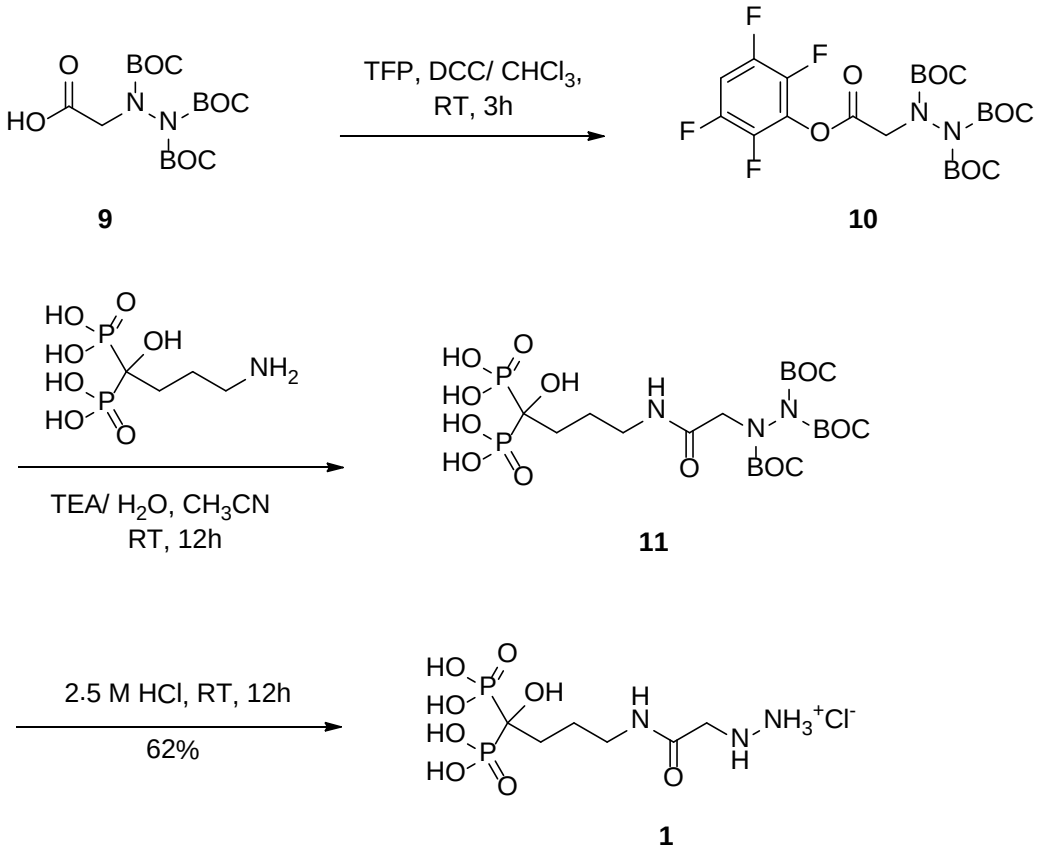

Synthesis of tri-tert-butyl 2-(2-oxo-2-(2,3,5,6-tetrafluorophenoxy)ethyl)hydrazine-1,1,2-tricarboxylate (10)

Tri-BOC-hydrazinoacetic acid (**9**) (90.0 mg, 0.231 mmol) and TFP (42.1 mg, 0.254mmol) were dissolved in 5 mL chloroform. DCC (52.3 mg, 0.254 mmol) in 5 mL chloroform was added dropwise to the reaction mixture and stirred at RT. The progress of the reaction was followed by TLC. After complete consumption of **9** (3 h), the 1,3-dicyclohexyl urea formed in the reaction mixture was removed by filtration, and the filtrate was evaporated *in vacuo*. The residue was then suspended in an adequate amount of hexane, the remaining 1,3-dicyclohexyl urea was removed by filtration, and the filtrate was evaporated *in vacuo* to obtain the crude compound **10**. The crude material was purified by column chromatography (hexane/acetone 85/15 v/v) to give the pure compound as a pale yellow liquid in 97% (120.5 mg) yield. ^{1}H NMR (CD_3CN): δ 7.25 (m, 1H), δ 3.20 (s, 2H) δ 1.45 (m, 27H). ^{13}C NMR ($CDCl_3$): δ 168.01 (s), δ 154.35 (s), δ 153.75 (s), δ 150.54 (s), δ 148.70 (s), δ 147.10 (s), δ 146.40 (s), δ 102.10 (s), δ 84.22 (s), δ 83.27 (s), δ 82.21 (s), δ 54.33 (m), δ 28.20 (s).

Synthesis of Compound 1

Compound **8** (50.0 mg, 0.154 mmol) was suspended in 1 mL of distilled water, and triethylamine (TEA) (93.2 mg, 0.923 mmol) was added to the suspension. After a few seconds of stirring at RT, the suspension became clear. The reaction was stirred at RT for 5 min. The compound **10** (124.3 mg, 0.231 mmol) was dissolved in 1.5 mL of acetonitrile and added to the reaction mixture. TEA (15.5 mg, 0.154 mmol) was added, and the reaction mixture was stirred at RT for 12 h. The reaction mixture was washed with

diethyl ether (10 mL) and evaporated *in vacuo*. The obtained solid was treated with 2 mL of 2.5 M HCl, and the solution was stirred at RT for 24 h. The solvent was removed *in vacuo*, and the crude product was sonicated twice in ethanol at RT for 2 h and filtered to obtain a white solid of pure compound **1** in 62% (31 mg) yield. ^{1}H NMR (D_2O): δ 3.78 (s, 2H), δ 3.28 (t, 2H), δ 1.99 (m, 2H), δ 1.84 (m, 2H). ^{13}C NMR (MeCN/D_2O): δ 170.41 (s), δ 74.17 (t), δ 51.58 (s), δ 40.50 (s), δ 31.75 (s), δ 24.17 (s). ^{31}P NMR (H_3PO_4/D_2O): δ 19.08. MS (+ ESI) : $[M + H]^+$ calculated for $C_6H_{18}N_3O_8P_2$: 322, found 322.

Scheme 2.9. Synthesis of HBP **2-7**

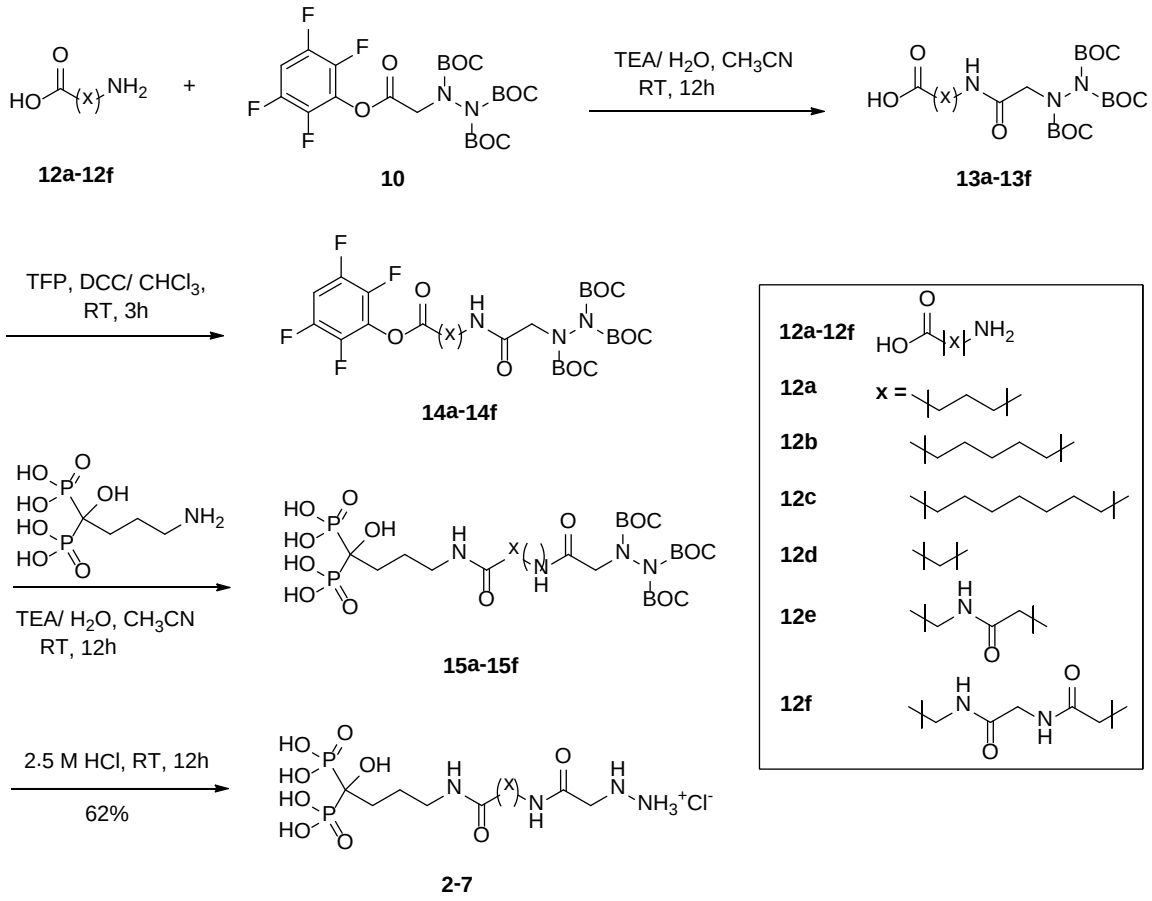

General Procedure for Synthesis of Compounds 13a-13f

Compound **12a-12f** (0.334 mmol, 1.0 equiv.) was suspended in 1 mL of distilled water, and TEA (0.668 mmol, 2.0 equiv.) was added to the suspension. After a few seconds of stirring at RT, the suspension became clear. The reaction was stirred at RT for 5 min. The compound **10** (0.401 mmol, 1.2 equiv.) was dissolved in 1.5 mL of acetonitrile, and the solution was added to the reaction mixture. TEA (0.167 mmol, 0.5 equiv.) was added, and the reaction mixture was stirred at RT for 12 h. The reaction mixture was washed with diethyl ether, and solvent was evaporated *in vacuo* to obtain crude compound **13a-13f**. The crude product **13a-13f** was used in the next reaction without further purification.

Compound 13a

Following the procedure shown for **13a-13f**, compound **13a** was obtained by amide coupling of compound **10** and 4-aminobutenoic acid (**12a**) as a semi solid in 97% yield. ^{1}H NMR ($CDCl_3$): δ 4.10 (s, 2H), δ 3.60 (d, 2H), δ 2.35 (m, 2H), δ 1.30 (m, 2H), δ 1.45 (m, 27H). ^{13}C NMR ($CDCl_3$): δ 182.70 (s), δ 170.70 (s), δ 154.30 (s), δ 153.40 (s), δ 150.56 (s) δ 84.24 (s), δ 83.56 (s), δ 82.10 (s), δ 54.30 (m), δ 39.41 (m), δ 35.60 (m), δ 28.41 (s), δ 23.42 (m).

Compound 13b

Following the procedure shown for **13a-13f**, compound **13b** was obtained by amide coupling of compound **10** and 6-aminohexanoic acid (**12b**) as a semi solid in 96% yield. ^{1}H NMR ($CDCl_3$): δ 4.03 (s, 2H), δ 3.33 (d, 2H), δ 2.21 (t, 2H), δ 1.61 (m, 2H), δ 1.45 (m, 27H), δ 1.28 (m, 2H). ^{13}C NMR ($CDCl_3$): δ 178.04 (s), δ 170.20 (s), δ 154.44 (s), δ

153.34 (s), δ 151.84 (s), δ 85.11 (s), δ 83.24 (s), δ 83.48 (s), δ 54.35 (m), δ 38.92 (m), δ 34.32 (m), δ 29.15 (s), δ 28.40 (s), δ 26.37 (s), δ 24.75 (s).

Compound 13c

Following the procedure shown for **13a-13f**, compound **13c** was obtained by amide coupling of compound **10** and 8-aminooctanoic acid (**12c**) as a semi solid in 95% yield. ^{1}H NMR ($CDCl_3$): δ 4.02 (s, 2H), δ 3.23 (m, 2H), δ 2.22 (t, 2H), δ 1.59 (m, 4H), δ 1.45 (m, 27H), δ 1.25 (m, 6H). ^{13}C NMR ($CDCl_3$): δ 178.40 (s), δ 170.05 (s), δ 154.14 (s), 151.25 (s), 151.19 (s), δ 85.17 (s), δ 85.39 (s), δ 83.89 (s), δ 38.90 (m), δ 34.00 (t), δ 30.10 (m), δ 29.12 (s), δ 29.65 (s), δ 26.58 (s), δ 24.54 (s).

Compound 13d

Following the procedure shown for **13a-13f**, compound **13d** was obtained by amide coupling of compond **10** and glycine (**12d**) as a semi solid in 95% yield. ^{1}H NMR ($CDCl_3$): δ 4.10 (s, 2H), δ 3.98 (s, 2H), δ 1.45 (m, 27H). ^{13}C NMR ($CDCl_3$): δ 174.56 (s), δ 168.46 (s), δ 154.46 (s), δ 153.86 (s), δ 150.65 (s) δ 84.52 (s), δ 83.16 (s), δ 82.45 (s), δ 54.93 (m), δ 45.91 (m), δ 28.22 (s).

Compound 13e

Following the procedure shown for **13a-13f**, compound **13e** was obtained by amide coupling of compond **10** and glycylglycine (**12e**) as a semi solid in 94% yield. ^{1}H NMR ($CDCl_3$): δ 4.02 (s, 2H), δ 3.99 (s, 2H), δ 3.80 (s, 2H), δ 1.45 (m, 27H). ^{13}C NMR

($CDCl_3$): δ 174.44 (s), δ 169.24 (s), δ 168.43 (s), δ 154.34 (s), δ 153.55 (s), δ 151.20 (s), δ 85.12 (s), δ 83.66 (s), δ 83.05 (s), δ 55.15 (m), δ 45.24 (m), δ 43.31 (m), δ 28.15 (s).

Compound 13f

Following the procedure shown for **13a-13f**, compound **13f** was obtained by amide coupling of compound **10** and glycylglycylglycine (**12f**) as a semi solid in 93% yield. ^{1}H NMR ($CDCl_3$): δ 4.01 (s, 2H), δ 3.98 (d, 2H), δ 3.91 (d, 2H), δ 3.80 (d, 2H), δ 1.42 (m, 27H). ^{13}C NMR ($CDCl_3$): δ 174.45 (s), δ 169.75 (s), δ 169.51 (s), δ 168.01 (s), δ 154.55 (s), 151.40 (s), 151.14 (s), δ 85.40 (s), δ 85.29 (s), δ 83.51 (s), δ 55.49 (m), δ 45.30 (m), δ 43.77 (m), δ 43.34 (s), δ 28.19 (s).

General Procedure for Synthesis of Compounds 14a-14f

Compound **13a-13f** (0.386 mmol, 1.0 equiv.) and TFP (0.425 mmol, 1.1 equiv.) were dissolved in 15 mL chloroform. DCC (0.425 mmol, 1.1 equiv.) in 10 mL chloroform was added dropwise to the reaction mixture and stirred at RT. The progress of the reaction was followed by TLC. After complete consumption of **13a-13f**, the 1,3-dicyclohexyl urea formed in the reaction mixture was removed by filtration, and the filtrate was evaporated *in vacuo*. The residue was then suspended in an adequate amount of hexane, the remaining 1,3-dicyclohexyl urea was removed by filtration, and the filtrate was evaporated *in vacuo* to obtain the crude compound **14a-14f**. The crude product was purified by column chromatography (DCM/MeOH 90/10 v/v) to obtain the pure compound as a pale yellow liquid.

Compound 14a

Following the procedure shown for **14a-14f**, compound **14a** was obtained from **13a** by treatment of TFP and DCC, as a sticky liquid. ^{1}H NMR ($CDCl_3$): δ 6.60 (s, 1H), δ 4.05 (s, 2H), δ 3.20 (d, 2H), δ 2.67 (m, 2H), δ 1.97 (m, 2H), δ 1.42 (m, 27H). ^{13}C NMR ($CDCl_3$): δ 182.47 (s), δ 170.12 (s), δ 154.10 (s), δ 153.45 (s), δ 151.10 (s), δ 148.69 (d), δ 147.23 (d), δ 146.80 (s), δ 102.10 (s), δ 84.58 (s), δ 83.74 (s), δ 82.36 (s), δ 54.33 (m), δ 39.45 (m), δ 33.56 (m), δ 23.47 (s), δ 28.56 (s).

Compound 14b

Following the procedure shown for **14a-14f**, compound **14b** was obtained from **13b** by treatment of TFP and DCC, as a sticky liquid. ^{1}H NMR ($CDCl_3$): δ 6.97 (s, 1H), δ 4.05 (s, 2H), δ 3.95 (s, 2H), δ 2.31 (m, 2H), δ 2.62 (m, 4H), δ 1.80 (m, 2H), δ 1.45 (m, 27H). ^{13}C NMR ($CDCl_3$): δ 177.12 (s), δ 170.89 (s), δ 154.69 (s), δ 153.78 (s), δ 151.11 (s), 148.60 (d), δ 147.05 (d), δ 146.44 (s), δ 102.10 (s), δ 85.25 (s), δ 83.73 (s), δ 83.92 (s), δ 54.33 (m), δ 38.96 (m), δ 33.56 (m), δ 29.78 (s), δ 28.40 (s), δ 26.58 (s), δ 24.45 (s).

Compound 14c

Following the procedure shown for **14a-14f**, compound **14c** was obtained from **13c** by treatment of TFP and DCC, as a sticky liquid. ^{1}H NMR ($CDCl_3$): δ 6.98 (s, 1H), δ 4.05 (s, 2H), δ 3.95 (s, 2H), δ 2.40 (s, 2H), δ 1.65 (m, 4H), δ 1.38 (m, 6H), δ 1.45 (m, 27H). ^{13}C NMR ($CDCl_3$): δ 178.58 (s), δ 170.89 (s), δ 154.45 (s), 151.69 (s), 151.51 (s), 148.72 (d), δ 147.20 (d), δ 146.40 (s), δ 102.10 (s), δ 85.93 (s), δ 85.54 (s), δ 83.12 (s), δ 38.95 (m), δ 33.50 (t), δ 30.32 (m), δ 29.45 (s), δ 29.10 (s), δ 26.70 (s), δ 25.73 (s).

Compound 14d

Following the procedure shown for **14a-14f**, compound **14d** was obtained from **13d** by treatment of TFP and DCC, as a sticky liquid. ^{1}H NMR ($CDCl_3$): δ 6.60 (s, 1H), δ 4.25 (s, 2H), δ 4.10 (s, 2H), δ 1.42 (m, 27H). ^{13}C NMR ($CDCl_3$): δ 174.02 (s), δ 168.32 (s), δ 154.21 (s), δ 153.14 (s), δ 150.78 (s), δ 148.72 (d), δ 146.89 (d), δ 146.10 (s), δ 101.80 (s), δ 84.12 (s), δ 83.85 (s), δ 82.64 (s), δ 54.41 (m), δ 45.00 (m), δ 28.44 (s).

Compound 14e

Following the procedure shown for **14a-14f**, compound **14e** was obtained from **13e** by treatment of TFP and DCC, as a sticky liquid. ^{1}H NMR ($CDCl_3$): δ 6.98 (s, 1H), δ 4.38 (s, 2H), δ 4.11 (s, 2H), δ 3.41 (s, 2H), δ 1.45 (m, 27H). ^{13}C NMR ($CDCl_3$): δ 170.28 (s), δ 169.52 (s), δ 167.00 (s), δ 156.00 (s), δ 151.12 (s), δ 150.02 (s), 148.23 (d), δ 147.45 (d), δ 146.69 (s), δ 102.47 (s), δ 85.67 (s), δ 85.00 (s), δ 83.90 (s), δ 55.87 (s), δ 45.65 (s), δ 43.06 (m), δ 28.14 (s).

Compound 14f

Following the procedure shown for **14a-14f**, compound **14f** was obtained from **13f** by treatment of TFP and DCC, as a sticky liquid. ^{1}H NMR ($CDCl_3$): δ 6.75 (s, 1H), δ 4.42 (d, 2H), δ 4.10 (m, 4H), δ 3.85 (d, 2H), δ 1.50 (m, 27H). ^{13}C NMR ($CDCl_3$): δ 170.81 (s), δ 170.10 (s), δ 170.05 (s), δ 165.87 (s), δ 156.00 (s), 154.80 (s), 151.20 (s), 148.48 (d), δ 147.23 (d), δ 146.10 (s), δ 103.76 (s), δ 85.79 (s), δ 85.51 (s), δ 84.07 (s), δ 55.96 (m), δ 49.46 (s), δ 43.61 (s), δ 40.82 (s), δ 28.11 (s).

General Procedure for Synthesis of Compounds 15a-15f

Compound **1** (0.154 mmol, 1.0 equiv.) was suspended in 1 mL of distilled water, and TEA (1.077 mmol, 7.0 equiv.) was added to the suspension. After a few seconds of stirring at RT, the suspension became clear. The reaction was stirred at RT for 5 min. The crude compound **14a-14f** (0.231 mmol, 1.5 equiv.) was dissolved in 1.5 mL of acetonitrile and added to the reaction mixture. TEA (0.154 mmol, 1.0 equiv.) was added, and the reaction mixture was stirred at RT for 12 h. The reaction mixture was washed with diethyl ether (10 mL) and evaporated *in vacuo* to obtain crude compound **15a-15f**. The crude product **15a-15f** was used in the next reaction without further purification.

Compound 15a

Following the procedure shown for **15a-15f**, compound **15a** was obtained by amide coupling of monosodium alendronate and compound **14a** in the basic condition as a white solid in 99% yield. ^{1}H NMR (D_2O): δ 4.12 (s, 2H), δ 3.27 (t, 2H), δ 3.12 (t, 2H), δ 2.28 (m, 2H), δ 1.95 (m, 2H), δ 1.80 (m, 4H), δ 1.42 (s, 27H). ^{13}C NMR (MeCN/D_2O): δ 177.50 (s), δ 171.22 (s), δ 154.56 (s), δ 153.48 (s), δ 151.94 (s), δ 85.08 (s), δ 75.40 (s), δ 74.00 (s), δ 71.40 (s), δ 52.33 (s), δ 49.17 (s), δ 41.65 (s), δ 34.78 (s), δ 32.66 (s), δ 31.42 (m), δ 29.15 (s), δ 25.02 (s).

Compound 15b

Following the procedure shown for **15a-15f**, compound **15b** was obtained by amide coupling of monosodium alendronate and compound **14b** in the basic condition as a white solid in 97% yield. ^{1}H NMR (D_2O): δ 4.09 (s, 2H), δ 3.15 (m, 4H), δ 2.23 (t, 2H), δ

1.98 (m, 2H), δ 1.83 (m, 2H), δ 1.58 (t, 2H), δ 1.51 (m, 2H), δ 1.45 (s, 27H), δ 1.31 (m, 2H). ^{13}C NMR (MeCN/D_2O): δ 178.47 (s), δ 170.85 (s), δ 159.5 (s), δ 15+6.50 (s), δ 151.08 (s) δ 108.32 (s), δ 75.30 (s), δ 75.00 (s), δ 71.38 (s), δ 52.33 (s), δ 49.03 (s), δ 41.56 (s), δ 40.76 (s), δ 37.25 (s), δ 32.54 (s), δ 29.53 (s), 29.05 (m), δ 26.56 (s), δ 25.04 (s).

Compound 15c

Following the procedure shown for **15a-15f**, compound **15c** was obtained by amide coupling of monosodium alendronate and compound **14c** in the basic condition as a white solid in 97% yield. ^{1}H NMR (D_2O): δ 4.09 (s, 2H), δ 3.15 (m, 4H), δ 2.21 (t, 2H), δ 1.95 (m, 2H), δ 1.81 (m, 2H), δ 1.55 (d, 4H), δ 1.45 (m, 27H), δ 1.25 (m, 6H). ^{13}C NMR (MeCN/D_2O): δ 178.74 (s), δ 159.55 (s), δ 148.80 (s), δ 144.25 (s), δ 142.98 (s), δ 85.08 (d) δ 76.75 (s), δ 75.42 (s), δ 71.37 (s), δ 48.90 (s), δ 47.55 (s), δ 41.63 (s), δ 40.94 (s), δ 37.45 (s), 32.67 (s), 31.38 (d), 29.70 (m), δ 29.04 (m), δ 27.45 (m), δ 26.99 (s), δ 25.01 (s).

Compound 15d

Following the procedure shown for **15a-15f**, compound **15d** was obtained by amide coupling of monosodium alendronate and compound **14d** in the basic condition as a white solid in 98% yield. ^{1}H NMR (D_2O): δ 4.21 (m, 2H), δ 3.95 (s, 2H), δ 3.21 (m, 2H), δ 1.95 (t, 2H), δ 1.82 (m, 2H), δ 1.47 (m, 27H). ^{13}C NMR (MeCN/D_2O): δ 163.50 (s), δ 160.50 (s), δ 151.10 (s), δ 148.00 (s), δ 146.20 (s), δ 84.50 (s), δ 79.15 (s), δ 78.56 (s), δ 74.50 (s), δ 51.25 (t), δ 43.65 (s), δ 33.75 (m) δ 29.54 (m), δ 24.30 (s), δ 22.50 (s).

Compound 15e

Following the procedure shown for **15a-15f**, compound **15e** was obtained by amide coupling of monosodium alendronate and compound **14e** in the basic condition as a white solid in 98% yield. ^{1}H NMR (D_2O): δ 4.21 (s, 2H), δ 4.05 (s, 2H), δ 3.92 (s, 2H), δ 3.12 (t, 2H), δ 1.95 (m, 2H), δ 1.82 (m, 2H). ^{13}C NMR (MeCN/D_2O): δ 171.25 (s), δ 170.89 (s), δ 169.55 (s), 157.00 (s), δ 155.22 (s), δ 151.45 (s), δ 96.58 (s), δ 84.26 (s), δ 83.87 (s) δ 81.05 (s), δ 53.60 (s), δ 42.50 (s), δ 41.08 (s), δ 38.90 (s), δ 31.50 (s), δ 29.50 (m), δ 23.24 (s).

Compound 15f

Following the procedure shown for **15a-15f**, compound **15f** was obtained by amide coupling of monosodium alendronate and compound **14f** in the basic condition as a white solid in 99% yield. ^{1}H NMR (D_2O): δ 4.22 (s, 2H), δ 4.06 (s, 2H), δ 4.01 (s, 2H), δ 3.92 (s, 2H), δ 3.15 (t, 2H), δ 1.92 (m, 2H), δ 1.81 (m, 2H), δ 1.45 (s, 27H). ^{13}C NMR (MeCN/D_2O): δ 175.54 (s), δ 173.75 (s), δ 173.61 (s), δ 172.72 (s), δ 160.01 (s), δ 159.23 (s), δ 158.25 (s), δ 84.79 (s), δ 76.72 (s), δ 75.39 (s), δ 71.36 (s), δ 55.48 (s), δ 44.07 (s), δ 41.55 (s), δ 32.48 (s), δ 31.30 (s), δ 31.21 (s), δ 29.09 (s).δ 25.03 (s).

General Procedure for Synthesis of Compounds 2-7

The crude solid of compound **15a-15f** (0.231 mmol, 1.5 equiv.) was treated with 2 mL of 2.5 M HCl, and the solution was stirred at RT for 24 h. The solvent was removed *in vacuo*, the crude product was sonicated twice in ethanol at RT for 2 h for purification. The white solid was filtered to obtain fine powder of pure compounds **2-7**.

Compound 2

Following the procedure shown for **2-7**, compound **15a** was obtained by acid treatment as a white solid in 63% yield. ^{1}H NMR (D_2O): δ 3.73 (s, 2H), δ 3.22 (t, 4H), δ 2.25 (t, 2H), δ 1.95 (m, 2H), δ 1.80 (m, 4H). ^{13}C NMR (MeCN/D_2O): δ 176.87 (s), δ 170.46 (s), δ 74.16 (t), δ 51.54 (s), δ 40.66 (s), δ 39.52 (s), δ 34.04 (s), δ 31.84 (s), δ 25.66 (t), δ 24.16 (s). ^{31}P NMR (H_3PO_4/D_2O): δ 19.32. MS (+ ESI) : $[M + H]^+$ calculated for $C_{10}H_{25}N_4O_9P_2$: 407.10, found 407.

Compound 3

Following the procedure shown for **2-7**, compound **15b** was obtained by acid treatment as a white solid in 59% yield. ^{1}H NMR (D_2O): δ 3.73 (s, 2H), δ 3.22 (q, 4H), δ 2.25 (t, 2H), δ 1.98 (m, 2H), δ 1.82 (m, 2H), δ 1.59 (t, 2H), δ 1.52 (t, 2H), δ 1.30 (m, 2H). ^{13}C NMR (MeCN/D_2O): δ 177.70 (s), δ 169.94 (s), δ 73.95 (t), δ 51.36 (s), δ 40.43 (s) δ 39.86 (s), δ 36.37 (s), δ 31.64 (s), δ 28.62 (s), δ 26.15 (s), δ 25.68 (s), δ 23.99 (s). ^{31}P NMR (H_3PO_4/D_2O): δ 19.14. MS (+ ESI) : $[M + H]^+$ calculated for $C_{12}H_{29}N_4O_9P_2$: 435.13, found 435.

Compound 4

Following the procedure shown for **2-7**, compound **15c** was obtained by acid treatment as a white solid in 57% yield. ^{1}H NMR (D_2O): δ 4.06 (s, 2H), δ 4.0 (s, 2H), δ 3.92 (s, 2H), δ 3.86 (s, 2H), δ 3.25 (t, 2H), δ 1.98 (m, 2H), δ 1.84 (m, 2H). ^{13}C NMR (MeCN/D_2O): δ 173.19 (s), δ 172.01 (s), δ 172.17 (s), δ 171.92 (s), δ 74.15 (t), δ 51.45 (s) δ 43.73 (s), δ

43.49 (s), δ 43.15 (s), δ 40.60 (s), δ 31.67 (s), δ 24.15 (s). ^{31}P NMR (H_3PO_4/D_2O): δ 19.15. MS (+ ESI) : $[M + H]^+$ calculated for $C_{14}H_{33}N_4O_9P_2$: 463.16, found 463.

Compound 5

Following the procedure shown for **2-7**, compound **15d** was obtained by acid treatment as a white solid in 55% yield. ^{1}H NMR (D_2O): δ 3.95 (s, 2H), δ 3.84 (s, 2H), δ 3.26 (t, 2H), δ 1.98 (m, 2H), δ 1.84 (m, 2H). ^{13}C NMR (MeCN/D_2O): δ 172.10 (s), δ 171.74 (s), δ 74.15 (t), δ 51.40 (s), δ 47.62 (s) δ 40.60 (s), δ 31.70 (s), δ 24.09 (s). ^{31}P NMR (H_3PO_4/D_2O): δ 19.16. MS (+ ESI) : $[M + H]^+$ calculated for $C_8H_{21}N_4O_9P_2$: 379.07, found 379.

Compound 6

Following the procedure shown for **2-7**, compound **15e** was obtained by acid treatment as a white solid in 56% yield. ^{1}H NMR (D_2O): δ 4.04 (s, 2H), δ 3.92 (s, 2H), δ 3.86 (s, 2H), δ 3.25 (t, 2H), δ 1.96 (m, 2H), δ 1.84 (m, 2H). ^{13}C NMR (MeCN/D_2O): δ 171.55 (s), δ 170.79 (s), δ 170.62 (s), δ 72.82 (t), δ 50.04 (s), δ 42.15 (s) δ 41.88 (s), δ 39.26 (s), δ 30.06 (s), δ 22.71 (s). ^{31}P NMR (H_3PO_4/D_2O): δ 19.08. MS (+ ESI) : $[M + H]^+$ calculated for $C_{10}H_{24}N_5O_{10}P_2$: 436.09, found 436.

Compound 7

Following the procedure shown for **2-7**, compound **15f** was obtained by acid treatment as a white solid in 54% yield. ^{1}H NMR (D_2O): δ 3.73 (s, 2H), δ 3.22 (q, 4H), δ 2.25 (t, 2H), δ 2.00 (m, 2H), δ 1.82 (m, 2H), δ 1.55 (t, 2H), δ 1.45 (t, 2H), δ 1.30 (s, 6H). ^{13}C NMR

(MeCN/D_2O): δ 178.82 (s), δ 170.70 (s), δ 74.58 (t), δ 52.25 (s), δ 49.01 (s), δ 41.25 (s), δ 40.95 (s), δ 37.36 (s), δ 32.54 (s), δ 29.73 (s), δ 29.57 (s), δ 27.41 (s), δ 26.88 (s), δ 24.81 (s). ^{31}P NMR (H_3PO_4/D_2O): δ 19.38. MS (+ ESI) : $[M + H]^+$ calculated for $C_{12}H_{27}N_6O_{11}P_2$: 493.11, found 493.

Figure 2.2. Structures of ester BPs (**16-18**)

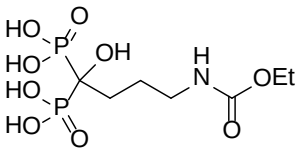

16

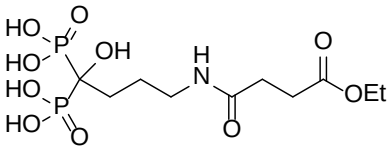

17

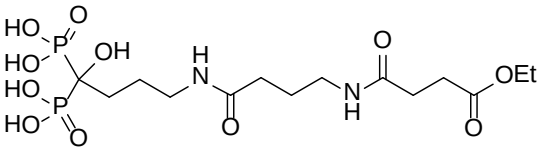

18

Scheme 2.10. Synthesis of ethoxy-bisphosphonates (**16-18**)

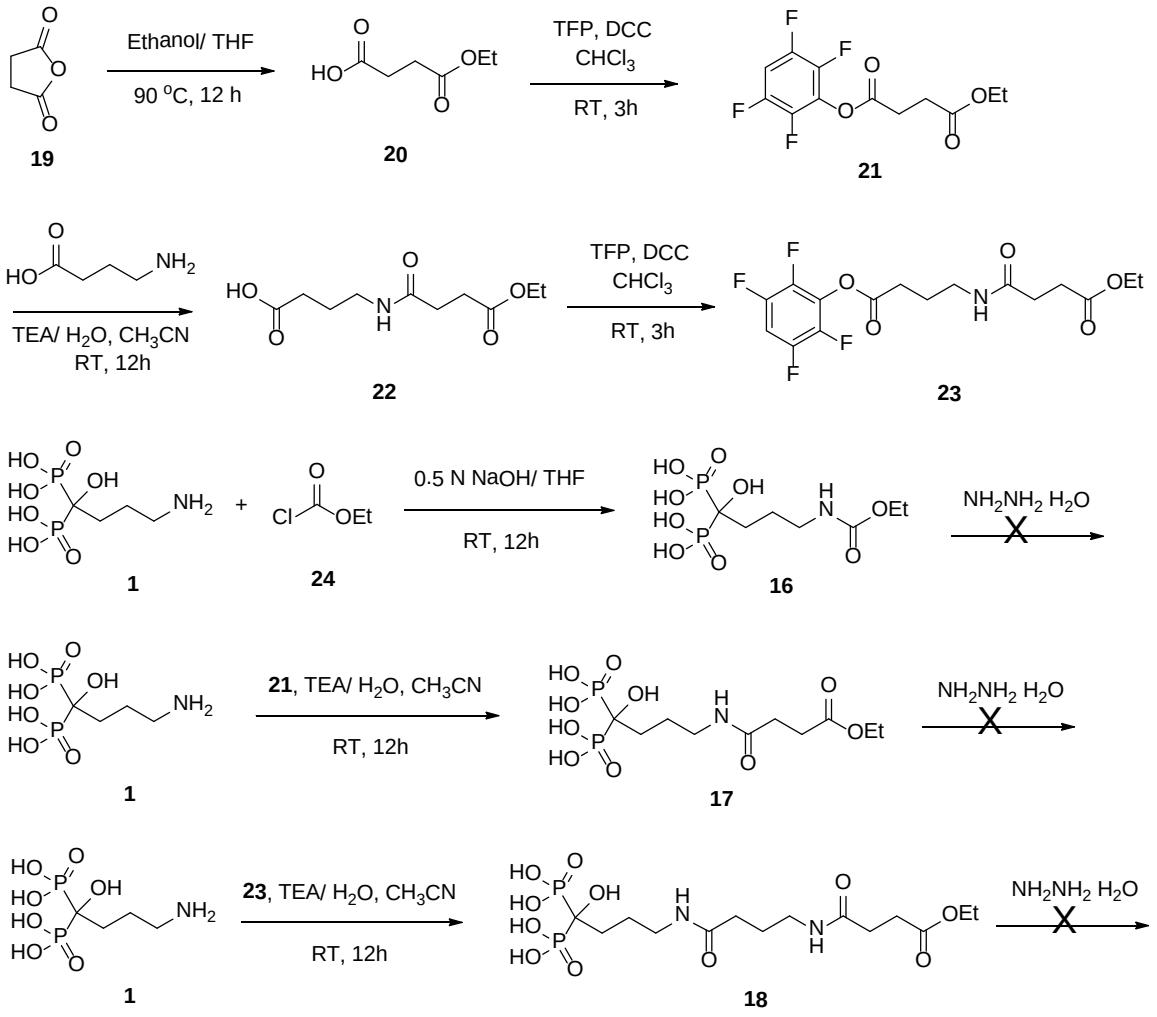

Synthesis of 4-ethoxy-4-oxobutanoic acid (20)

Succinic anhydride (**19**) (1.0 g, 10.0 mmol) was dissolved in 25 mL THF. Ethanol (0.51 g, 11.0 mmol) was added to the reaction mixtute and refluxed it at 90 °C for 12 h. The progress of the reaction was followed by TLC. After complete consumption of succinic anhydride, the solvent was evaporated in vacuo. The product was purified by column chromatography (hexane/acetone 80/20 v/v) to obtain the pure 4-ethoxy-4-oxobutanoic acid as a white solid. Yield: 95% (1.4 g). ^{1}H NMR ($CDCl_3$): δ 4.07 (q, 2H), δ 2.61 (m, 4H), δ 1.21 (t, 3H). ^{13}C NMR ($CDCl_3$): δ 178.50 (s), δ 172.23 (s), δ 61.3 (s), δ 29.1 (d), δ 14.2 (s).

Synthesis of ethyl (2,3,5,6 tetrafluorophenyl) succinate (21)

Compound **20** (1.00 g, 6.859 mmol) and TFP (1.25 g, 7.534 mmol) were dissolved in 20 mL chloroform. DCC (1.55 g, 7.534 mmol) was dissolved in 10 mL chloroform and the solution was added dropwise to the reaction mixture. The reaction was stirred at RT, and the progress of the reaction was followed by TLC. After complete consumption of starting material, the solid formed in the reaction mixture was removed by filtration, and the filtrate was evaporated *in vacuo* to obtained crude product. The crude material was purified by column chromatography (hexane/acetone 80/20 v/v) to give the pure compound as a white solid in 99% (0.99 g) yield. ^{1}H NMR ($CDCl_3$): δ 6.97 (m, 1H), δ 4.18 (q, 2H) δ 3.00 (t, 2H), δ 2.78 (t, 2H), δ 1.21 (t, 3H). ^{13}C NMR ($CDCl_3$): δ 171.00 (s), δ 169.30 (s), δ 149.23 (m), δ 143.80 (m), δ 138.20 (s), δ 102.10 (t), δ 60.80 (s), δ 29.1 (d), δ 14.2 (s).

Synthesis of 4-(4-ethoxy-4-oxobutanamido)butanoic acid (22)

4-Amino butanoic acid (0.35 g, 3.394 mmol) was suspended in 15 mL distilled water, and TEA (1.03 g, 10.182 mmol) was added to the suspension. After a few seconds of stirring at RT, the suspension became clear. The reaction was stirred at RT for 5 min. Compound **21** (1.10 g, 3.734 mmol) was dissolved in 10 mL of acetonitrile, and the solution was added dropwise to the reaction mixture. TEA (0.34 g, 3.394 mmol) was added, and the reaction mixture was stirred at RT for 12 h. The reaction mixture was washed with diethyl ether, and solvent was evaporated *in vacuo*. The crude product was purified by column chromatography (DCM/MeOH 80/20 v/v) to give the pure compound **22** as a sticky solid in 62% (0.48 g) yield. ^{1}H NMR ($CDCl_3$): δ 6.58 (bs, 1H), δ 4.82 (bs, 1H), δ 4.11 (q, 2H), δ 3.47 (t, 2H), δ 3.10 (m, 2H), δ 2.62 (t, 2H), δ 2.25 (t, 2H), δ 1.83 (m, 2H), δ 1.25 (t, 3H).

Synthesis of ethyl 4-oxo-4-((4-oxo-4-(2,3,5,6-tetrafluorophenoxy)butyl)amino)butanoate (23)

Compound **22** (0.78 g, 3.377 mmol) and TFP (0.62 g, 3.714 mmol) were dissolved in 15 mL chloroform. DCC (0.76 g, 3.714 mmol) was dissolved in 7 mL chloroform, and the solution was added dropwise to the reaction mixture. The reaction was stirred at RT, and the progress of the reaction was followed by TLC. After complete consumption of starting material, the solid formed in the reaction mixture was removed by filtration, and the filtrate was evaporated *in vacuo* to obtained crude product. The crude material was purified by column chromatography (hexane/acetone 75/25 v/v) to give the pure compound **23** as a white solid in 95% (1.2 g) yield. ^{1}H NMR ($CDCl_3$): δ 6.97 (m, 1H), δ

5.90 (bs, 1H), δ 4.18 (q, 2H) δ 3.40 (q, 2H), δ 2.70 (m, 4H), δ 2.42 (t, 2H), δ 1.95 (t, 2H), δ 1.22 (t, 3H).

Synthesis of (4-((ethoxycarbonyl)amino)-1-hydroxybutane-1,1-diyl)diphosphonic acid (16)

Compound **1** (0.50 g, 1.832 mmol) was dissolved in 2 mL of 0.5N NaOH. Ethyl chloroformate (**24**) (0.397 g, 3.663 mmol) was dissolved in 1 mL THF, and the solution was added dropwise to the reaction mixture. The reaction was stirred at RT for 12 h. The reaction mixture was washed with diethyl ether and evaporated *in vacuo* to obtain the product as a sodium salt, which was then used in the next reaction without further purification. ^{1}H NMR (D_2O): δ 3.85 (q, 2H), δ 2.92 (t, 2H), δ 1.75 (m, 2H), δ 1.60 (m, 2H), δ 1.00 (t, 3H). ^{13}C NMR (MeCN/D_2O): δ 161.8 (s), δ 76.38 (t), δ 64.60 (s), δ 43.73 (s), δ 33.63 (s), δ 26.65 (s), δ 16.67 (s).

Synthesis of (4-(4-ethoxy-4-oxobutanamido)-1-hydroxybutane-1,1-diyl)diphosphonic acid (17)

Compound **1** (0.40 g, 1.465 mmol) was suspended in 10 mL of distilled water, and TEA (1.036 g, 10.256 mmol) was added to the suspension. After a few seconds of stirring at RT, the suspension became clear. Ethyl (2,3,5,6 tetrafluorophenyl) succinate (0.47 g, 1.612 mmol) was dissolved in 15 mL of acetonitrile, and added into the reaction mixture. TEA (0.15 g, 1.465 mmol) was added, and the reaction mixture was stirred at RT for 12 h. The reaction mixture was washed with diethyl ether and evaporated *in vacuo* to obtain crude product (0.38 g) as a white solid, which was then used in the next reaction without

further purification. ^{1}H NMR (D_2O): δ 4.16 (q, 2H), δ 3.21 (t, 2H), δ 2.65 (t, 2H), δ 2.55 (t, 2H), δ 1.90 (m, 4H), δ 1.25 (q, 3H). ^{13}C NMR (MeCN/D_2O): δ 173.80 (s), δ 168.20 (s), δ 64.50 (t), δ 53.30 (s), δ 31.80 (s), δ 22.20 (s), δ 21.50 (s), δ 20.85 (s), δ 14.80 (s), δ 4.75 (s). MS (MALDI TOFMS) : $[M - H]^+$ calculated for $C_{10}H_{20}NO_{10}P_2$: 376, found 376.

Synthesis of (4-(4-(4-ethoxy-4-oxobutanamido)butanamido)-1-hydroxybutane-1,1-diyl)diphosphonic acid (18)

Compound **1** (0.70 g, 2.564 mmol) was suspended in 10 mL of distilled water, and TEA (1.813 g, 17.949 mmol) was added to the suspension. The reaction mixture was stirred for 5 min at RT. After a few seconds of stirring at RT, the suspension became clear. Ethyl 4-oxo-4-((4-oxo-4-(2,3,5,6-tetrafluorophenoxy)butyl)amino)butanoate (1.068 g, 2.821 mmol) was dissolved in 15 mL of acetonitrile and added to the reaction mixture. TEA (0.258 g, 2.564 mmol) was added, and the reaction mixture was stirred at RT for 12 h. The reaction mixture was washed with diethyl ether (10 mL) and evaporated *in vacuo* to obtain crude compound (4-(4-(4-ethoxy-4-oxobutanamido)butanamido)-1-hydroxybutane-1,1-diyl)diphosphonic acid (0.65 g) as a white solid, which was then used in the next reaction without further purification. ^{1}H NMR (D_2O): δ 4.18 (q, 2H), δ 3.55 (t, 2H), δ 3.25 (m, 2H), δ 2.65 (dd, 4H), δ 2.30 (t, 2H), δ 2.02 (m, 2H), δ 1.90 (m, 4H), δ 1.29 (t, 3H). ^{13}C NMR (MeCN/D_2O): δ 182.81 (s), δ 175.55 (s), δ 175.02 (s), δ 72.48 (t), δ 62.92 (s), δ 40.69 (s), δ 39.50 (s), δ 39.00 (s), δ 33.39 (s), δ 28.20 (s), δ 26.05 (s), δ 24.50 (s), δ 24.00 (s), δ 13.80 (s).

Scheme 2.11. Synthesis of aldehyde-bisphosphonate

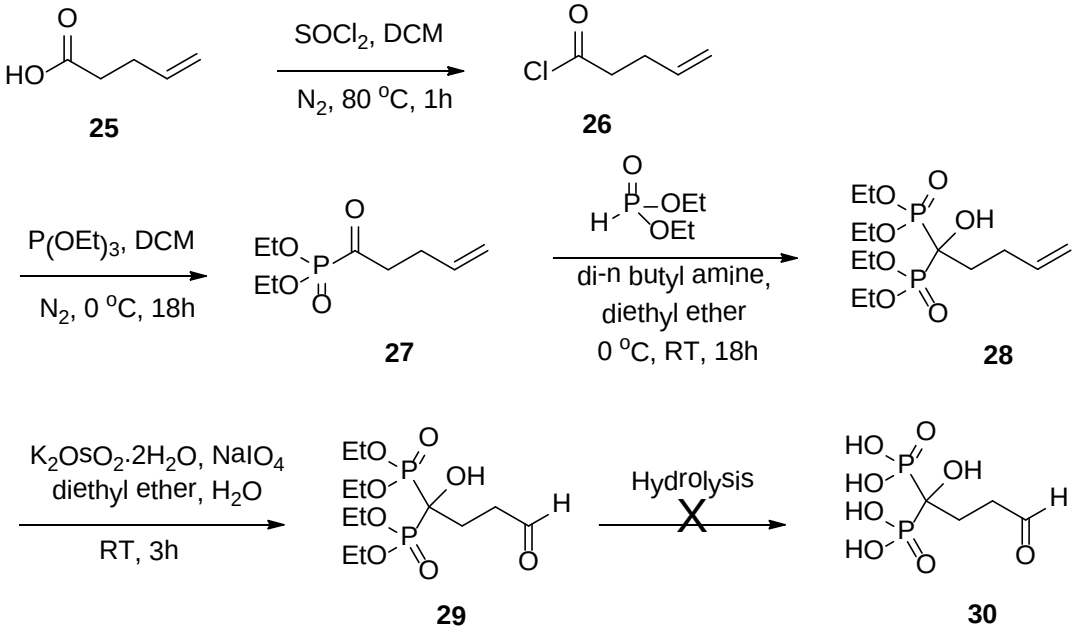

Synthesis of pent-4-enoyl chloride (26)

4-Pentenoic acid (**25**) (1.00 g, 9.988 mmol) was dissolved in 10 ml of DCM, and thionyl chloride (1.42 g, 11.985 mmol) was added dropwise at RT. The reaction mixture was refluxed at 80 °C for 2 h. The solvent was removed by evaporated *in vacuo* to obtain the product as a liquid, which was then used in the next reaction without further purification.

Synthesis of diethyl pent-4-enoylphosphonate (27)

4-Pentenoic acid chloride (**26**) (1.00 g, 8.439 mmol) was dissolved in 10 mL DCM, and the reaction flask was cooled at 0 °C. Triethyl phosphite (1.40 g, 8.439 mmol) was added dropwise in the reaction mixture with rapid stirring. After addition was complete, the reaction mixture was allowed to warm to RT. The reaction mixture was stirred at RT for overnight, and the solvent was removed under reduced pressure to obtain the product (**27**). The product was purified with column chromatography (hexane/acetone 85/15 v/v), and the pure product **27** was isolated as a liquid in 81% (1.5 g) yield.

Synthesis of tetraethyl (1-hydroxypent-4-ene-1,1-diyl)bis(phosphonate) (28)

Hydrogen diethyl phosphite (0.63 g, 4.545 mmol) and di-n-butylamine (0.59 g, 4.545 mmol) were dissolved in 20 mL diethyl ether, and the reaction mixture was stirred at RT for 5 min. The reaction mixture was cooled at 0 °C. Compound **27** (1.0 g, 4.545 mmol) was slowly added in the reaction mixture with a rapid stirring at 0 °C. After addition was complete, the reaction was allowed to warm to the RT, and then was stirred overnight. The solvent was removed under reduced pressure to obtain a crude product. The purification was done with column chromatography (hexane/acetone 80/20 v/v) to obtain

the pure product **28** in 93% (1.50 g) yield. ^{1}H NMR ($CDCl_3$): δ 5.8 (m, 1H), δ 5.1 (m, 1H), δ 4.6 (m, 1H), δ 4.2 (m, 8H), δ 2.22 (m, 2H), δ 1.82 (m, 2H), δ 1.28 (m, 12H).

Synthesis of tetraethyl (1-hydroxy-4-oxobutane-1,1-diyl)bis(phosphonate) (29)

Compound **28** (0.20 g, 0.559 mmol) was dissolved in 2 mL distilled water and 2 mL diethyl ether, and $K_2OsO_4.2H_2O$ (0.01 g, 0.028 mmol) was added into reaction mixture. The reaction was stirred for 2 min, and $NaIO_4$ (0.30 g, 1.397 mmol) was added in aliquots over 30 min with vigorous stirring. The reaction was stirred vigorously at RT overnight. The organic and aqueous layers were separated from each other. The aqueous layer was extracted with diethyl ether, and all organic layers were combined together. The organic layer was washed with brine, dried over Na_2SO_4, filtered, and concentrated. The residue was purified with column chromatography (hexane/acetone 80/20 v/v) to obtain the pure product **28** in 70% (140 mg) yield. ^{1}H NMR ($CDCl_3$): δ 4.78 (m, 1H), δ 4.18 (m, 8H), δ 2.6 (t, 2H), δ 2.23 (m, 2H), δ 1.28 (m, 12H).

RESULTS AND DISCUSSION

Our goal was to design novel BPs that demonstrate high binding affinity to bone mineral and contain a functional group that could be used to conjugate therapeutic agents to BPs through an acid-labile linkage. In addition to the above goal, our other goal was to synthesize the bifunctional BPs which could conjugate to the proteins in a selective manner, and immobilize them on solid surface for tissue engineering applications. Substituents (R^1 and R^2) at the geminal carbon of the BP contribute toward the bone

affinity; in particular, the presence of a hydroxyl at R^1 enhances bone affinity by enabling tridentate binding to HA (*20, 98, 99*). In that regard, we chose 1-hydroxy-1,1-bisphosphonic acid as the basic backbone of bifunctional BPs.

The designed 1-hydroxy-1,1-bisphosphonic acid backbone has a hydroxyl at R^1, while the R^2 substituent was used to introduce a different functional group that could be subsequently used for attachment of therapeutic agents. The attachment of a therapeutic agent to BP is possible through several reversible and irreversible linkages, such as amide, ester, imine, hydrazone, ether, and thioether coupling. Ester and thioester linkages are too labile and are not capable of surviving in systemic circulation (*90*). However, esterase activity in the plasma readily hydrolyzes esters and thioesters. Moreover, the rate of hydrolysis of ester and thioester could vary with the concentration of esterase interacting with the conjugate and the steric hindrance around the linkage (*16, 90*). The disulfide is also a too-labile bond, and readily gets reduced in presence of glutathione (*100*). The current approaches that employ cleavable linkages are either too labile to ensure delivery of the drug to the desired site, or show limited release providing inadequate availability of drug for action (*90, 91*). A strategy that involves labile conjugation to one of the phosphonate groups of BP could compromise the affinity of the corresponding BP-drug conjugate toward bone, because it is through the phosphonate groups that BPs bind to the mineral matrix (*91*). However for drug delivery at wound healing sites and resorption sites, where the pH is acidic (*101, 102*), acid-labile linkages such as those provided by hydrazones and imines are more appropriate. Imine hydrolyses rapidly at pH $\leq$ 7.0 (*103*), while hydrazone is stable at physiological pH. Further, the rate of hydrolysis of the hydrazone linkage increases gradually with decrease in pH from 7.4

(*104*, *105*). Therefore, the hydrazone linkage presents advantages over the imine linkage when sustained drug release is desired at the bone surface. Hence, the hydrazine functionality was introduced in 1-hydroxy-1,1-bisphosphonic acid at R^2 to obtain bifunctional HBPs.

The attachment of protein to BPs is possible by several methods of conjugation. Amide, ester, thioester, ether, thioether, and disulfide coupling are commonly used methods for protein conjugation. Since proteins generally have several amine and carboxylate groups, which could participate in amide coupling, the selective conjugation is difficult by amide coupling. Similarly, there could be more than one thiol group in the protein, and therefore, disulfide and thioether couplings are also in general not selective ways of conjugation. Moreover, thiols in the protein are generally involved in formation of secondary or tertiary structure through disulfide linkages. As a result, BP attachment via thiol conjugation could disturb the protein conformation and result in loss of protein bioactivity. The ester, thioester, and imine linkages are fairly unstable, and could not serve the purpose of protein immobilization. However, the hydrazone linkage seems very promising due to its strong and stable nature at physiological pH. The hydrazone linkage could be achieved by reaction of aldehyde and hydrazine functionality. It is a nucleophilic substitution reaction, and feasible under slightly acidic pH (less than physiological pH). Under such acidic conditions, other nucleophilic groups of proteins (amines, thiols, hydroxyls) are protonated and remain nonreactive. The hydrazone linkage between BP and protein could be achieved by reacting hydrazine of the BP with an aldehyde on the protein (the latter can be obtained by periodate treatment of N-terminal serine or threonine). In other words, BPs with a hydrazine functional group

could be conjugated to protein via hydrazone linkage. In that regard and in order to achieve selective conjugation of proteins for their immobilization on solid surfaces as well as conjugation of therapeutic agents for their targeted delivery to bone, bifunctional BPs with the hydrazine functionality at their R^2 substituent were designed.

Retention of protein activity after its immobilization on a solid surface is essential for its successful application in the design of biomaterials and tissue engineering. The protein could lose its activity by a small change in its conformation (*106*). Therefore, a proper distance between the immobilized protein and the immobilization surface is necessary. With a very small distance between the immobilized protein and the immobilization surface, the protein may interact with the surface and lose its bioactivity. Similarly, too-large of a distance may cause a lining of the protein on the surface, which could lose the bioactivity of protein. Moreover, for the targeted delivery of a drug to bone, the HBP-drug conjugate should not only be the stable during systemic circulation, but should also get cleaved at the desired site. On one hand, drug conjugation or the unwanted folding of the conjugate could create steric hindrance and prevent the release of the drug at the bone site. On the other hand, the attached drug might lose its activity or drug potency due to the steric interactions between the BP and the bone surface. Therefore, to optimize the distance between the immobilized protein and the immobilization-surface, as well as to avoid a loss of drug activity due to its steric interactions with bone surface, we have designed and synthesized HBPs with several spacers of varying length.

Similar to the length of the spacer, the hydrophobicity of the spacer, used for conjugation of BP to the therapeutic agent might change the drug potency of the

conjugated therapeutic agent. BP-conjugated protein might interact with the spacer used for the conjugation and cause a change in its conformation and bioactivity. However, the interactions between the spacer and conjugated therapeutic agent or protein might vary with the nature of the immobilized protein and the hydrophobicity of the spacer. Moreover, the bioavailability of the conjugate may vary with the change in hydrophobicity of the BP or the BP-conjugate. Therefore, various spacers of different hydrophobicity are introduced between two functional units of bifunctional BPs.

Considering the factors mentioned above, we have synthesized seven bifunctional hydrazine-bisphosphonates (HBPs) (**1-7**). These novel BPs with hydroxyl group as R^1 substituent, could bind Ca^{2+} of HA in a tridentate manner, and show an enhanced affinity to HA. The R^2 substituent has a hydrazine functionality attached through various spacers of varying length and hydrophobicity. The list of synthesized HBPs is shown in Figure 2.1.

All seven HBPs were synthesized from the monosodium alendronate (**8**), which is a widely prescribed drug in the treatment of osteoporosis. Monosodium alendronate was synthesized by one pot synthesis method according to a previously reported procedure (Scheme 2.7) (*81, 107*). The reaction was done in an inert atmosphere, where 4-aminobutanoic acid was treated with phosphorous acid, and phosphorous trichloride in methanesulfonic acid, followed by subsequent hydrolysis. The reaction either starts with nucleophilic addition of the phosphorous of H_3PO_3 to the carbonyl carbon of the 4-aminobutanoic acid, or 4-aminobutanoic acid reacts with PCl_3 and forms an acid chloride and then undergoes nucleophilic addition of H_3PO_3. The carbonyl group gets reformed after the attachment of one phosphonate, and allows a second nucleophilic attack by

H_3PO_3. The hydrolysis of the reaction allows the formation of two phosphonates with one hydroxyl group at the alpha carbon of the product. Methanesulfonic acid was used as a solvent in the reaction, which keeps the reaction mixture in the liquid state and allows the complete conversion of 4-aminobutanoic acid to α-hydroxy-bisphosphonic acid. The pH adjustment at 4.4 with addition of NaOH allows the formation of monosodium salt of the α-hydroxy-bisphosphonic acid. The white solid of monosodium salt of α-hydroxy-bisphosphonic acid was treated with 95% ethanol and filtered to remove the excess starting materials and reagents from the reaction mixture. The resultant white product was dried under vacuum to obtain a pure white powder of monosodium alendronate. The product was recovered with an excellent yield of 87% and characterized with ^{1}H NMR, ^{31}P NMR, ^{13}C NMR, and mass spectrometry.

The synthesis of HBP **1** is outlined in Scheme 2.8. Compound **10** was prepared by dropwise addition of *N*,*N´*-dicyclohexylcarbodiimide (DCC) in chloroform to a mixture of tri-BOC-hydrazinoacetic acid (**9**) and 3,5,6-tetrafluorophenol (TFP) in chloroform at room temperature (RT). Compound **10** is the tetrafluorophenol ester of tri-BOC-hydrazinoacetic acid. The four fluorines attached to phenol increased the electrophilicity of the carbonyl carbon of compound **10**. Therefore, compound **10** became very reactive towards nucleophiles such as amines. Monosodium alendronate was then coupled with compound **10** in the presence of triethylamine (TEA) at RT. Since monosodium alendronate is not soluble in non-aqueous solvents, distilled water was used as a solvent for the amide coupling reaction. TFP is a side product of the amide coupling reaction, which was removed by washing the reaction mixture with diethyl ether. Some of the TEA in the reaction mixture was eliminated with diethyl ether extraction, while the remaining

TEA was removed by *in vacuo* evaporation of the reaction mixture. The product obtained after *in vacuo* evaporation was a sticky solid, which was then dissolved in 2.5 M HCl and kept stirred at RT for 24 h. HCl treatment removed the BOC groups from the hydrazine and formed a chloride salt of HBP **1**. The solvent was removed *in vacuo*, and the crude product was sonicated twice in ethanol at RT for 2 h and filtered to obtain pure HBP **1** (Scheme 2.8).

HBPs **2-7** are synthetic analogues of HBP **1**, in which length and hydrophobicity of the HBPs was varied by introducing various spacers, such as 4-aminobutyric acid (**12a**), 6-aminohexanoic acid (**12b**), 8-aminooctanoic acid (**12c**), glycine (**12d**), glycylglycine (**12e**), and glycylglycylglycine (**12f**), respectively (Scheme 2.9). The spacers **12d**, **12e**, and **12f** are poly-glycines, which are multiple glycines coupled with amide linkages. Poly-glycine spacers are hydrophilic, which were introduced in between alendronate and hydrazinoacetic acid to increase the length and hydrophilicity of HBPs. The spacers **12a**, **12b**, **12c** are aliphatic long chain amino acids, which were introduced in between alendronate and hydrazinoacetic acid to increase the length and hydrophobicity of HBPs. All the spacers are amino acids, having a carboxylate functionality at one end and an amine functionality at the other end. These spacers were coupled with compound **10** in the presence of TEA at RT. The solvent used was CH_3CN because of the solubility of both the starting materials, and its ease of *in vacuo* evaporation. The reaction mixture was washed with diethyl ether and the solvent was removed with *in vacuo* evaporation to obtain compounds **13a-13f**. Compounds **14a-14f** are activated esters, which were prepared by treatment of **13a-13f** with TFP, and DCC in $CHCl_3$. Using similar strategies as those employed in the synthesis of HBP **2**, compounds **14a-14f** were coupled with

monosodium alendronate, followed by the removal of hydrazine protection with the treatment of HCl to obtain HBPs **2-7**. All HBPs were purified by sonication in ethanol and characterized with ^{1}H NMR, ^{31}P NMR, ^{13}C NMR, and elemental analysis. The general scheme of synthesis of HBPs **2-7** is shown in Scheme 2.9.

Other than the method used for the synthesis of HBPs **1-7**, we designed the method for the synthesis of hydrazide-BPs from ester-BPs. In particular, we synthesized several spacers having acid functionality at one terminal and ester functionality at the other terminal. These bifunctional spacers were conjugated to the alendronate (**8**) to obtain several ester-BPs of different length. The structures of the synthesized ester-BPs are shown in Figure 2.2.

The ester-BPs of various length spacers were treated with hydrazine monohydrate to obtain hydrazide-BP (Scheme 2.4). In brief, the five-membered ring of succinic anhydride was opened with 1.1 equivalent of ethanol to obtain monoester (**20**) selectively. The acid functionality of monoester was activated by treatment of TFP and DCC to obtain its tetraflurophenol ester (**21**), which is reactive towards amines at basic conditions. The activated ester was coupled with 4-aminobutanoic acid to get compound **22**. This elongated spacer (**22**) having a carboxylate functionality at one end, was activated by TFP and DCC to obtain its tetraflurophenol ester (compound **23**). Both the spacers (**21** and **23**) were coupled to alendronate with amide coupling to get ester-BPs **17** and **18**. The shortest ester-BP (**16**) was synthesized by treatment of ethyl chloroformate with alendronate. Ethyl chloroformate is highly nucleophilic, and reacts immediately with the amine of alendronate. The ester-BPs (**16**, **17**, and **18**) were obtained in good yield. The ester-BPs were refluxed with hydrazine monohydrates in methanol to obtain

bifunctional hydrazide-BPs according to the previously reported procedure (*108*), however only traces of the desired product were detected.

Using a previously reported procedure, we could not isolate the hydrazide-BPs as a major product, even when the reaction was repeated several times by varying reaction conditions, such as moles of reagent, solvent, temperature, and time of the reaction. In most of the attempted reactions, we could not obtain hydrazide-BP. After the reaction workup, the ^{1}H NMR analysis of the reaction mixture showed the alendronate as a major product. Hydrazine monohydrate, used for conversion of ester to hydrazine, is also an alkali, and has similar properties to ammonia. Therefore, it is highly possible that hydrazine monohydrate hydrolyzed the amide linkage in ester-BP, and decomposed it into smaller molecules like alendronate. In addition, the starting materials of the reaction were only soluble in water or highly polar solvents. The monitoring of the reaction by thin layer chromatography (TLC) was also a difficult task due to the solubility properties of the reactant or the product. It was also challenging to remove the excess of hydrazine monohydrate from the reaction mixture. Overall, due to the reversible nature of the reaction and other difficulties in the synthesis, we did not pursue the synthesis of hydrizide-BPs any further; however, we could synthesized bifunctional ester-BPs with different length spacers.

We also designed aldehyde-BPs considering the reactivity of aldehydes toward hydrazines and amines. Aldehyde reacts with amine at a neutral or basic environment to form an imine. Aldehyde also reacts with hydrazine at acidic conditions to form a hydrazone. Since aldehyde-BPs could be coupled to proteins through imine or hydrazone linkages, we designed a method for synthesis of aldehyde-BPs as shown in Scheme 2.11.

The α-hydroxy-bisphosphonic acid is hydrophilic and difficult to purify; therefore, we designed α-hydroxy-bisphosphonate esters, which are easier to purify and can be hydrolyzed back to bisphosphonic acid. The synthesis was started with various length aliphatic acids, such as 3-butenoic acid, 4-pentenoic acid, 6-heptenoic acid, and 10-undecenoic acid. These acids have a terminal double bond at one end, which could be oxidized to an aldehyde. The synthesis of aldehyde-BPs was performed according to a previously reported procedure (*109*), and is shown in scheme 2.11. In brief, the synthesis was started with formation of pent-4-enoyl chloride **(26)** by refluxing 4-pentenoic acid **(25)** with thionyl chloride in DCM under nitrogen at 80 °C. Since, compound **26** is very reactive and moisture sensitive, it was used in the next reaction without further purification. The triethyl phosphate was added to the crude compound **26**, and the reaction was stirred overnight to obtain compound **27**. The crude product **27** was purified by column chromatography, and then treated with hydrogen diethyl phosphite to obtain BP **28**. The ethylene bond of **28** was oxidized with potassium osmate dihydrate and sodium meta periodate to obtain compound **29**. Compound **29** has an aldehyde at one terminal and ethyl phosphate groups at the other terminal. The last step of hydrolysis of compound **29** for conversion of ethyl phosphate into phosphoric acid was tried in several ways, such as by refluxing in 6M HCl, stirring in concentrated HCl, refluxing in concentrated HCl, as well as treatment with trimethyl silyl bromide and water; however, the isolation of the desired product (compound **30**) was found difficult.

Compound **30** was the desired product of the hydrolysis of compound **29**, which has two phosphoric acid groups at one terminal and an aldehyde at other terminal. The failure of the reaction could be due to the hydrolysis conditions. The aldehyde is a very

reactive species, and even the oxygen in air slowly oxidizes it. Moreover, in the aqueous acidic environment the rate of oxidation of aldehyde is much faster than at a neutral environment. Therefore, it is highly possible that the aqueous acidic environment of hydrolysis oxidized the aldehyde of compound **29**, and might have prevented the formation of compound **30**.

CONCLUSIONS

Overall, we attempted three different methods for synthesis of various bifunctional BPs, such as hydrazide-BP, aldehyde-BP, and hydrazine-BP. The synthesis of hydrazide-BP failed in the last step of synthesis, in which hydrazine monohydrate hydrolyzed the ester-BP into the starting material instead of hydrazide formation. The isolation of the aldehyde-BP failed due to the instability of aldehyde in an acidic environment. However, we have reported the straightforward synthesis of novel, bifunctional HBPs having two phosphonates at one terminal and a hydrazine at the other terminal. The seven derivatives of HBPs (**1-7**), having various spacers of different length and hydrophobicity, were synthesized and characterized by ^{1}H NMR, ^{13}C NMR, ^{31}P NMR, and mass spectrometry. The therapeutic agents with aldehyde or ketone functional groups could be conjugated to the HBPs and immobilized on bone or HA surface to explore further applications.

CHAPTER THREE

ENHANCED AFFINITY BIFUNCTIONAL BISPHOSPHONATES FOR TARGETED DELIVERY OF THERAPEUTIC AGENTS TO BONE

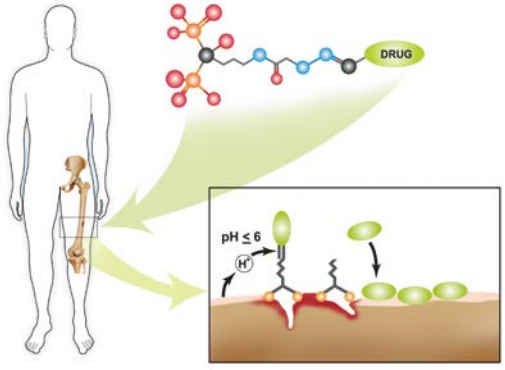

Active targeting of therapeutic agents to bone reduces drug toxicity and improves drug bioavailability at the desired site (*110*). Bone tissue is characterized by constant remodeling, whereby it continuously undergoes formation and resorption; perturbations in bone remodeling are associated with several metabolic bone diseases, such as osteoporosis (*6, 8, 111*). Therefore, molecules that inhibit bone resorption or stimulate bone formation show drug activity against various skeletal disorders (*112*). Although a range of therapeutic agents is available to treat skeletal disorders (*31*), their clinical application is hampered by their uptake in non-targeted sites and the consequent undesired side effects (*11*).

Several bisphosphonates (BPs) show anti-resorptive properties and are being prescribed in the treatment of skeletal diseases (*31-33*). BPs are stable analogues of naturally occurring pyrophosphate and have high affinity to bone and hydroxyapatite

(HA) (*20*). Besides the two phosphonate groups, BPs have two other substituents (R^1 and R^2) on their geminal carbon (Figure 1.2). BPs with a hydroxyl or an amine group at R^1 facilitate tridentate binding to bone and HA, and show an increased affinity to these materials (*98, 99*). The overall nature of the R^2 substituent also contributes toward enhancing the bone-seeking ability and pharmacological properties of BPs (*20, 113*).

Recently, a number of drug targeting and drug delivery strategies have been reported using a range of delivery vehicles, such as polymer scaffolds, liposomes, dendrimers, micelles, hydrogels, peptides, and antibodies (*44, 45, 114-119*). However, drug targeting to bone sites requires molecules that have high affinity to bone. Besides BPs, other molecules, such as D-aspartic acid octapeptide,(*44, 45*) polymalonic acid,(*46*) and tetracycline(*47, 48*) show affinity to bone. BPs have advantage over other molecules because their affinity can be tuned by changing their R^1 and R^2 substituents. Moreover, in addition to being prescribed as drugs, BPs are also being studied for drug targeting, and drug delivery to bone (*49, 89-93*), including the administration of radiopharmaceuticals and imaging agents to bone for diagnostic applications (*50, 94-97*). For the purpose of drug targeting to bone, various strategies of BP-drug conjugation have been investigated by us and others (*16, 49-52*). Ideally, for targeted drug delivery to bone, BP-drug conjugates should have a stable linkage between the BP and drug molecule that can survive during systemic circulation of the conjugate following parenteral administration, and at the same time be labile at the bone surface to release the drug locally. Most of the strategies mentioned above employ agents that are conjugated to BPs through stable, non-cleavable linkages resulting in the administration of the complete conjugate to the treatment site (*49, 50, 89, 94-96*). Current approaches that employ cleavable linkages are

either too labile to ensure delivery of the drug to the desired site (*90*, *91*), or show limited release providing inadequate availability of drug for action (*90*). A strategy that involves labile conjugation to one of the phosphonate groups of BP could compromise the affinity of the corresponding BP-drug conjugate toward bone, because it is through the phosphonate groups that BPs bind to the mineral matrix (*91*).

Herein, we report a novel strategy for targeted delivery of therapeutic agents to sites of low pH, such as bone resorption lacunae and areas of wound healing, through their conjugation to enhanced affinity bifunctional BPs with a pH-triggered cleavable linkage. In particular, we have used seven novel hydrazine-bisphosphonates (HBPs) (**1-7**), which have a hydroxyl group as R^1, while R^2 contains a hydrazine functionality attached through spacers of various length and hydrophobicity (Figure 2.1). Furthermore, experiments were performed to explore the binding affinity, cytotoxicity, drug conjugation, and pH triggered drug release of HBPs.

EXPERIMENTAL SECTION

Materials: The osteoblastic cell line MC3T3-E1 was obtained from American Type Culture Collection (CRL-2593; ATCC, Rockville, MD). Alpha minimum essential medium (αMEM) and fetal bovine serum (FBS) were purchased from GIBCO-Invitrogen (Carlsbad, CA). The BCA protein assay kit was obtained from ThermoFisher Scientific (Rockford, IL). The cell proliferation reagent WST-1 was purchased from Roche (Mannheim, Germany). Ac-DEVD-AFC was obtained from Enzo Life Sciences (Plymouth Meeting, PA). 4-Aminobutanoic acid and 2,3,5,6-tetrafluorophenol (TFP)

were purchased from Alfa Aesar (Ward Hill, MA). *N,N′*-Dicyclohexylcarbodiimide (DCC), triethylamine (TEA), tri-BOC-hydrazinoacetic acid (TBHA), reagent grade hydroxyapatite powder, potassium hydroxide, sodium acetate, sodium chloride, sodium hydroxide, etoposide, tris(hydroxymethyl)aminomethane hydrochloride (Tris-HCl), 4-(2-hydroxyethyl)piperazine-1-ethanesulfonic acid (HEPES), 3-[(3-cholamidopropyl)dimethylamino]-1-propanesulfonate (CHAPS), ethylenediaminetetraacetic acid disodium salt dehydrate (EDTA), sodium fluoride (NaF), sodium orthovanadate, leupeptin hemisulfate salt, aprotinin bovine, phenylmethylsulfonylfluoride, DL-dithiothreitol (DTT), glycerol, and triton X-100 were purchased from Sigma-Aldrich (St. Louis, MO). Calcium chloride, hydrochloric acid, and potassium dihydrogen phosphate were obtained from EMD Chemicals (Gibbstown, NJ). Acetonitrile, chloroform, dichloromethane (DCM), diethyl ether, dimethyl sulfoxide (DMSO), hexane, and phosphoric acid were purchased from Mallinckrodt (Hazelwood, MO). The NMR solvents deuterium oxide and deuterated chloroform were purchased from Cambridge Isotope Laboratories (Andover, MA).

Apparatus: ^{1}H NMR, ^{31}P NMR, and ^{13}C NMR spectra were obtained on a Varian INOVA 400 MHz spectrometer (Palo Alto, CA). HA crystal growth experiments were performed using an Isotemp Refrigerated Circulator and pH meter (Fisher Scientific, Pittsburgh, PA). UV-vis spectra were obtained with an Agilent 8453 UV-visible spectrophotometer (Agilent Technologies, Santa Clara, CA). Deionized water was produced using a Milli-Q water purification system (Millipore, Bedford, MA).

Crystal Growth Inhibition Assay for Binding Affinity Study. As BPs target bone surfaces under active formation and resorption of HA (*120*), a crystal growth inhibition assay was performed to measure the affinities of HBPs to HA. This method has commonly been used to examine BP binding affinity.(*24, 121*) Kinetic experiments of HA crystal growth were performed in a nitrogen atmosphere in magnetically stirred (400 rpm) double-jacketed vessels at pH 7.4 and 37.0 ± 0.1 °C, as described in a previously reported procedure (*24, 121*). In brief, the reaction solution with final ionic strength of 0.15 M was prepared by mixing calcium chloride (2.0 mmol), potassium dihydrogen phosphate (2.0 mmol) and sodium chloride (132.0 mmol) followed by degassing and filtration. The titrant with final ionic strength of 0.15 M was prepared by mixing calcium chloride (2.0 mmol), potassium hydroxide (10.0 mmol) and sodium chloride (134.0 mmol) followed by degassing and filtration. The reaction was initiated by adding 5 mg seed mass of HA crystallites into 100 mL of reaction solution. The constant thermodynamic driving force for growth of HA crystal was maintained by keeping the pH constant at 7.4 with addition of titrant. The volume of titrant added was recorded as a measure of HA crystal growth. Crystal growth inhibition experiments were performed in presence of at least six different concentration of each of HBPs (**1-7**). For a positive control, experiments were performed in presence of six different concentration of alendronate (**8**), whereas for a negative control, experiments were performed in absence of any BP.

Cell Culture. The MC3T3-E1 cells were cultured in pre-warmed αMEM medium that was supplemented with 10% FBS at 37 °C in a humidified atmosphere composed of

5% CO_2. The cells were seeded into 96-well plates at a density of 1×10^4 cells/well for *in vitro* quantification of intracellular protein and caspase activity. One day after seeding, the cultures were treated with various concentrations (10^{-6}, 10^{-5}, 10^{-4} M) of HBPs. Cells without HBPs were used as a negative control, while cells treated with 10^{-6}, 10^{-5}, or 10^{-4} M of etoposide were used as positive controls. The plates were incubated again for 24, 48, 72 h before use for further analysis. The experiments were conducted in triplicate and repeated at least three times to ascertain the reproducibility of the results.

Intracellular Protein Quantification. Intracellular protein was measured using a commercially available BCA assay kit. Briefly, the medium was removed, and the adherent cells were washed with PBS. The cultures were lysed by 10-min incubation in 50 µL of lysate buffer (20 mM Tris-HCl, pH 7.4, 150 mM NaCl, 1mM EDTA, 10mM NaF, 1mM sodium orthovanadate, 5 µg/ml leupeptin, 0.14 U/ml aprotinin, 1mM phenylmethylsulfonylfluoride, and 1% (v/v) Triton X-100), followed by 2 s of sonication. Volumes of 10 µL of the cell lysate samples and standards (solutions of known concentrations of bovine serum albumin) were added to the wells of a 96-well microtiter plate followed by addition of 200 µL of the working reagent; the well contents were mixed thoroughly by shaking the plate for 2 min. The plate was incubated at 37 °C for 30 min and then cooled to RT. The absorbance of the samples was measured at 562 nm on a plate reader. The amount of protein in the sample was calculated using a standard plot.

Cell Cytotoxicity Assay. The cytotoxicity of the HBPs was determined using a colorimetric WST-1 assay. The assay was conducted after 72 h of HBP treatment in

accordance with the manufacturer's instructions. In brief, cultures in 96-well plates were incubated with 10 µL/well of cell proliferation reagent WST-1 at 37 °C for 60 min in a humidified atmosphere composed of 5% CO_2. The plate was cooled to RT, and the absorbance of the samples was measured at 450 nm on a plate reader.

Apoptosis Assay. Apoptosis was determined by measuring the intracellular caspase-3 activity. The cultures were lysed by 10 min of incubation in 50 µL of lysate buffer (20 mM Tris-HCl, pH 7.4, 150 mM NaCl, 1mM EDTA, 10mM NaF, 1mM sodium orthovanadate, 5 µg/ml leupeptin, 0.14 U/ml aprotinin, 1mM phenylmethylsulfonylfluoride, and 1% (v/v)Triton X-100), followed by 2 s of sonication. The cell lysate was treated with 50 µM Ac-DEVD-AFC in 50 mM HEPES buffer (pH 7.4, 100 mM NaCl, 0.1% CHAPS, 10 mM DTT, 1mM EDTA, and 10% (v/v) glycerol) at RT for 60 min in the dark. The caspase-3 activity was determined by measuring the fluorescence at λ_{em}=510 nm (λ_{ex}=485).

Synthesis of Compound 32. Compound **1** (10.0 mg, 0.028 mmol) was suspended in 10 mL of distilled water. The reaction mixture was acidified with 10 µL of acetic acid. 4-Nitro benzaldehyde (**31**) (8.4 mg, 0.056 mmol) was dissolved in DMSO and added to the above suspension. The reaction was stirred at RT for 48 h. The solvent was evaporated *in vacuo* to obtain crude product **32**. Compound **32** was dissolved in water and washed with ethyl acetate to remove excess reactant **31**. The water layer containing **32** was used in the next reaction without further purification.

Scheme 3.1. Synthesis, immobilization of model drug-BP conjugate, and incubation at 37 °C in acetate solutions of various pH. Hatched area represents HA particles.

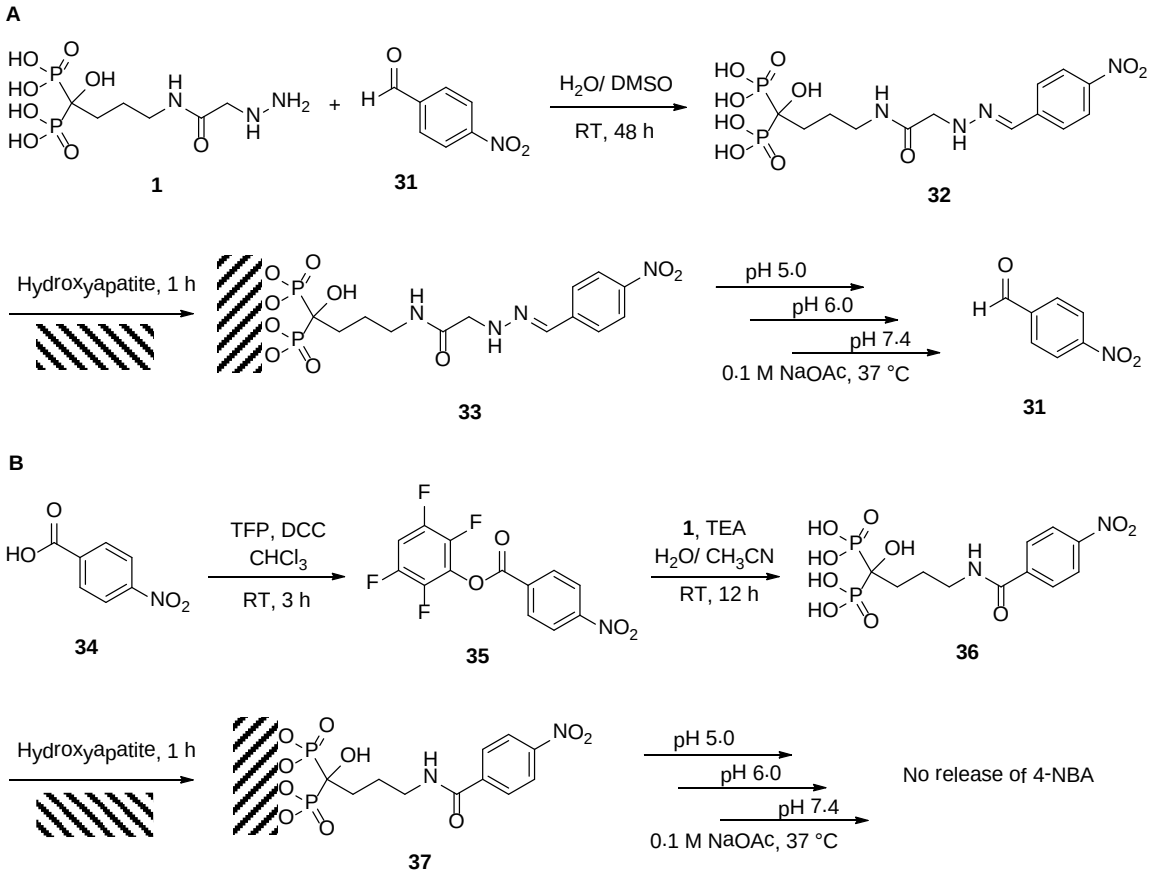

Synthesis of Compound 35. 4-Nitro benzoic acid (**34**) (100.0 mg, 0.598 mmol) and TFP (109.3 mg, 0.658 mmol) were dissolved in 5 mL acetone. DCC (135.8 mg, 0.658 mmol) in 5 mL acetone was added drop-wise to the reaction mixture and stirred at RT. The progress of the reaction was followed by TLC. After complete consumption of **34** (3 h), the 1,3-dicyclohexyl urea formed in the reaction mixture was removed by filtration, and the filtrate was evaporated *in vacuo*. The residue was then suspended in an adequate amount of acetonitrile, the remaining 1,3-dicyclohexyl urea was removed by filtration, and the filtrate was evaporated *in vacuo* to obtain crude compound **35**. Compound **35** was used in the next reaction without further purification.

Synthesis of Compound 36. Compound **8** (60.0 mg, 0.185 mmol) was suspended in 1 mL of distilled water and TEA (111.9 mg, 1.108 mmol) was added to the suspension. After a few seconds of stirring at RT, the suspension became clear. The reaction was stirred at RT for 5 min. Crude compound **35** (92.2 mg, 0.277 mmol) was dissolved in 1.5 mL of acetonitrile and added to the reaction mixture. TEA (18.7 mg, 0.185 mmol) was added, and the reaction mixture was stirred at RT for 12 h. The reaction mixture was washed with 10 mL diethyl ether several times and the water layer was lyophilized to obtain a sticky solid. The reaction product was then sonicated twice in ethanol for 2 h at RT and filtered to obtain pure compound **36**. ^{1}H NMR (D_2O): δ 8.33 (d, 2H), δ 7.95 (d, 2H), δ 3.45 (t, 2H), δ 1.98 (m, 4H). ^{31}P NMR (H_3PO_4/D_2O): δ 18.23. MS (- ESI) : 397 $[M-H]^-$.

***In vitro* Studies of Drug Targeting and Drug Release.** Compound **32** is a HBP-drug conjugate, where a model drug (4-NBA) was conjugated to HBP **2** via hydrazone linkage. The conjugate was immobilized on HA surface and studied for its release at various pH solutions. In brief, compound **32** (1 mg) in water was equally distributed into three Eppendorf tubes and diluted to get 1.0 mL of total volume each. Excess of HA (50.0 mg) was added to each Eppendorf tube, and the tubes were stirred at RT for 0.5 h. After centrifugation at 1000 rpm for 5 min, the supernatant was discarded. The HA was washed twice with 1.0 mL water, followed by centrifugation, and the supernatant was discarded. A volume of 1.0 mL acetate solution (0.1 M sodium acetate, 0.05 M sodium chloride) of pH 5.0, 6.0, and 7.4 was added in three Eppendorf tubes, respectively. The Eppendorf tubes were incubated at 37 °C with continuous shaking. The suspensions were centrifuged at particular time points, and the absorbance of the supernatants was measured (λ = 265 nm, 1-cm cuvette) to calculate the amount of 4-NBA released from the immobilized conjugate.

For the control studies, the above experiment was repeated with compound **36**. Compound **36** was a BP-drug conjugate, where the model drug (4-NBA) was conjugated to alendronate via amide linkage. The conjugate was immobilized on the HA surface and studied for its release at various pH solutions. In brief, compound **36** (1 mg) in water was equally distributed into three Eppendorf tubes and diluted to get 1.0 mL of total volume each. Excess of HA (50.0 mg) was added to each Eppendorf tube, and the tubes were stirred at RT for 0.5 h. After centrifugation at 1000 rpm for 5 min, the supernatant was discarded. The HA was washed twice with 1 mL water, followed by centrifugation, and the supernatant was discarded. A volume of 1.0 mL acetate solution (0.1 M sodium

acetate, 0.05 M sodium chloride) of pH 5.0, 6.0, and 7.4 was added in three Eppendorf tubes, respectively. The Eppendorf tubes were incubated at 37 °C with continuous shaking. The suspensions were centrifuged at particular time points, and the absorbance of the supernatants was measured (λ = 265 nm, 1-cm cuvette) to calculate the amount of 4-NBA released from the immobilized conjugate.

RESULTS AND DISCUSSION

Over the last two decades, several BPs have been widely used in clinical setting for the treatment of various bone diseases. After administration of BPs, they bind to bone surfaces where they are internalized into osteoclasts and cause their apoptosis (*36, 41, 122*). In other words, BPs control the bone resorption by executing osteoclasts. However, this could be a drawback of the BP treatment because it disturbs the bone remodeling cycle. In general, bone remodeling is the life-long process, where osteoblasts and osteoclasts work simultaneously for bone formation and bone resorption, respectively. Bone formation and bone resorption are interdependent processes and therefore, osteoblastic function of bone formation is also gets affected by controlling osteoclastic bone resorption. Along with controlling bone resorption, subsequent bone formation at resorption sites is crucial; this can be achieved by delivering therapeutic agents to bone resorption sites using bisphosphonates. Active drug targeting at sites of bone metastases and calcified neoplasms using polymeric carrier was reported previously. Alendronate and an anti-angiogenic agent, TNP-470, were conjugated to N-(2-hydroxypropyl)methacrylamide (HPMA) through a cathepsin K sensitive tetrapeptide

(Gly-Gly-Pro-Nle) (*36, 123*). Because of alendronate conjugation, HPMA was found to be distributed to bone tumors and the endothelial compartments of bone metastases with a good antitumor efficacy. However, one could eliminate the polymeric carrier and make a simpler and smaller conjugate by coupling drugs directly to high affinity BPs via hydrolyzable bonds. Therefore, we used HBPs (**1-7**), whose synthesis have been described in Chapter Two, for demonstration of delivery of drug molecules, including bone growth factors, at bone resorption sites.

HBPs have two phosphonates at one terminal and a hydrazine at other terminal. In general, hydrazine reacts with aldehyde at lower pH at which aliphatic amines are not reactive. Therefore, a selective reaction of HBPs with an aldehyde-containing drug molecule could be possible to obtain a HBP-drug conjugate. However for the targeted drug delivery at bone, it is important that the HBP-drug conjugate should not only be stable during systemic circulation, but also bind to the bone surface before releasing the drug at the desired site. The attached drug may sterically affect this interaction between the BP and the bone surface. Therefore, HBPs (**1-7**) with several spacers of varying length and hydrophobicity were designed for this type of the drug delivery application.

In general, BPs have high affinity to bone mineral. Moreover, after administration of BPs, they tend to target bone over other parts of the body. However, not all BPs have the same binding affinity, which varies with their structural characteristics. The two phosphonates are the most important because of their mineral affinity, but the mineral affinities of BPs change with their other two substituents (R^1 and R^2). Specifically, BPs having hydroxyl or amine group at their R^1 substituent show increased affinity to bone. Similarly, the R^2 substituent might affect the bone affinity of BPs. Therefore, the binding

affinities of the HBPs were measured and compared with alendronate, which is a commercially available BP having high affinity to HA. BPs are known to inhibit the crystal growth of HA and target bone surfaces under active formation and resorption of HA (*120*). Therefore, a crystal growth inhibition assay, which is a widely used method for determination of binding affinity of BP,(*24, 121*) was performed to measure the affinities of HBPs to HA. During the experiments, a favorable environment for crystal growth of HA was maintained. The crystal growth of HA was measured in presence of various concentration HBPs. The pH was maintained at 7.4 by addition of titrant, and the volume of titrant added was recorded as a measure of HA crystal growth. A range of experiments were performed in presence of various concentrations of HBPs and alendronate. For every experiment of HA crystal growth, a plot of the volume of titrant added vs time was generated. A typical set of plots is depicted in Figure 3.1. The growth rate (*R*) at any instant can be described by

$$R = \beta \frac{\mathrm{d}V}{\mathrm{dt}} \qquad \text{(S1)}$$

where d*V*/dt is the rate of titrant addition, and β is a constant whose value reflects the titrant concentration with respect to the surface area of HA during crystal formation; β was considered as constant for all experiments.

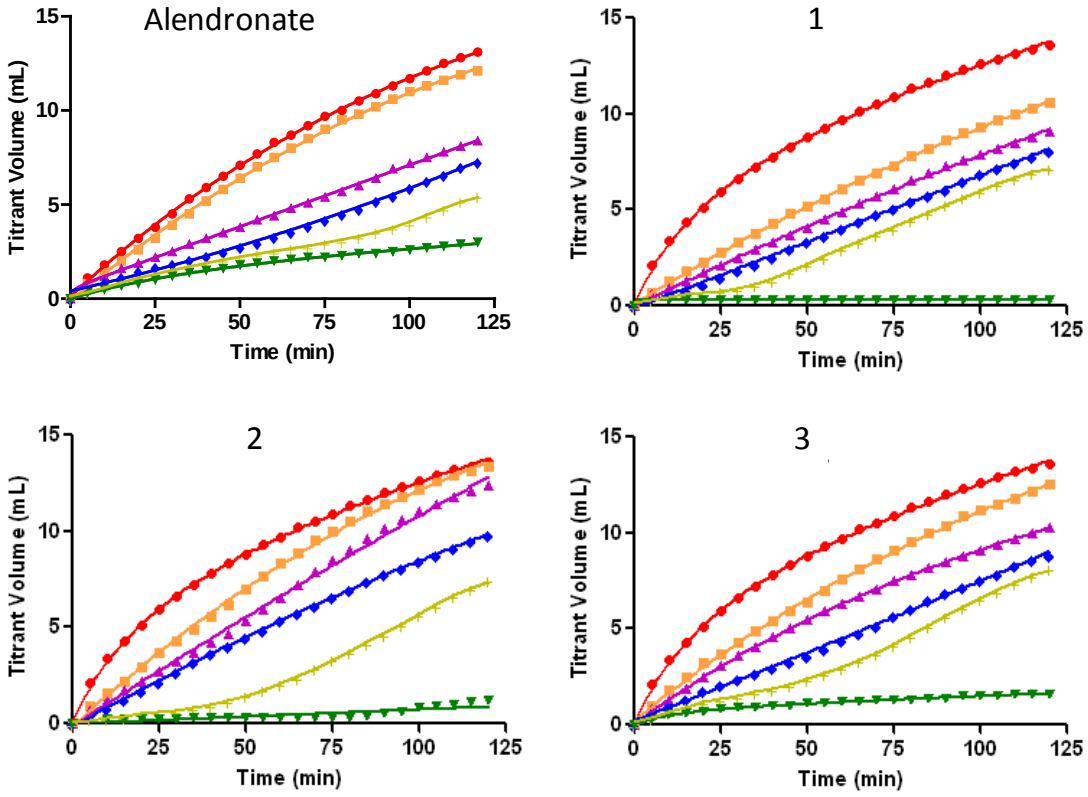

Figure 3.1. Plots of HA crystal growth in presence of varying concentrations of alendronate and HBPs (**1-3**) at pH 7.4 and 37 °C (seed mass = 5 mg); ●, ■, ▲, ♦, +, ▼ represent the concentrations of HBPs, 0, 1.0×10^{-7}, 2.5×10^{-7}, 5.0×10^{-7}, 7.5×10^{-7}, and 10×10^{-7} M, respectively.

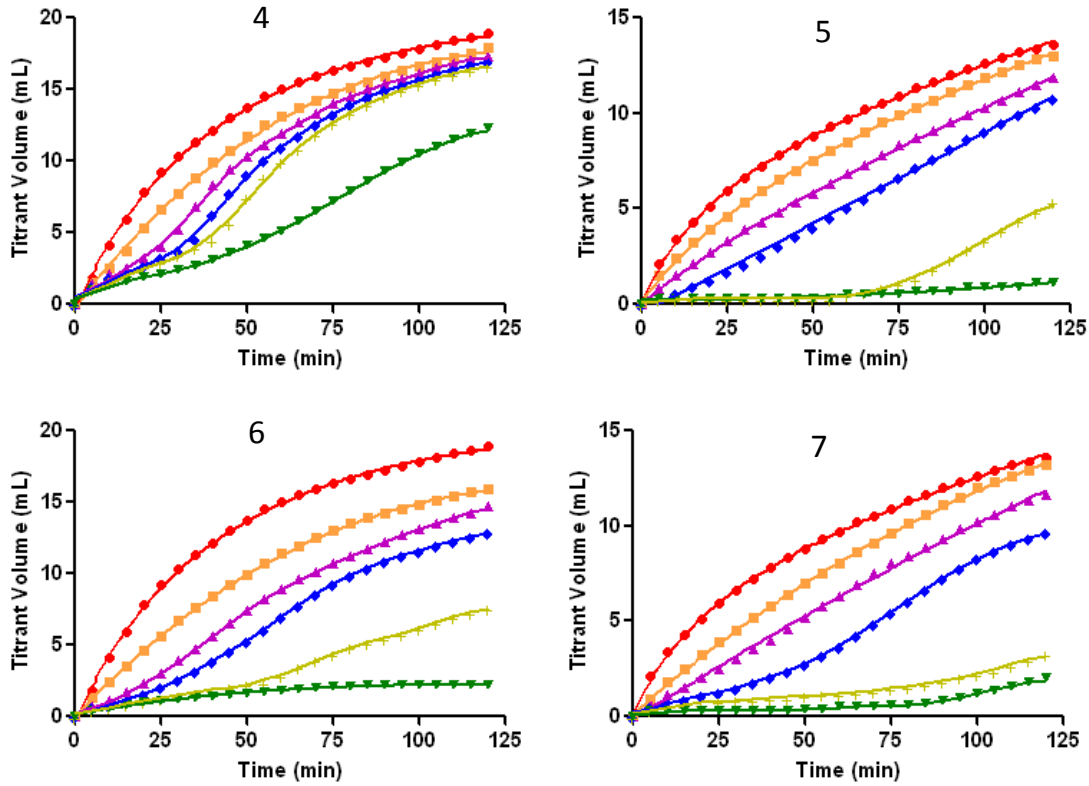

Figure 3.2. Plots of HA crystal growth in presence of varying concentrations of HBPs (**4-7**) at pH 7.4 and 37 °C (seed mass = 5 mg); ●, ■, ▲, ♦, +, ▼ represent the concentrations of HBPs, 0, 1.0×10^{-7}, 2.5×10^{-7}, 5.0×10^{-7}, 7.5×10^{-7}, and 10×10^{-7} M, respectively.

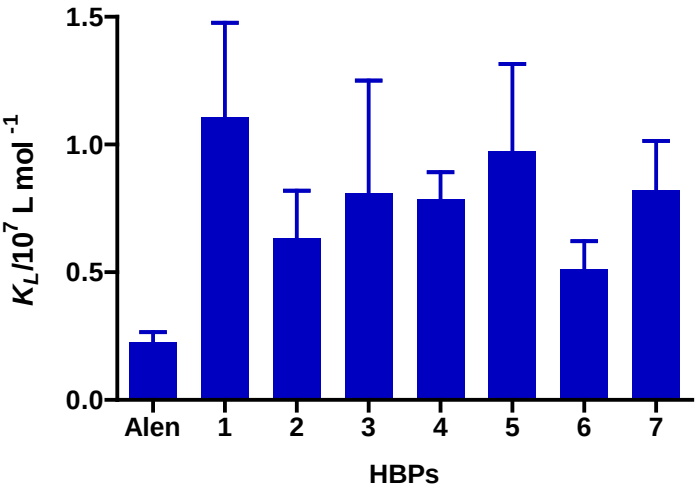

Figure 3.3. Relative adsorption affinity constants (K_L) of alendronate (**Alen**) and HBPs **1-7** measured at varying concentrations of BPs (C=1.0 × 10^{-7}, 2.5 × 10^{-7}, 5.0 × 10^{-7}, and 7.5 × 10^{-7} M) at pH 7.4 and 37 °C. Data are the average ± one standard deviation (n = 4).

It can be noted from Figure 3.1 and 3.2 that the HA crystals appear to grow non-linearly during the early stage of the experiment due to initial seeding of the HA crystals. The flat line parallel to the X-axis indicates the complete prevention of crystal growth. A pseudo-Langmuir adsorption isotherm can be used to describe the rates of HA crystal growth and can be expressed by

$$\frac{R_0}{R_0 - R_i} = 1 + \frac{1}{K_L C} \qquad \text{(S2)}$$

where C is the concentration of BP added, and R_0 and R_i are the rates of HA crystal growth in the absence and presence of BP, respectively.

By rearranging equations S1 and S2, the relative adsorption affinity constants (K_L) can be described by

$$K_L = \frac{\frac{dV_0}{dt} - \frac{dV_i}{dt}}{C\,\frac{dV_i}{dt}} \qquad \text{(S3)}$$

where dV_0/dt and dV_i/dt are the rates of titrant addition at early stage of the experiment in the absence and presence of BP, respectively.

The relative trend of binding affinities of alendronate (1) and HBPs (**1**-7) at various concentrations of BPs is shown in Figure 3.3. The shorter length HBPs (2 and 3) showed significantly higher binding affinities than alendronate ($p<0.05$). Overall, all seven HBPs showed high binding affinities to HA, which makes them suitable for drug targeting.

Apart from its targeting ability, the ideal drug-carrier should not induce unnecessary toxic effects, especially against bone-forming cells (osteoblasts). HBPs could also have toxic affects towards other cells and tissues or affect cell differentiation, which could cause substantial morbidity (*124*). The primary purpose of this study was to

demonstrate the potential of HBPs for targeted delivery of the attached drugs at bone-resorption sites through *in vitro* experiments. Therefore, HBPs at various concentrations (10^{-6} - 10^{-4} M) were evaluated for their possible cytotoxicity and apoptotic effect against pre-osteoblasts. The intracellular protein measured after 24, 48, and 72 h treatment of HBPs, showed no abnormal changes in cell proliferation (Figure 3.4). The amount of protein in the HBP-treated cells was similar to the control over the period of 72 h. Cell viability studies were performed and metabolic activity was quantified using the commercially available WST-1 kit. MC3T3-E1 cells exposed to HBPs for 72 h showed activity similar to that of control (Figure 3.5). Although, the metabolic activity of cells exposed to 10^{-4} M HBPs for 72 h showed 10% decrease in cell viability, the difference was not statistically significant.

Because caspases are required for cell apoptosis, the possibility of HBP-induced cell apoptosis was evaluated by measuring caspase-3 activity. Caspase-3 is a cysteine-aspartic acid protease and cleaves Ac-DEVD-AFC releasing the fluorogenic AFC, which can be quantified by fluorescence spectroscopy (*125*). Apoptosis of MC3T3-E1 pre-osteoblasts was confirmed by treatment with 10^{-6}, 10^{-5}, or 10^{-4} M etoposide for 72 h, which resulted in 2-3 fold increase in caspase-3 activity (results not shown). As shown in Figure 3.5, however, HBPs did not induce apoptosis in MC3T3-E1 pre-osteoblasts after 72 h of exposure; all treatments resulted in statistically similar levels of caspase activity. Because HBPs showed no apoptotic and cytotoxic effects on pre-osteoblasts, HBPs could be utilized as a vehicle for drug delivery applications.

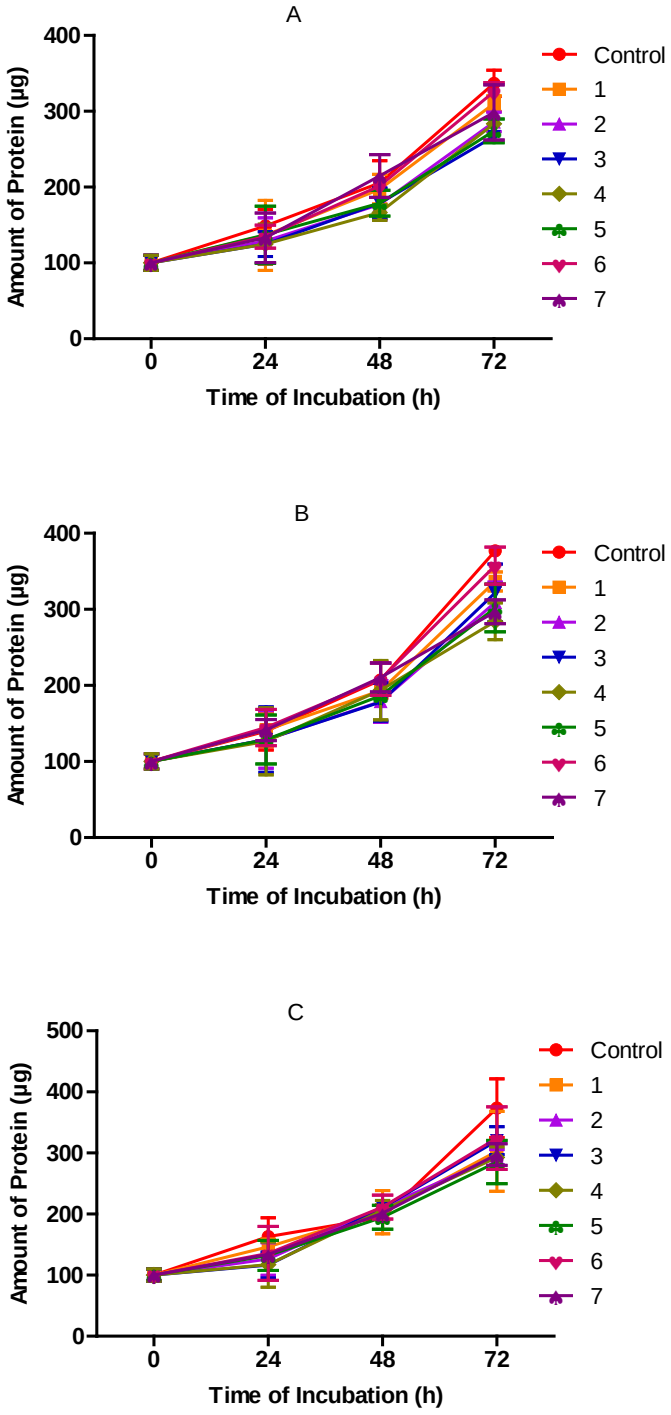

Figure 3.4. Intracellular protein contents showing MC3T3-E1 cell growth for 72 h after HBP treatment. Plots A, B, and C show results for exposure to HBPs at 1×10^{-6}, 1×10^{-5}, and 1×10^{-4} M, respectively. Error bars denote standard deviations.

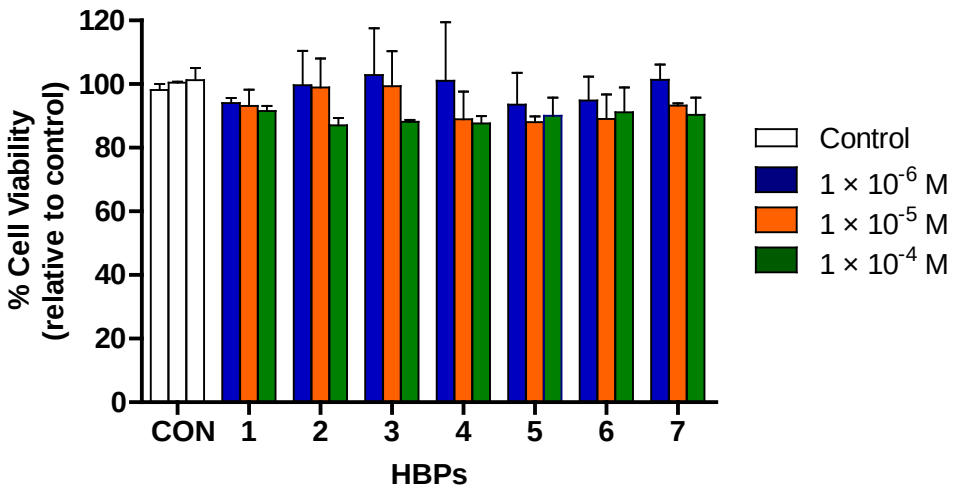

Figure 3.5. MC3T3-E1 cell viability measured after 72 h of incubation with no HBP (CON) and HBPs **1-7** at different concentrations (1×10^{-6}, 1×10^{-5}, and 1×10^{-4} M). The data are expressed as percentage of the control. The white, blue, orange, and green bars represent treatment of no HBP (control), 1×10^{-6}, 1×10^{-5}, and 1×10^{-4} M HBPs, respectively. Error bars denote standard deviations.

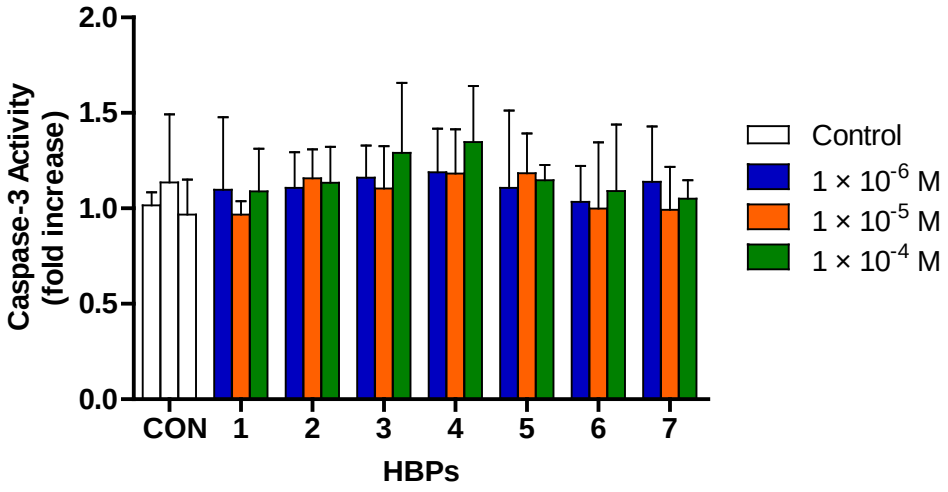

Figure 3.6. Apoptosis of MC3T3-E1 cells measured 72 h following addition of no HBP (CON) and HBPs **1-7** at three different concentrations (1×10^{-6}, 1×10^{-5}, and 1×10^{-4} M). The data are expressed as percentage of the control. The white, blue, orange, and green bars represent treatment of no HBP (control), 1×10^{-6}, 1×10^{-5}, and 1×10^{-4} M HBPs, respectively. Error bars denote standard deviations.

HBP **1** was used to demonstrate the targeted delivery of therapeutic agents to bone. In particular, *in vitro* drug targeting to HA and drug release from the HA surface was demonstrated using 4-NBA as a model drug. 4-NBA was conjugated with HBP **1** in DMSO/water, and then the conjugate was immobilized on HA by adding excess of HA particles to the reaction mixture at RT. HA with the attached conjugate was separated by centrifugation and washed thoroughly with water to remove unconjugated 4-NBA (Scheme 3.1). The triggered release of 4-NBA from the immobilized 4-NBA-HBP conjugate on HA was demonstrated at various pH as shown in Figure 3.7. HA with the attached conjugate was resuspended in 0.1 M sodium acetate (pH 5.0, 6.0 or 7.4) and incubated at 37 °C. The suspensions were centrifuged at particular time points, and the absorbance of the supernatants was measured at 265 nm using a UV-vis spectrophotometer to calculate the amount of released 4-NBA. It was observed that in the first 12 h of incubation, there was approximately 60%, 30% and 20% of 4-NBA released from the immobilized conjugate at pH 5.0, 6.0, and 7.4, respectively.

To confirm that release of 4-NBA occurs via hydrazone cleavage rather than through desorption of the conjugate from the HA surface, 4-NBA was conjugated to alendronate (**8**) through formation of an amide bond. The conjugate was immobilized on HA surface by adding excess of HA particles, and then the particles were washed thoroughly with water to remove unconjugated 4-NBA and non-specifically adsorbed conjugate molecules. HA with the attached conjugate was treated similarly as described above, and the amount of released 4-NBA was measured by UV-vis spectroscopy (Scheme 3.1). From the control experiments, it was observed that there was no significant release of 4-NBA through desorption from the immobilized conjugate **37** (Figure 3.7).

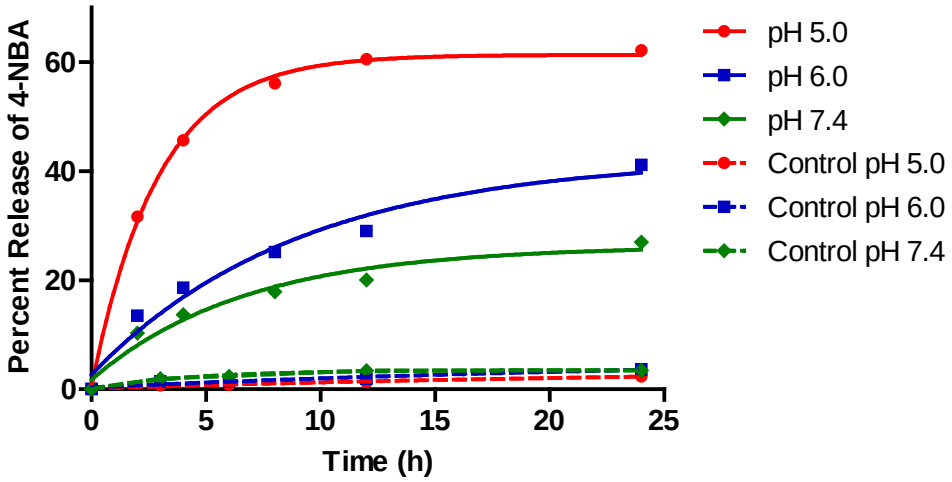

Figure 3.7. Percent release of 4-NBA (percentage of cleaved hydrazone bonds) from the immobilized conjugate on HA surface at 37 °C. Solid line and dotted line represent 4-NBA release from **33** and **37**, respectively.

CONCLUSIONS

In conclusion, we have reported the use of bifunctional HBPs (**1-7**) for targeted delivery of therapeutic agents to bone. Through the HA crystal growth inhibition assays, some of the HBPs showed significantly higher binding affinities to HA than alendronate. Through *in vitro* experiments, HBPs demonstrated no apoptotic and cytotoxic effects on MC3T3-E1, a pre-osteoblast cell. 4-NBA, a model drug, was bound to HA through a HBP, and its *in vitro* release at various pH was recorded. It was observed that hydrolysis of hydrazone bonds in the conjugate and subsequent release of 4-NBA was slow at physiological pH, but much faster at pH lower than physiological, such as the pH in bone resorption sites and sites of wound healing (*101, 102*). Consequently, HBP-drug conjugates could be useful in locally delivering attached drugs to the resorptive microenvironment of bone tissue. Overall, this approach should improve the therapeutic index by boosting pharmacological efficacy and diminishing undesirable side effects.

CHAPTER FOUR

ORIENTED IMMOBILIZATION OF PROTEINS ON HYDROXYAPATITE SURFACE USING BIFUNCTIONAL BISPHOSPHONATES AS LINKERS

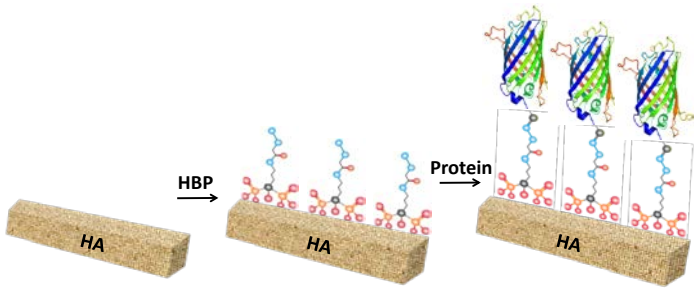

Approaches to immobilize proteins are widely investigated because of their diverse applications in various fields such as protein microarrays, biosensors, biotechnology, chemical manufacturing, nanotechnology, single molecule enzymology, and drug discovery (*126*). Oriented immobilization methods that maintain the native structure and proper orientation of the target protein are desirable because through oriented immobilization the proteins can be predisposed in a manner that is optimal for binding to their respective ligands. Proteins have been immobilized on surfaces via three different approaches: physical adsorption, bioaffinity binding, and covalent bonding. Physical adsorption is the most straightforward type of immobilization in which proteins are adsorbed on the surface with weak non-covalent interactions. Conversely, because of the random and weak nature of the attachment, proteins may lose their activity as a result of blocking of the active site or leaching from the surface after immobilization (*74*). Bioaffinity immobilization of proteins is mainly based on the specific interaction between

two biomolecules, such as enzymes binding to surfaces modified with their corresponding substrates, cofactors, or inhibitors. The use of bioaffinity for immobilization may result in blockage of the active site of the protein and reduction of its activity. In addition, bioaffinity is usually a reversible interaction under specific conditions, and therefore it may lead to reversible immobilization (*127, 128*). Covalent immobilization yields proteins bound to a solid surface through a strong covalent linkage. Functional groups, such as amines, carboxylates, thiols or hydroxyls, in the side chain of exposed amino acids in the protein have been used in the formation of irreversible linkages with surfaces (*74*). Since multiple copies of the same functional group usually exist on the protein's surface, covalent immobilization is usually not selective. Oriented immobilization is achieved only when the protein contains just one copy of the reactive functional group, which is usually realized through selective chemical reactions or by protein engineering (*75*). Several methods, such as Staudinger ligation, thiol-ene reaction, thiazolidine ring formation, cycloaddition, and Diels-Alder product formation, have been explored for oriented immobilization of proteins and small molecules for various applications (*75, 76, 129*). However, they have not been adequately explored for bone implant applications.

A host of materials, such as titanium, stainless steel, cobalt-based alloys, and HA, have been explored as bone implant materials (*62*). Naturally occurring HA has similar composition to bone mineral and, therefore, it has been widely used for orthopedic implants as well as an implant coating material. The interface between implants and the body plays a crucial role in determining success or failure of the prosthesis. Stability of the bone-to-implant interface can be improved chemically by incorporating organic

material and physically by optimizing the surface topography of implants (*64-66*). Covering the implant surface with biomolecule is one of the most effective ways of stimulating specific cell and tissue response at the bone-implant interface (*67-69*). Moreover, oriented immobilization of therapeutic biomolecules on HA could provide additional benefits to implants, such as faster osseointegration, prevention of infection, etc. Herein, a novel, versatile approach of oriented immobilization of proteins is described, by employing rationally designed bifunctional bisphosphonates.

Bisphosphonates (BPs) are chemical analogues of endogenous pyrophosphate and have been investigated for protein immobilization applications on natural and artificial biomaterials, such as bone and HA (*51, 130-132*). BPs are bone-seeking molecules, having high affinity to bone and HA. They are organic molecules with, typically, two substituents (R^1 and R^2) in their structure, along with two phosphonate groups attached to their geminal carbon. Various BP analogues and their conjugates have been utilized in treatment of skeletal diseases, such as osteoporosis, bone metastasis, and hypercalcemia (*33, 133*). Further, BPs have been used to administer radiopharmaceuticals and imaging agents for diagnostic purposes (*94*). Studies have also focused on determining the affinity to bone and HA of BPs conjugated with protein (*130-132*). However, to date, BPs have not been conjugated site-selectively to proteins. In the aforementioned studies, BPs were attached non-specifically to multiple sites of proteins, which led to random orientation of proteins on the surface (*51*). In this study, our objective was to demonstrate that bifunctional BPs could facilitate the oriented immobilization of proteins on HA. Toward this goal, we used seven bifunctional HBPs, with various length and lipophilicity, as linkers between the protein and the HA surface. All seven HBPs, whose synthesis have

been described in Chapter Two, were demonstrated to have high affinity towards HA surface (described in Chapter Three) (*134*). EGFP with an N-terminal serine and *β*-lactamase with an N-terminal threonine were used as model proteins to demonstrate their site-specific immobilization on the HA surface. Specifically, both proteins were oxidized selectively to obtain an N-terminal aldehyde and immobilized on the HA surface through HBPs. The overall purpose of the present studies was to investigate the feasibility of oriented immobilization of protein on HA through HBPs and to evaluate the bioactivity of HBP-immobilized protein. Such biomaterials should find application in bone regeneration and targeted protein delivery therapies.

EXPERIMENTAL SECTION

Materials. Reagent grade HA powder, 4-(2-hydroxyethyl)piperazine-1-ethanesulfonic acid sodium salt (HEPES), tris(hydroxymethyl)aminoethane hydrochloride (Tris-HCl), ampicillin, isopropyl-1-*β*-D-thiol-1-galactopyranoside (IPTG), ethylenediaminetetraacetic acid (EDTA), 2,4,6-trinitrobenzenesulfonic acid (TNBS), sodium borate decahydrate, potassium hydroxide, sodium acetate, sodium chloride, sodium hydroxide, sodium periodate, ethylene glycol, agarose, *β*-lactamase from *Enterobacter cloacae*, Luria Bertani (LB) broth were purchased from Sigma-Aldrich (St. Louis, MO). Calcium chloride, hydrochloric acid, potassium dihydrogen phosphate, and sodium phosphate were obtained from EMD Chemicals (Gibbstown, NJ). The pEGFP vector was obtained from Clontech Laboratories (Mountain View, CA). The pTWIN1 vector and all restriction endonucleases were obtained from New England BioLabs

(Ipswich, MA). Oligonucleotide primers used in PCR were custom-synthesized by Integrated DNA Technologies (Coralville, IA). The BCA assay kit was purchased from Pierce Chemical (Rockford, IL). All solutions and buffers were prepared using deionized water, which was produced using a Milli-Q water purification system (Millipore, Bedford, MA). All chemicals were reagent grade or better.

Apparatus. All UV-vis spectroscopy experiments were performed with an Agilent 8453 UV-visible spectrophotometer (Agilent Technologies, Santa Clara, CA). All UV-vis spectroscopy readings are background-subtracted. Fluorescence measurements were performed on a Cary Eclipse fluorescence spectrophotometer (Varian, Walnut Creek, CA). Polymerase chain reactions (PCR) were performed in a Perkin-Elmer GeneAmp PCR system 2400 (Norwalk, CT). Cell lysates were centrifuged using an Avanti J-25I centrifuge (Beckman Coulter, Brea, CA). HA samples were centrifuged using centrifuge-5417R (Eppendorf, Wesseling-Berzdorf, Germany).

Substrate and Linkers Used for Protein Immobilization. Reagent grade HA powder was used as solid support for immobilization experiments. Slurries of HA in various buffers were used without any pretreatment for protein immobilization. Seven HBPs (**1**-**7**) of various length and lipophilicity, whose synthesis have been described in Chapter Two (*134*), were used as linkers between the HA and the protein for immobilization of proteins (Figure 2.1).

Modification of Proteins. Two different proteins were used as model proteins, EGFP and *β*-lactamase. EGFP and *β*-lactamase were oxidized at their N-terminus, which was a serine and threonine, respectively.

The gene encoding EGFP was cloned by PCR using plasmid pEGFP as the template and the primers, GGT GGT TGC TCT TCC AAC TCG ACT CTA GAG GAT CCC CGG GTA CCG (forward) and GGT CTG CAG TTA CTT GTA CAG CTC GTC CAT GCC GAG (reverse). The restriction enzymes SapI (forward primer) and PstI (reverse primer) digestion sites are underlined. The PCR product was purified with agarose gel electrophoresis, and then doubly digested with SapI and PstI. The pTWIN1 vector was similarly digested with the same pair of enzymes. After digestion, the PCR product and the vector were gel-purified and ligated to yield plasmid pTWIN1-EGFP. In this construct, a stretch of 12 residues "STLEDPRVPVAT" was added to the N-terminus of EGFP. This sequence serves two purposes. First, it introduced a serine at the N-terminus of the protein after internal self-splicing, which can be used after oxidation (*vide infra*) for immobilization. Second, it worked as a spacer between the surface and EGFP to reduce the risk of compromising fluorescence emission. The DNA sequence of the pTWIN1-EGFP was confirmed by DNA sequencing (Davis Sequencing, Davis, CA). Plasmid pTWIN1-EGFP was then transformed into *E. coli* cells for protein expression. Cells were grown in cultures of LB broth containing 100 μg/mL of ampicillin at 37 °C with shaking at 250 rpm. When the OD600 of the culture reached 0.6-0.7, expression was induced with the addition of 100 μg/mL of IPTG. Cultures were incubated for an additional four hours under the same conditions. The cells were harvested by centrifugation at 6000 rpm for 20 min at 20 °C. The supernatant was discarded, and the

pellet was resuspended in 5 mL of Tris-HCl buffer (20 mM Tris-HCl, 500 mM NaCl, 1 mM EDTA, pH 8.5). Resuspended bacteria were sonicated on ice for 5 min with 10-s on/off pulses to lyse the cells. The cellular debris was removed by centrifugation for 25 min at 10,000 rpm and 20 °C. The protein in the supernatant was purified using affinity chromatography according to the manufacturer's recommendations (Green Fluorescent Protein Purification Kit, BIO-RAD Laboratories, Hercules, CA). Briefly, the supernatant containing the protein was added to the binding buffer (4 M $(NH_4)_2SO_4$, pH 7.0) to obtain a protein-buffer solution (2 M $(NH_4)_2SO_4$, pH 7.0). The disposable column was equilibrated with 2 M $(NH_4)_2SO_4$, pH 7.0, and then loaded with the protein-buffer solution. The column was washed for a total of three times with a wash buffer (1.3 M $(NH_4)_2SO_4$, pH 7.0). The bound EGFP protein was eluted with a low salt elution buffer (10 mM Tris-HCl, 1 mM EDTA, pH 7.0). The purity of the eluting fractions was evaluated by SDS-PAGE using 12.5% polyacrylamide PhastGels (GE Healthcare, Piscataway, NJ) followed by gel development using silver staining. The protein concentration was measured using the BCA protein assay with bovine serum albumin (BSA) as the standard.

EGFP was oxidized using a sodium periodate treatment, which converts the N-terminal serine to an N-terminal aldehyde moiety (*135*). Purified EGFP at a concentration of 1.0 mg/mL in phosphate buffer (10 mM sodium phosphate, 200 mM NaCl, pH 7.0) was used for the reaction. Sodium periodate was prepared freshly in water and added into the EGFP solution at 5-fold molar excess. The mixture was incubated for 20 min at room temperature (RT). The reaction was quenched by the addition of 7-fold molar excess of ethylene glycol over sodium periodate (Scheme 4.1). The reaction mixture was then

dialyzed against the same buffer (10 mM sodium phosphate, 200 mM NaCl, pH 7.0) overnight at 4 °C.

β-Lactamase was treated with sodium periodate to convert the N-terminal threonine to a N-terminal aldehyde (Scheme 4.1). The reaction mixture was dialyzed against HEPES buffer (50 mM HEPES, pH 7.4) overnight at 4 °C. The concentration of the proteins was determined using the BCA protein assay with BSA as the standard.

Measurement of Fluorescence and Enzyme Activity of Modified Proteins. Equal amounts of EGFP and oxidized EGFP in phosphate buffer (10 mM sodium phosphate, 200 mM NaCl, pH 7.0) were used for fluorescence measurement to determine the change in fluorescence after oxidation. The fluorescence of EGFP and oxidized EGFP were measured at excitation and emission wavelengths of 485 and 520 nm, respectively, under the same conditions.

Enzymatic activities of *β*-lactamase and oxidized *β*-lactamase were measured to determine the effect of oxidation on protein activity. Equal amount of *β*-lactamase and oxidized *β*-lactamase were used for kinetic experiments. The enzymatic activity of *β*-lactamase and oxidized *β*-lactamase was measured using the substrate cefazolin. *β*-Lactamase catalyzes the hydrolysis the *β*-lactam ring of cefazolin, leading to a decrease in absorbance at 263 nm. In particular, *β*-lactamase and oxidized *β*-lactamase in HEPES buffer (50 mM HEPES, pH 7.4) were incubated with a 100 μM cefazolin solution freshly prepared in the same buffer for 20, 40, 60, 80, and 100 s at RT. The absorbance at 263 nm was measured for each sample, and the absorbance *vs* time was plotted.

Surface Modification with HBPs. HBPs were immobilized on HA particles and quantified by reaction with TNBS, which reacts with hydrazine groups to form trinitrophenyl derivatives (*136-138*). HA particles (1.0 mg) were treated with 1 x 10^{-4} M HBPs in HEPES buffer (50 mM HEPES, pH 7.4) for 1 h at RT. The samples were washed thoroughly with the same buffer followed by deionized water (Scheme 4.1). HA particles without treatment with HBP were used as control. HBP-treated samples along with the control were incubated with 0.1% (w/v) TNBS in 3% (w/v) sodium borate at 70 °C for 5 min. The samples were washed with deionized water and then hydrolyzed with 1 M NaOH at 70 °C for 10 min. The released yellow product was proportional to the number of hydrazine groups. The amount of immobilized HBPs was measured indirectly by measuring the absorbance of the hydrolyzed reaction products at 410 nm. Standard curves were prepared by direct hydrolysis of TNBS in 1 M NaOH.

Immobilization and Quantification of Protein. EGFP was immobilized on HA particles using seven HBPs (**1**-**7**). HBP-modified HA particles (1.0 mg) were treated with 0.1 mg of oxidized EGFP in phosphate buffer (10 mM sodium phosphate, 200 mM NaCl, pH 7.0) for 1 h at 4 °C (Scheme 4.1). For the control studies, oxidized EGFP was simply adsorbed on HA particles under the same conditions. The samples were centrifuged for 5 min at 3,000 rpm, and the amount of immobilized EGFP was determined by measuring the fluorescence of the supernatant at excitation and emission wavelengths of 485 and 520 nm, respectively.

β-Lactamase was immobilized on HA particles using seven HBPs (**1**-**7**). For immobilization on the HA particles, 1.0 mg of HBP-modified HA particles were treated

with 0.3 mg of oxidized *β*-lactamase in HEPES buffer (50 mM HEPES, pH 6.5) for 1 h at RT (Scheme 4.1). For the control studies, *β*-lactamase was simply adsorbed on HA particles under the same conditions. The samples were thoroughly washed with HEPES buffer (50 mM HEPES, pH 7.0) and deionized water. The amount of *β*-lactamase immobilized on HA was measured using the BCA protein assay with BSA as the standard by a slight modification in the manufacturer's protocol. *β*-Lactamase immobilized HA samples were incubated directly in the working reagent of BCA assay for 1 h at 37 °C. The samples were centrifuged for 5 min at 3,000 rpm, and the absorbance of the supernatants was measured at 570 nm.

Enzymatic Activity of *β*-Lactamase and Determination of Kinetic Constants. The enzymatic activity of *β*-lactamase immobilized on HA particles, adsorbed *β*-lactamase, and free *β*-lactamase in solution was measured using the substrate cefazolin and monitoring the hydrolysis reaction at 263 nm. Briefly, cefazolin solutions were prepared at different concentrations (0, 20, 40, 60, 80, 100, 120, 140, 160, 180, 200 μM) in HEPES buffer (50 mM HEPES, pH 7.4). A fixed volume of *β*-lactamase immobilized HA particles was added to each cefazolin solution and treated for 15 s at RT. Similarly, HA particles with adsorbed *β*-lactamase and free *β*-lactamase in solution were exposed to various concentrations of cefazolin for 15 s at RT. Each reaction mixture was centrifuged immediately, and the absorbance of the supernatant was measured at 263 nm. The reaction rates were calculated from the change in absorbance. The substrate saturation curves of various *β*-lactamase samples with cefazolin were fitted into Michaelis-Menten

kinetics using GraphPad, and the corresponding K_M, k_{cat}, and k_{cat}/K_M values were calculated.

Statistical Analysis. Data presented are mean ± standard deviation. A minimum of three replicates were used for each experiment. One-way analysis of variance (ANOVA) was conducted using GraphPad software (San Diego, CA). The results were considered significantly different when $p < 0.05$.

RESULTS AND DISCUSSION

Immobilization of biomolecules has been the subject of active investigation. To ensure activity, factors such as the interaction between the biomolecule and the immobilization surface, and the orientation of the biomolecule on the surface need to be considered (*139*). Various methods have been explored for immobilization of proteins on solid surfaces, including several bone implant interfaces (*70-73*). However, the majority of the methods employed are based on linking the protein covalently to the implant surface via surface-exposed functional groups on the protein, including amino, carboxylate, and thiol groups. Such methods result in linkages that are mostly random, and multiple bonds may form between each protein molecule and the surface. Therefore, such immobilization approaches may compromise the activity of the protein. In addition, the active site of the immobilized protein may be blocked during random immobilization, which may lead to drastically decreased bioactivity. In addition, the structure of the protein may also be affected by protein-surface interactions and/or steric hindrance.

Oriented immobilization may minimize or overcome the drawbacks of random orientation. Successful oriented immobilization requires selective functionalization of biomolecules, tailoring of the surface, or both (*136*). Various approaches have been explored for oriented immobilization of biomolecules. Most of these approaches rely on the formation of a specific covalent linkage between the protein and the target surface or a specific interaction between two biomolecules (*76*). However, oriented immobilization has been rarely reported for immobilization of biomolecules on biomaterials.

In this study, EGFP and *β*-lactamase were used as model proteins to develop an oriented immobilization method of proteins on mineralized biomaterials, such as HA. EGFP is a green fluorescent protein, which was modified genetically to contain an N-terminal serine. On the other hand, *β*-lactamase is an enzyme produced by a broad spectrum of bacteria that hydrolyzes *β*-lactam antibiotics to produce a change in the absorption spectrum, which can be used to monitor enzymatic activity. It is a very efficient catalyst and instills resistance to *β*-lactam antimicrobial agents, such as penicillins, cephalosporins, and cefamycins, by breaking their four-member ring structure. *β*-Lactamase from *Enterobacter cloacae* has a threonine at its N-terminus. Serine and threonine are the only amino acids that have a vicinal amino alcohol. Vicinal diols and amino alcohols can be oxidized with periodate to obtain an aldehyde functional group that can be used for attachment. In our work, the N-terminal serine and threonine in EGFP and *β*-lactamase, respectively, were oxidized with periodate to obtain a single aldehyde, which was used to attach the proteins to the HA surface. The rate of oxidation of vicinal diol is 100-1000 fold slower than vicinal amino alcohol (*140*). Therefore, this

method of generating N-terminal aldehydes could also be applied to glycoproteins without degrading the carbohydrate region.

The fluorescence emission at 520 nm of EGFP and oxidized EGFP were measured and compared. No significant change in fluorescence was observed after oxidation of EGFP. To evaluate the effect of oxidation of *β*-lactamase, the enzymatic activities of the same amount of *β*-lactamase and oxidized *β*-lactamase were determined using 100 μM cefazolin as the substrate. The enzymatic activity of *β*-lactamase was reduced by about 30% upon periodate treatment, indicating that oxidation has some effect on the protein. Therefore, it can be stated that sodium periodate oxidation of the N-terminus serine or threonine of a protein might affect the activity of the protein, and this could vary from protein to protein. Other than vicinal amino alcohols and diols, amino acids that can be oxidized by periodate treatment are methionine, cysteine, tyrosine, tryptophan and histidine. However, these amino acids are much less reactive toward periodate. Under the mild experimental conditions used for the oxidation of N-terminal serine and threonine of EGFP and β-lactamase, respectively, damage to other periodate-reactive groups of the proteins is limited, which is manifested by no change in the fluorescence of EGFP and limited change in the activity of β-lactamase.

Scheme 4.1. Oriented immobilization of *β*-lactamase and EGFP on HA through HBPs

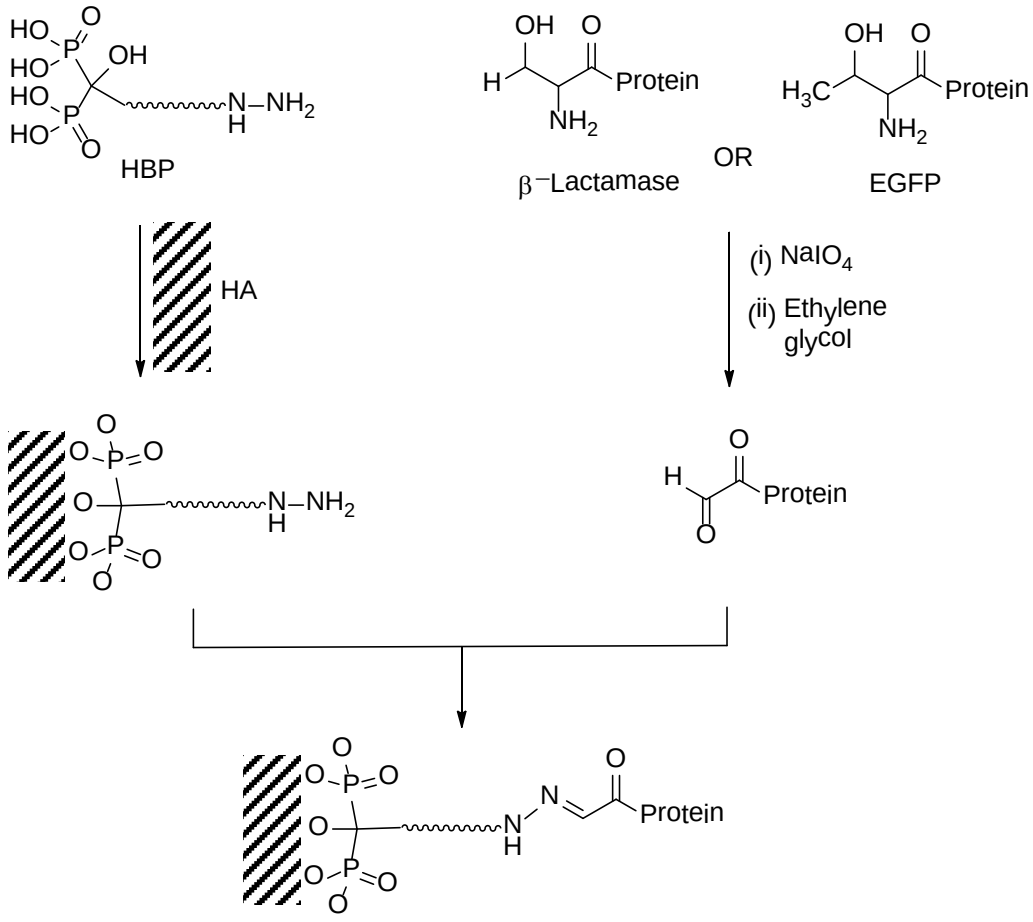

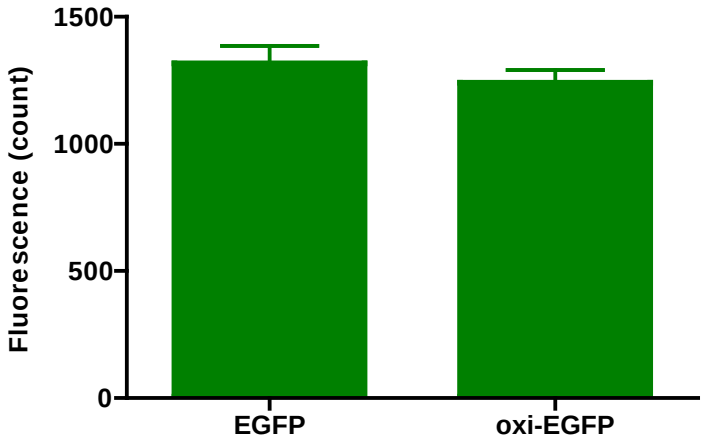

Figure 4.1. Fluorescence of the equal amount of EGFP and oxidized-EGFP in phosphate buffer (10 mM sodium phosphate, pH 7.0, 200 mM NaCl) at RT. Data are average ± one standard deviation (n = 3).

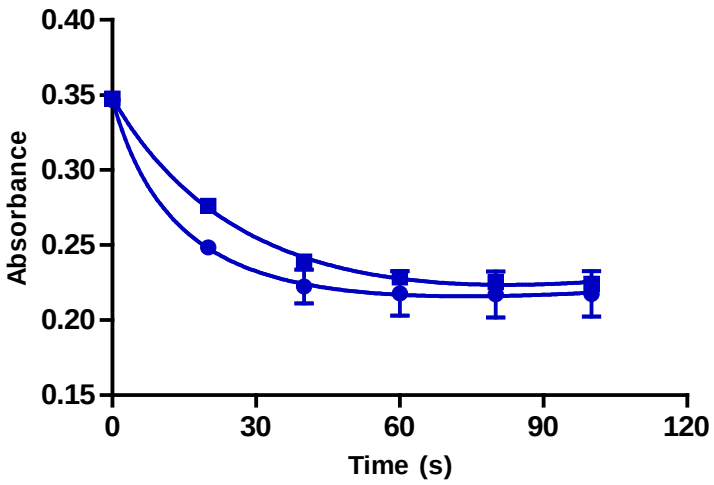

Figure 4.2. Enzyme activity of *β*-lactamase and oxidized *β*-lactamase on 100 µM cefazolin in HEPES buffer (50 mM HEPES, pH 7.4); ●, ■ represent *β*-lactamase, and oxidized *β*-lactamase. Data are the average ± one standard deviation (n = 3). Some error bars are obstructed by the points and are overlapped with each others.

In this study, HA was used as a solid surface for protein immobilization. The unit cell of HA has a chemical formula of $Ca_{10}(PO_4)_6(OH)_2$, with two primary sites capable of binding, namely, Ca^{2+} for anions and PO_4^{3-} for cations (*20*). HA has a similar composition as that of the mineral component of bone, and is a bioactive prosthetic material, which can undergo *in vivo* bone bonding (*141, 142*). Because of these properties, HA has been widely used in bone implant applications. Moreover, as a result of the development of several effective coating techniques, such as direct current plasma spraying, radio frequency plasma spraying, and suspension plasma spraying, HA has been broadly used as a coating material for various metal implants (*142, 143*). Given the extensive use of HA in bone implant applications, the focus in this study was the site-specific immobilization of proteins on the HA surface. Since BPs have a high affinity toward HA, bifunctional BPs were used as linkers between proteins and the HA surface.

BPs have been approved for the treatment of various skeletal diseases and, therefore, are biocompatible and could be used for implant modification. BPs have excellent anti-resorptive properties and affinity to bone. The two phosphonates of BPs account for their bone-seeking ability via Ca^{2+} chelation. However, the R^1 and R^2 groups of BPs also contribute to their bone affinity. Since, BPs with hydroxyl or amine at R^1 demonstrate tridentate binding and, thus, higher affinity to bone or HA (*20*), for this study we chose a series of hydrazine-BP (HBP) derivatives previously reported by our laboratory. The enhanced affinity of HBPs was measured using a crystal growth inhibition study (*24, 134*). HBPs have a hydrazine on their R^2 substituent that is linked with various length and lipophilicity spacer arms to the bisphosphonate group. Hydrazine reacts with aldehyde at low pH (4.5 to 7.4) (*144-147*), where the lysine amine groups of

the protein are protonated, rendering them unreactive. Moreover, hydrazines react faster than amines to aldehydes and ketones, and reaction of hydrazines with aldehydes results in the formation of a stable hydrazone bond. In that regard, HBPs are well-suited bifunctional linkers for the oriented immobilization of proteins containing an aldehyde, and were used to target and immobilize proteins on the surface of HA particles.

It has been observed that several factors affect the bioactivity of immobilized proteins, including the surface density of functional groups as well as the length and lipophilicity of the spacer between the surface and the protein (*148-150*). Higher density of functional groups on the surface could cause a higher number of immobilized biomolecules, which may result in steric hindrance as a result of crowding, thus blocking the active site of biomolecules. A lower density of functional groups should result in a lower number of the immobilized biomolecules, but this does not necessarily cause improvement in the accessibility and activity of the biomolecule (*151*); the latter could occur if the site from which the biomolecule is immobilized misorients the protein in a way that its binding/active site is blocked by the immobilization surface. In other words, the activity of the biomolecule does not solely depend on the density of the functional groups on the surface or the number of biomolecules immobilized on the surface. The objective was to investigate the effect of the above-mentioned factors on the accessibility and activity of the immobilized protein. Therefore, HBPs of various length and lipophilicity were used for immobilization of proteins. The surface density of hydrazines on the HA surface following treatment with various HBPs was determined with a TNBS assay as shown in Figure 4.3. The TNBS assay is generally used for the detection of amine groups, however, it has also been used for quantification of hydrazines (*137*, *138*).

The results of the TNBS assay show that neither the length nor the lipophilicity of the spacer affects significantly the surface density of the hydrazine on the surface of HA.

Oxidized EGFP was immobilized on the HBP-modified HA particles, and the amount of immobilized EGFP was measured using fluorescence. The extent of binding was determined by measuring the difference between the fluorescence of the supernatant before and after the immobilization of oxidized EGFP on HA (Figure 4.4). The change in length and lipophilicity of HBPs had no statistically significant effect on the amount of EGFP immobilized. However, it was observed that the use of HBPs as linkers for the immobilization of EGFP increased significantly the amount of EGFP immobilized over EGFP that was simply adsorbed on HA ($p<0.05$). The lower amount of adsorbed EGFP can be explained by the tendency of HA to adsorb proteins with an overall positive charge while repelling proteins that are overall negatively charged (*152*, *153*). EGFP has a pI of 5.7 and possesses an overall negative charge at pH of 7.0, which is the pH at which the experiments were conducted. On the contrary, bisphosphonates have high affinity for HA. Consequently, modification with HBP results in higher amounts of immobilized EGFP.

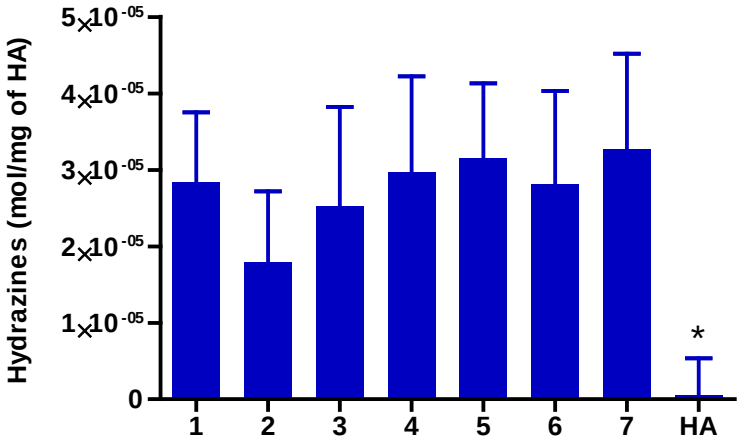

Figure 4.3. Surface density of hydrazine groups on HA surfaces modified with seven different HBPs (**1**-**7**) by TNBS assay. An amount of 1 mg HA particles was treated with 1 × 10^{-4} M of the corresponding HBP (**1**-**7**). HA refers to unmodified HA. Data are the average ± one standard deviation (n = 9). (* indicates the values are significantly different from others $p<0.05$).

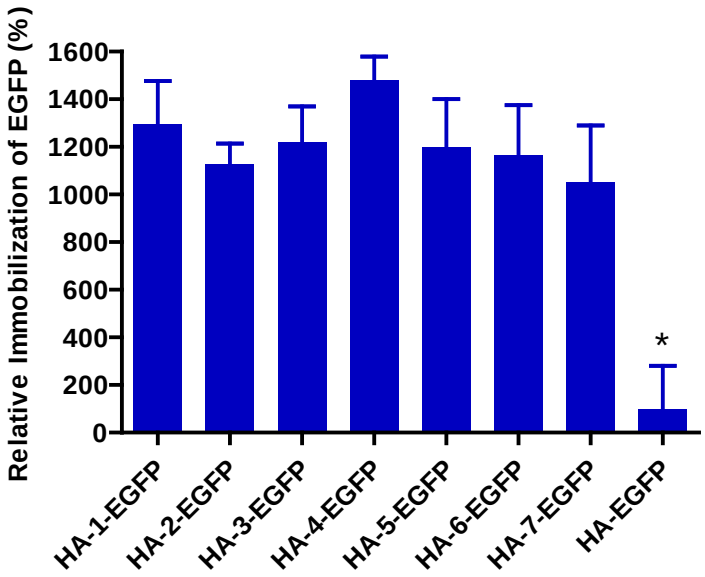

Figure 4.4. Immobilization of EGFP on HA surfaces determined by fluorescence. EGFP was immobilized on HA surfaces via seven different HBPs (**1**-**7**) and by simple adsorption. The corresponding EGFP is denoted as HA-1-EGFP through HA-7-EGFP. HA-EGFP refers to EGFP physically adsorbed on HA in the absence of HBP. The Y-axis is normalized relative to the amount of EGFP immobilized by adsorption (HA-EGFP). Data are the average ± one standard deviation (n = 3). (* indicates the values are significantly different from others $p<0.05$).

Oxidized *β*-lactamase was also immobilized on the HBP-modified HA particles through a stable hydrazone linkage between the aldehyde at the N-terminus of oxidized *β*-lactamase and surface hydrazines. The amount of immobilized *β*-lactamase was measured using the BCA assay (Figure 4.5). The lowest binding was observed when *β*-lactamase was attached to HA through the shorter chain HBP **1** and **5** ($p<0.05$). *β*-Lactamase that was simply adsorbed on HA and immobilized through HBP **2**, **3**, **4**, **6**, and **7** gave statistically indistinguishable results in terms of the amount of immobilized enzyme ($p<0.05$). In general, HA has an elevated affinity to proteins that possess a positive charge (*152, 153*). *β*-Lactamase from *Enterobacter cloacae* has a pI of 7.8 (*154*), and therefore the protein has an overall positive charge at pH 6.5, which is the pH at which the experiments were conducted. This explains why *β*-lactamase adsorbs readily on HA. From Figure 4.5, it can also be stated that the lipophilicity of the HBPs does not show any significant effect on the amount of immobilized *β*-lactamase.

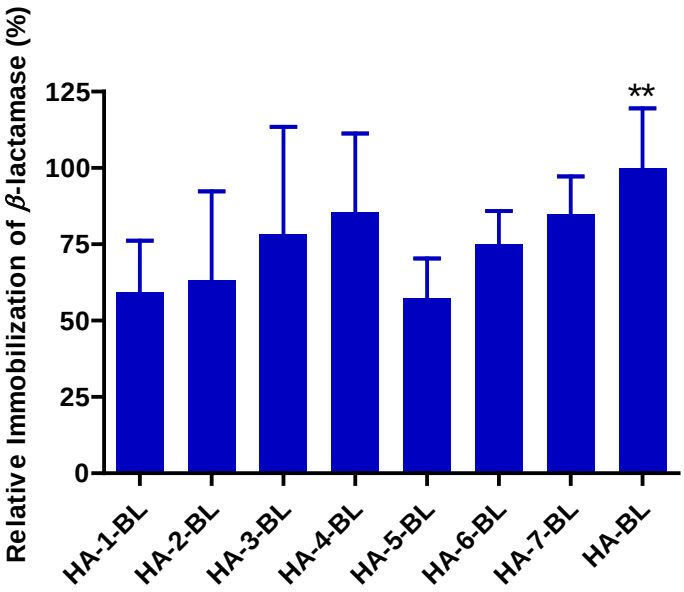

Figure 4.5. Immobilization of *β*-lactamase on HA surfaces determined by the BCA protein assay. *β*-Lactamase was immobilized on HA surfaces via seven different HBPs (**1**-**7**) (HA-1-BL through HA-7-BL) and by simple adsorption (HA-BL). The Y-axis is normalized relative to the amount of *β*-lactamase immobilized by adsorption (HA-BL). Data are the average ± one standard deviation (n = 6). (** indicates the values are significantly different from HA-1-BL and HA-5-BL $p<0.05$).

The enzymatic activities of HBP-immobilized *β*-lactamase and adsorbed *β*-lactamase were determined through the hydrolysis of the substrate cefazolin. For comparison purposes, the activity of free *β*-lactamase in solution was also measured using the same substrate under similar reaction conditions. The hydrolysis of cefazolin was also determined in the presence of "bare" HA and HBP-modified HA as negative controls. The reaction data were fitted to a Michaelis-Menten kinetic model. The Michaelis constant (K_M) and the maximum velocity (V_{max}) were calculated using GraphPad. The turnover number of *β*-lactamase (k_{cat}), which represents the maximum number of the substrate molecules that undergoes hydrolysis per catalytic site of the active enzyme per unit time, was also calculated using the following equation.

$$k_{cat} = \frac{V_{max}}{[E]} \quad \text{S1}$$

where $[E]$ is the enzyme concentration. The catalytic efficiency, k_{cat}/K_M, of immobilized *β*-lactamase, adsorbed *β*-lactamase, and free *β*-lactamase in solution were calculated. In general, the catalytic efficiency of the enzyme indicates how fast the chemical reaction proceeds in the forward direction.

The kinetic parameters obtained with cefazolin and surface-immobilized *β*-lactamase, adsorbed *β*-lactamase, and free *β*-lactamase in solution are shown in Table 1. The K_M values of the immobilized *β*-lactamase were all higher than free *β*-lactamase in solution. The k_{cat} and k_{cat}/K_M values of immobilized *β*-lactamase were all lower than free *β*-lactamase in solution. From these findings, it can be concluded that the enzymatic activity of immobilized *β*-lactamase is reduced compared to free *β*-lactamase in solution. This is consistent with prior literature that indicates higher K_M and lower k_{cat} values when

enzymes are immobilized (*155*, *156*). However, the K_M values for immobilized *β*-lactamase are significantly lower than that of adsorbed *β*-lactamase ($p<0.05$). The k_{cat} values of immobilized *β*-lactamase, which indicate the number of cefazolin molecule hydrolyzed per *β*-lactamase molecule per second, were also significantly higher than that of adsorbed *β*-lactamase ($p<0.05$). Therefore, *β*-lactamase immobilized through HBPs hydrolyzed the substrate more effectively than adsorbed *β*-lactamase. Specifically, the catalytic efficiencies of *β*-lactamase immobilized through HBP **1**, **2**, **5**, and **6** were significantly higher than those of adsorbed *β*-lactamase ($p<0.05$). As stated above, statistically equivalent amounts of the enzyme were attached on HA when *β*-lactamase was simply adsorbed or immobilized through HBP **2**, **3**, **4**, **6**, and **7**. Despite having the same amount of immobilized enzyme, the lowest turnover number was observed with adsorbed *β*-lactamase. This is because direct adsorption of the protein leads to random orientation on the surface, which may result in loss of structural integrity and activity because of steric hindrance and interactions with the HA surface (*157*, *158*). Overall, HBP-immobilized *β*-lactamase showed higher k_{cat} than adsorbed *β*-lactamase.

Further work will be necessary to determine the actual orientation of the immobilized protein on the HA surface. Since this strategy of oriented immobilization of proteins was developed using HA, which is widely used as a bone implant material, the next logical step would be to orient bone-related proteins on the HA implant surface to improve cell/tissue interactions with the implant surface.

Table 4.1. Kinetic parameters describing the enzymatic activity of free *β*-lactamase in solution, adsorbed *β*-lactamase, and immobilized *β*-lactamase through HBPs[a]

***β*-Lactamase in various form**	K_M (10^{-6} M)	k_{cat} (10^{-3} s^{-1})	k_{cat}/K_M (s^{-1} M^{-1})
Free *β*-lactamase in solution	24.2 ± 3.8	7.43 ± 0.47	310 ± 34
Adsorbed *β*-lactamase	124 ± 25	1.36 ± 0.26	11.1 ± 1.2
β-Lactamase immobilized through HBP **1**	70.7 ± 5.0	3.73 ± 0.03	52.9 ± 3.2
β-Lactamase immobilized through HBP **2**	81.2 ± 8.9	2.88 ± 0.10	35.6 ± 2.6
β-Lactamase immobilized through HBP **3**	85.0 ± 5.0	1.90 ± 0.07	22.3 ± 0.7
β-Lactamase immobilized through HBP **4**	82.3 ± 8.3	1.82 ± 0.07	22.3 ± 1.5
β-Lactamase immobilized through HBP **5**	77.3 ± 4.1	3.84 ± 0.14	49.8 ± 4.2
β-Lactamase immobilized through HBP **6**	80.9 ± 5.2	2.64 ± 0.04	32.7 ± 2.4
β-Lactamase immobilized through HBP **7**	89.7 ± 6.4	2.02 ± 0.00	22.8 ± 1.6

[a] Data are represented by mean values (n = 3) ± standard deviation.

CONCLUSIONS

Oriented immobilization of proteins on solid surfaces anchors them at preferred locations enhancing their usefulness for a target desired application. Immobilization of proteins in their bioactive as well as accessible state is critical for inducing their specific biological actions. The objective of the present work was to demonstrate the ability of bifunctional HBPs to immobilize a target protein in an oriented manner on HA surfaces, a type of biomaterial widely used in orthopedic implants. It was expected that such functionalization of the HA surface with a protein would result in improved bioactivity compared to simply adsorption. Our data demonstrate that the length or lipophilicity of HBPs have no significant effect on the amount of protein (EGFP and β-lactamase) immobilized on HA surface. Regarding the study of β-lactamase immobilized through various HBPs, we demonstrated that the immobilized enzyme had enhanced bioactivity compared to adsorbed β-lactamase. In summary, we showed that HBPs could be used for effective and bioactive immobilization on HA of any protein that has an intrinsic N-terminal serine or threonine or onto which either of these amino acids can be introduced at the N-terminus. It is envisioned that the proposed approach of oriented immobilization of bioactive proteins will broaden the possibility of immobilizing a wide variety of therapeutic proteins and peptide agents onto biomaterial surfaces, thus, potentially improving the biocompatibility of orthopedic implants.

CHAPTER FIVE

BIFUNCTIONAL BISPHOSPHONATES FOR DELIVERING PTH (1-34) TO BONE MINERAL WITH ENHANCED BIOACTIVITY

Targeted drug delivery has been widely studied and is of high importance in medical technology (*116*). It reduces systemic drug toxicity by targeting the delivery of drugs to the desired site. It distributes the drug with a more uniform effect at the desired site and reduces the frequency of drug dosage (*110*). Because of the benefits of targeted delivery over conventional delivery of drugs, various drug delivery vehicles, such as nano/micro particles (*159-161*), dendrimers, polymeric micelles (*162*), liposomes (*163, 164*), and hydrogels (*165, 166*), have been explored. Drug delivery to bone tissue requires a vehicle that could direct the drug-containing system or drug itself to bone mineral. This has been explored by using molecules that have a high affinity to bone mineral, such as BPs (*16, 20*), D-aspartic acid octapeptide (*44, 45*), polymalonic acid (*46*), and tetracycline (*47, 48*).

Delivering drug molecules to bone for enhancing bone regeneration or treating osteogenesis is a topic of prime importance. Various bioactive macromolecules, such as bone morphogenetic proteins (BMPs), basic fibroblast growth factor (FGF), insulin-like growth factors (IGFs), platelet-derived growth factor (PDGF), transforming growth factor-β (TGF-β), and vascular endothelial growth factor (VEGF), have been found to stimulate proliferation and differentiation of bone forming cells and could be used for bone regeneration (*167*). These biomolecules bind to cell surface receptors to initiate

such effects. A challenge in the targeted delivery of the therapeutic protein or macromolecule to bone through conjugation to a bone-seeking agent is the effect of the latter on bioactivity. For example, the conjugate upon binding to bone should orient the therapeutic agent in a manner that makes it available for optimal binding to its cell surface receptor. Delivery of macromolecules using multiple BPs has been reported before (*52, 130, 132, 168-170*). Since proteins have multiple reactive functional groups, their selective attachment to the delivery vehicle through a single amino acid residue is difficult. Non-selective attachment of the delivery vehicle and/or attachment of multiple delivery vehicles to a single protein molecule could cause a loss of bioactivity of the protein. On the other hand, selective attachment of the therapeutic protein through a single amino acid residue to a single molecule of the delivery vehicle should be more favorable as maintaining the bioactivity of the protein.

In general, BPs are chemical analogues of pyrophosphate that have high affinity to bone mineral. Several BPs are widely used as anti-resorptive agents in the treatment of several bone diseases (*171, 172*). BPs are also being explored for targeting of therapeutic agents to bone tissue, including radiopharmaceuticals and imaging agents (*49, 50, 89-97*). Although protein conjugation to BPs has been studied, the interactions of the resultant conjugates with bone-related cells or tissue have not been adequately explored. Further, delivering therapeutic protein in its bioactive form could be possible by its selective attachment through a single amino acid residue on the protein to a high affinity BP molecule, and this has not been adequately explored. Herein, we propose to deliver an osteogenic peptide, parathyroid hormone (PTH), to bone by designing a conjugate in which a single molecule of BP is attached to the N-terminus of PTH.

PTH is an 84 amino acid peptide hormone that plays important physiological roles, including calcium regulation and bone remodeling. PTH (1-34), a 34 amino acid peptide derived from the N-terminus of the PTH, retains most of the functions of PTH of the hormone. Depending on the concentration and mode of administration, PTH (1-34) can have anabolic or catabolic effects. In general, high and sustained doses of PTH result in bone resorption, but intermittent doses of higher amounts or infusion of low doses leads to bone formation (*77, 78*). PTH (1-34) was used in all of the studies described herein and is denoted as PTH throughout for simplicity. Oral delivery of PTH as well as many other therapeutic peptides is not useful because of their degradation in the gastrointestinal (GI) track. Therefore, PTH is generally administered through injections. However, the injected PTH gets distributed throughout the body and does not become selectively adsorbed in bone tissue for bone regeneration. However, attachment of a high affinity BP to the N-terminus of PTH could deliver the peptide to bone in a selective manner and orient the molecules on the bone surface for enhanced cell interactions.

Herein, we report a novel strategy for delivering PTH to bone tissue through conjugation to a single molecule of high affinity bifunctional BP. In particular, we have conjugated PTH to HBPs of varying length and lipophilicity, whose synthesis has been described in Chapter Two (*134*). The conjugates were immobilized on bone wafers, and the cell responses to the immobilized PTH were assessed using pre-osteoblast, MC3T3-E1 cells. Furthermore, experiments were performed to explore the binding affinity of the HBP-PTH conjugates (or ability of HBPs to deliver the attached PTH to bone) and drug potency of the HBPs toward controlling osteoclastic bone resorption using macrophagic/pre-osteoclastic RAW 264.7 cells.

EXPERIMENTAL SECTION

Materials. The pre-osteoblastic MC3T3-E1 (CRL-2593) and macrophagic/pre-osteoclastic RAW 264.7 (TIB-71) cell lines were obtained from American Type Culture Collection (ATCC, Rockville, MD). Alpha minimum essential medium (αMEM), Dulbecco's Modified Eagle's Medium (DMEM), and fetal bovine serum (FBS) were purchased from GIBCO-Invitrogen (Carlsbad, CA). The bicinchoninic acid (BCA) and Micro BCA protein assay kits were obtained from ThermoFisher Scientific (Rockford, IL). The cell proliferation reagent WST-1 was purchased from Roche (Mannheim, Germany). Ac-DEVD-AFC was obtained from Enzo Life Sciences (Plymouth Meeting, PA). Bovine aprotinin, 3-[(3-cholamidopropyl)dimethylamino]-1-propanesulfonate (CHAPS), DL-dithiothreitol (DTT), etoposide, ethylenediaminetetraacetic acid disodium salt dihydrate (EDTA), glycerol, 4-(2-hydroxyethyl)piperazine-1-ethanesulfonic acid (HEPES), Hoechst 33258, isobutylmethylxanthine (IBMX), leupeptin hemisulfate salt, orthovanadate, PTH (1-34), phenylmethylsulfonylfluoride, potassium hydroxide, propidium iodide, reagent grade hydroxyapatite powder, sodium acetate, sodium chloride, sodium hydroxide, sodium fluoride (NaF), sodium tris(hydroxymethyl)aminomethane hydrochloride (Tris-HCl), and Triton X-100 were purchased from Sigma-Aldrich (St. Louis, MO). Calcium chloride, hydrochloric acid, and potassium dihydrogen phosphate were obtained from EMD Chemicals (Gibbstown, NJ). Centrifugal filter units with a nominal molecular weight limit (NMWL) of 3 kDa were purchased from Millipore (Billerica, MA).

Hydrazine-Bisphosphonates (HBPs). Seven HBPs (**1-7**) of various length and lipophilicity were synthesized according to the previously reported procedure (*81, 107, 134*) (Figure 2.1). Although each HBP has the same terminal functional groups, they have spacers of varying length and lipophilicity between the phosphonate and hydrazine functionalities. These HBPs were selectively conjugated to oxidized PTH through a hydrazone linkage and used as vehicle for delivering PTH to bone in an oriented manner (further described in subsequent sections).

***In vitro* Activity of HBPs.** BPs are used in clinical settings for treatment of bone diseases as well as various types of cancers. Since HBPs are structural derivatives of the alendronate, which is widely used as anti-resorptive agent in the treatment of various skeletal diseases, and have never been studied for their drug potency, the *in vitro* activities of HBPs were studied on preosteoclastic RAW 264.7 cells.

To study the *in vitro* proapoptotic activity of HBPs, RAW 264.7 cells were cultured in pre-warmed DMEM medium that was supplemented with 10% FBS at 37 °C in a humidified atmosphere composed of 5% CO_2. The cells were seeded into 24-well plates at a density of 40×10^4 cells/well for *in vitro* quantification of intracellular protein and caspase-3 activity. One day after cell seeding, the cultures were treated with various concentrations (10^{-6}, 10^{-5}, 10^{-4} M) of HBPs. Cells without HBPs were used as a negative control, while cells treated with 10^{-6}, 10^{-5}, or 10^{-4} M of etoposide were used as positive controls. The plates were incubated again for 24, 48, and 72 h before their use for further analysis. The experiments were conducted in triplicate and repeated at least three times to ascertain the reproducibility of the results.

Intracellular Protein Quantification. Intracellular protein was measured using a commercially available BCA assay kit. Briefly, the medium was removed, and the adherent cells were washed with PBS. The cultures were lysed by 10-min incubation in 50 µL of lysate buffer (20 mM Tris-HCl, pH 7.4, 150 mM NaCl, 1mM EDTA, 10 mM NaF, 1 mM sodium orthovanadate, 5 µg/ml leupeptin, 0.14 U/ml aprotinin, 1mM phenylmethylsulfonylfluoride, and 1% (v/v) Triton X-100), followed by 2 s of sonication. Volumes of 10 µL of the cell lysate samples and standards (solutions of known concentrations of bovine serum albumin) were added to the wells of a 96-well microtiter plate followed by addition of 200 µL of the working reagent; the well contents were mixed thoroughly by shaking the plate for 2 min. The plate was incubated at 37 °C for 30 min and then cooled to room temperature (RT). The absorbance of the samples was measured at 562 nm on a plate reader. The amount of protein in the sample was calculated using a standard curve prepared with albumin.

Fluorescence Microscopy. The number of apoptotic and necrotic cells was determined by staining the cultures with propidium iodide and Hoechst 33258. Propidium iodide is membrane impermeant for live cells and stains only dead cells by binding to their DNA. A stock solution of 1.5 mM propidium iodide was made by dissolving 1 mg of propidium iodide in 1 mL of deionized water and storing in the dark at 2–6 °C. For cell staining, cultures were treated with propidium iodide at a final concentration of 0.5 µM while kept on ice for 20-30 min. The cultures were analyzed using fluorescent microscopy. The apoptotic cells were quantified using Hoechst 33258 reagent. The cultures were treated with 5 µg/mL of Hoechst 33258 and incubated for 10 min at 37 °C.

The apoptotic cells were determined using fluorescent microscopy in the dark. The necrotic cells were determined by subtracting the number of apoptotic cells (quantified by Hoechst staining) from the total number of dead cells (quantified by propidium iodide staining). The cell images were processed using ImageJ software (A public domain Java image processing and analysis program inspired by National Institutes of Health).

Apoptosis Assay. Apoptosis was determined by measuring the intracellular caspase-3 activity. The cultures were lysed by 10 min of incubation in 50 µL of lysate buffer (20 mM Tris-HCl, pH 7.4, 150 mM NaCl, 1 mM EDTA, 10 mM NaF, 1 mM sodium orthovanadate, 5 µg/ml leupeptin, 0.14 U/ml aprotinin, 1 mM phenylmethylsulfonylfluoride, and 1% (v/v) Triton X-100), followed by 2 s of sonication. The cell lysate was treated with 50 µM Ac-DEVD-AFC in 50 mM HEPES buffer (100 mM NaCl, 0.1% CHAPS, 10 mM DTT, 1 mM EDTA, and 10% (v/v) glycerol, pH 7.4) at RT for 60 min in the dark. The caspase-3 activity was determined by measuring the fluorescence at λ_{em}=510 nm (λ_{ex}=485).

Selective Oxidation of PTH and Site-specific Conjugation of HBPs to PTH. To facilitate the selective conjugation of PTH to HBP, the N-terminal serine residue of PTH was selectively oxidized to an aldehyde functionality (Scheme 5.1) (*135*, *173-175*). In brief, PTH was dissolved in HEPES buffer (50 mM, pH 7.0) at 41 µg/mL of concentration. Freshly dissolved sodium periodate in deionized water was added to the PTH solution at 2-fold molar excess. The mixture was incubated in the dark for 10 min at RT. The reaction was quenched by the addition of 10-fold molar excess of glycerol over

sodium periodate. The reaction mixture was then filtered through centrifugal filter units of 3 kDa NMWL to remove the byproduct of the reaction and excess reagents. The oxidized PTH was diluted in HEPES buffer (50 mM, pH 7.0) to a final concentration of 41 μg/mL. The oxidized PTH was conjugated to HBPs in a site-specific manner through the generated N-terminal aldehyde. In particular, PTH was treated with 10-fold molar excess of HBPs in acetate buffer (100 mM sodium acetate, 50 mM NaCl, pH 6.0) for 2 h at RT. The reaction mixtures were purified and concentrated using centrifugal filter units to obtained pure HBP-PTH conjugates.

Bioactivity of HBP-PTH Conjugates. The viability and apoptotic effects of the HBP-PTH conjugates on pre-osteoblastic cells (MC3T3-E1) and pre-osteoclastic cells (RAW 264.7 cells) were also determined. In brief, MC3T3-E1 and RAW 264.7 cells were cultured in αMEM and DMEM medium, respectively, at 37 °C in a humidified atmosphere containing 5% CO_2. Both media were supplemented with 10% FBS. The cells were seeded into 96-well plates at a density of 0.5×10^4 cells/well and incubated for 24 h, followed by addition of various concentrations (7.3×10^{-10}, 7.3×10^{-9}, 7.3×10^{-8} M) of PTH and HBP-PTH conjugates along with positive and negative controls. After 24, 48, and 72 h of incubation of the cultures, cell viability, intracellular protein content, and caspase-3 activity of the cells were measured according to the procedure described above (in section '*In vitro* activity of HBPs'). The cell viability of the HBP-PTH conjugates was determined using a colorimetric WST-1 assay in accordance with the manufacturer's instructions. The cultures in 96-well plates were incubated with 10 μL/well of cell proliferation reagent WST-1 at 37 °C for 60 min in a humidified atmosphere composed

of 5% CO_2. The plate was cooled to RT, and the absorbance of the samples was measured at 450 nm on a plate reader. The experiments were conducted in triplicate and repeated at least three times to ascertain the reproducibility of the results.

***In vitro* Mineral Binding Affinity of HBP-PTH Conjugates and PTH.** The mineral affinity of the HBP-PTH conjugates and PTH were determined using an HA binding assay according to a previously reported procedure (*52, 168, 170*). In brief, 100 µL samples (HBP-PTH conjugates and PTH) were diluted to 800 µL with HEPES buffer (50 mM, pH 7.0) to obtain a peptide or peptide conjugate concentration in the range of 10-30 µg/ mL. The diluted samples were then added to microcentrifuge tubes containing 1 mg of HA (in triplicate). For a positive control (i.e., 0% binding), the samples were incubated in microcentrifuge tubes without HA. As a negative control, HEPES buffer without peptide or conjugates were incubated in microcentrifuge tubes. All samples were shaken for 2 h at RT and centrifuged to separate non-bound peptide from bound peptide. The concentration of the non-bound peptide or peptide conjugate was determined using the Micro BCA assay according to the manufacturer's protocol. In a typical experiment, 150 µL of the supernatant and BSA standards were added to 150 µL of working reagent in a 96-well plate and mixed thoroughly by shaking the plate for 2 min. The plate was incubated for 30 min at 37 °C and then cooled to RT, followed by measuring the absorbance at 562 nm on a plate reader. The peptide concentration of the supernatant was determined using the Micro BCA standard plot. The percent HA binding was calculated using the following equation:

$$\%\ \text{HA binding} = \frac{[(\text{Peptide conc. with HA}) - (\text{Peptide conc. without HA})]}{(\text{Peptide conc. with HA})} \times 100$$

Scheme 5.1. Selective oxidation of N-terminal serine of PTH and site-specific conjugation of the oxidized PTH to HBPs though hydrazone linkage

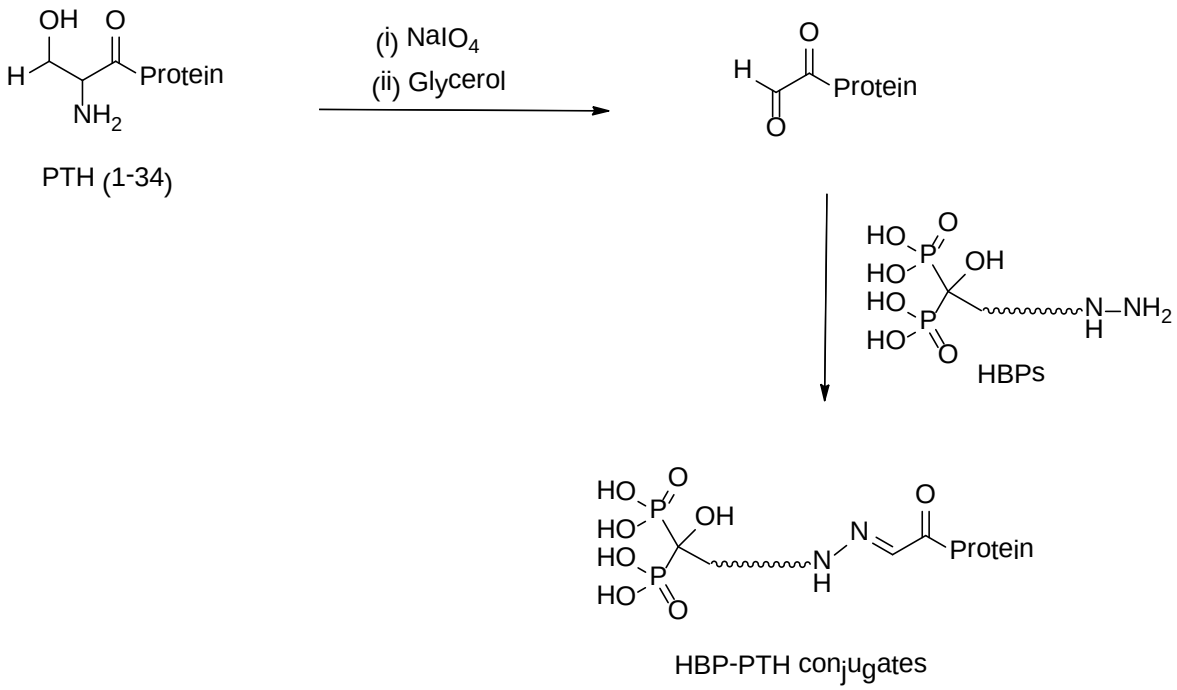

Immobilization and Bioactivity of PTH on Bone Surface. The HBP-PTH conjugates were immobilized on bone wafers (Scheme 5.2). Bone wafers were prepared from the midshaft cortical bone of a bovine femur. Cortical bone was first machined into a rod with 5 mm × 5 mm square cross-section and then sliced into 500 μm thick wafers. The bone wafers were thoroughly washed with deionized water and HEPES buffer (50 mM, pH 7.0). One hundred μL of sample aliquots (HBP-PTH conjugates and PTH) were diluted to 800 μL with HEPES buffer (50 mM, pH 7.0) to obtain a peptide or peptide conjugate concentration in the range of 10-30 μg/ mL. The diluted samples were then added to a 48-well plate containing a single bone wafer per well (in triplicate). The plate was incubated for 2 h at RT with continuous shaking. The supernatant was removed from each well, and the concentration of unattached protein was determined using the Micro BCA assay. The concentration of the immobilized or adsorbed peptide on bone wafers was calculated by subtracting the peptide concentration of the supernatant from the total peptide concentration added to bone wafer.

Scheme 5.2. *In vitro* targeting the HBP-PTH conjugates to bone surface. The conjugates were immobilized on bone wafers by simple mixing of conjugate solution to the bone wafers.

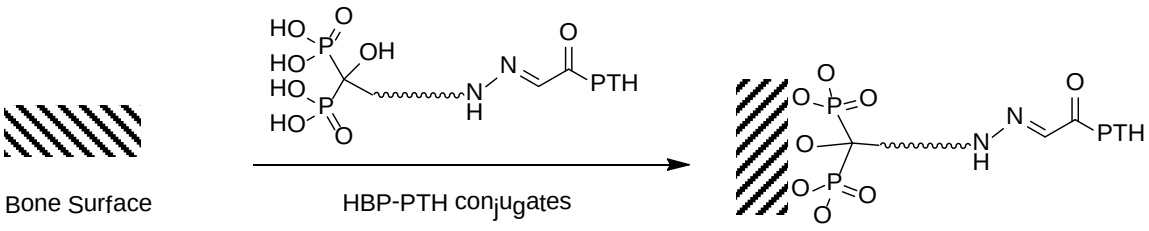

The bone wafers were washed twice with HEPES buffer (50 mM, pH 7.0) followed by a single wash with phenol red-free αMEM (supplemented with 10% FBS and 0.5 mM IBMX). The bioactivity of the adsorbed PTH and immobilized PTH through various HBPs on bone wafers were determined by measuring the intracellular cAMP contents in cells cultured on the bone wafers. In a typical experiment, pre-osteoblastic MC3T3-E1 cells were cultured in phenol red-free αMEM supplemented with 10% FBS. The cells were pretreated with 0.5 mM IBMX and seeded on each bone sample of the prepared 48-well plate at a density of 50,000 cells/well. The average amount of PTH immobilized per bone wafers (determined using the Micro BCA assay) was calculated, and the same amount of PTH and oxidized PTH were added to cell culture as a positive control. The plate was incubated for 15 min at 37 °C in a humidified atmosphere containing 5% CO_2, and the cultures were lysed directly in the medium with 0.1 M HCl. Intracellular cAMP was measured using a commercially available immuno-assay kit following the manufacturer's instructions. The cAMP data were normalized by the amount of DNA in each well, using a Hoechst assay as described in a previously reported procedure. In brief, standard solutions of DNA were prepared by serial dilution of calf thymus DNA with phenol red-free αMEM supplemented with 10% FBS and 0.5 mM IBMX. The cell lysates and the DNA standards were treated with Hoechst 33258 (0.5 μg/mL of a final concentration) in the dark for 10 min, followed by fluorescence measurement (λ_{ex} = 356 nm, λ_{em} = 458 nm). The data were corrected by subtracting the amount of cAMP/DNA produced by unstimulated (no PTH) cell cultures. The amount of cAMP/DNA produced by the immobilized and adsorbed PTH was determined.

Statistical Analysis. Data presented are mean ± standard deviation. A minimum of three replicates were used for each experiment. One-way analysis of variance (ANOVA) was conducted using GraphPad software (San Diego, CA). The results were considered significantly different when $p < 0.05$.

RESULTS

HBPs and Their *In vitro* Anti-resorptive Activities. The structures of HBPs (**1-7**) having spacers of different length and hydrophobicity are shown in Figure 2.1. These HBPs have not been studied for their anti-resorptive / proapoptotic properties. Therefore, *in vitro* activities of HBPs were determined using pre-osteoclast, RAW 264.7 cells. Results from the caspase-3 activity assay showed that, except for HBP **4**, HBPs at concentrations from 10^{-6} to 10^{-4} M did not have apoptotic effects on pre-osteoclasts as shown in Figure 5.1. HBP **4** did not show a significant apoptotic affect at the concentration range of 10^{-6} to 10^{-5} M, however at higher concentration (10^{-4} M), it showed about 3-4 fold higher apoptotic effect than control ($p < 0.05$). Similarly, alendronate also showed a significantly higher apoptotic affect than control ($p < 0.05$). Alendronate at 10^{-4} M concentration showed 1.5-2 fold higher apoptotic effect than HBP **4** at 10^{-4} M concentration ($p < 0.05$).

Results obtained by fluorescent microscopy support the data obtained from the caspase-3 experiments. As shown in Figure 5.2, no significant apoptosis of RAW 264.7 cells in response to HBPs was observed except for HBP **4**. HBP **4** at 10^{-4} M concentration resulted in significant numbers of apoptotic RAW 264.7 cells similar to alendronate ($p <$

0.05). HBP **4** at 10^{-4} M concentration caused almost 4- to 5-fold more apoptosis than did the control. Figure 5.2 also compares necrosis vs. apoptosis. Overall, necrosis caused by treatment with HBP or alendronate was much smaller than apoptosis. Similar to control, HBPs did not induced significant necrosis in RAW 264.7 cells. However, alendronate at 10^{-4} M concentration caused significantly higher necrosis than did the control and the other HBPs ($p < 0.05$).

***In vitro* Bioactivity of HBP-PTH Conjugates.** By measuring the metabolic activity of the cells after 72 h of treatment with HBP-PTH, it was found that pre-osteoblastic and pre-osteoclastic cells proliferated similar to the controls, where no conjugate was added. Moreover, the apoptosis assays also supported the results obtained from the viability assay and showed no significant apoptosis of pre-osteoclastic and pre-osteoblastic cells following HBP-PTH treatment for 72 h (Figures 5.3 and 5.4). Overall, the viability and apoptosis assays after 72 h of treatment with HBP-PTH on RAW 264.7 and MC3T3-E1 cells showed no significant difference in comparison to the control. Moreover, there was no significant effect of length and lipophilicity of the HBPs in the HBP-PTH conjugates in terms of cell metabolic activity and cytotoxicity.

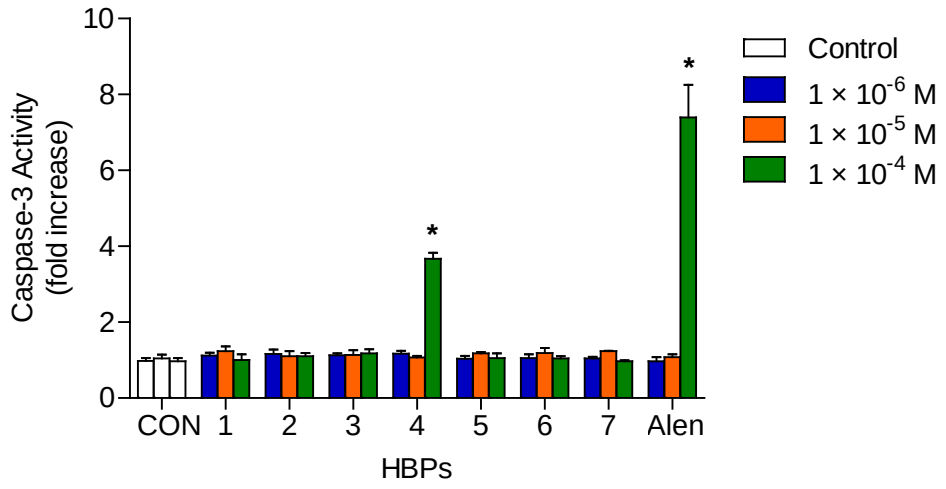

Figure 5.1. Quantification of apoptosis of osteoclastic RAW 264.7 cells by caspase-3 measurement. The cells were lysed, and caspase-3 produced by the cells was measured after 24 h of incubation with no BP (CON), HBPs (**1-7**) and alendronate (Alen) at different concentrations (1×10^{-6}, 1×10^{-5}, and 1×10^{-4} M). Error bars denote standard deviations ($n \geq 3$). (* indicates the values are significantly different from others $p<0.001$).

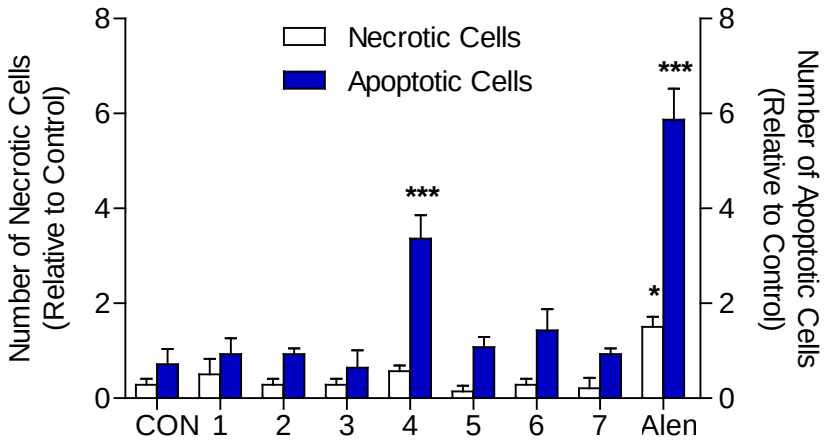

Figure 5.2. Quantification of apoptosis and necrosis of osteoclastic RAW 264.7 cells by fluorescent microscopy. The cells were stained using propidium iodide and Hoechst 33258 after 24 h of incubation with no BP (CON) and HBPs (**1-7**) at different concentrations (1×10^{-6}, 1×10^{-5}, and 1×10^{-4} M). The apoptotic and necrotic cells were determined by fluorescence microscopy and quantified using Image J software. The data are expressed as fold increase relative to the control. Error bars denote standard deviations ($n \geq 3$). (* indicates the values are significantly different from others, and *** indicates the values are significantly different from others and each other $p<0.05$).

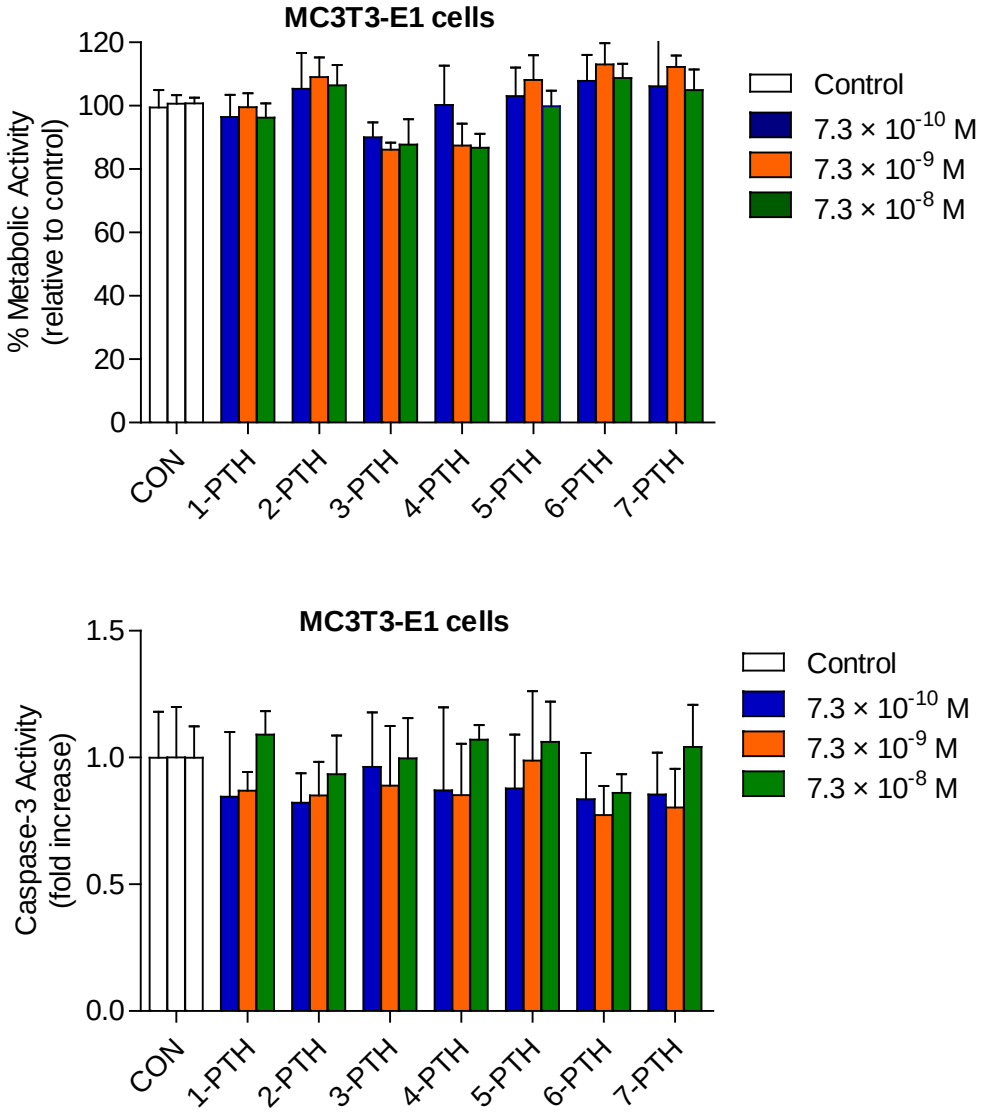

Figure 5.3. Percent cell viability and apoptosis of osteoblastic MC3T3-E1 cells measured after 72 h of incubation with no HBP-PTH (CON) and HBP-PTH conjugates at different concentrations (7.3×10^{-10}, 7.3×10^{-9}, and 7.3×10^{-8} M). Error bars denote standard deviations ($n \geq 3$).

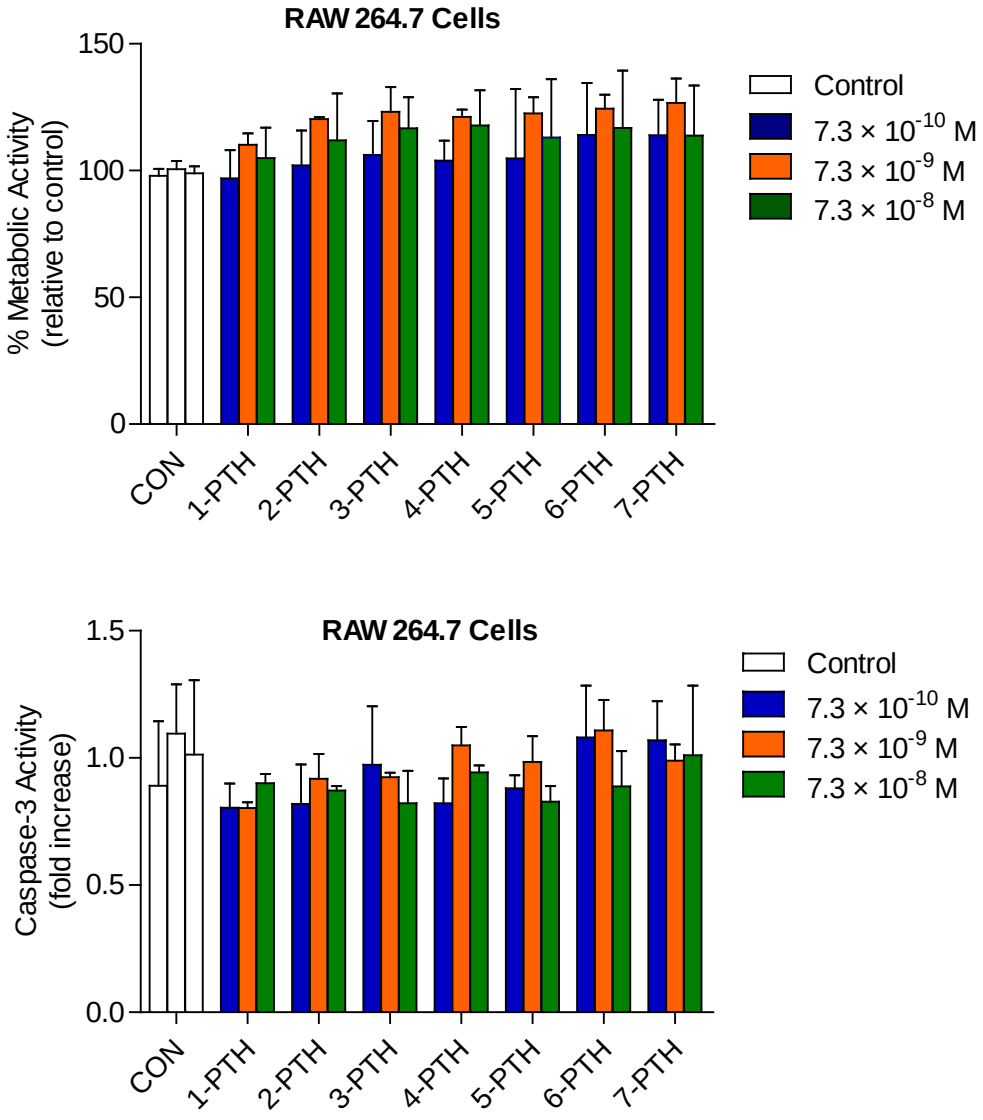

Figure 5.4. Percent cell viability and apoptosis of osteoclastic RAW 264.7 cells measured after 72 h of incubation with no HBP-PTH (CON) and HBP-PTH conjugates at different concentrations (7.3×10^{-10}, 7.3×10^{-9}, and 7.3×10^{-8} M). Error bars denote standard deviations ($n \geq 3$).

***In vitro* Mineral Binding Affinity of HBP-PTH Conjugates and PTH.** Mineral binding affinity of the HBP-PTH conjugates and PTH, determined using an HA binding assay, showed that the overall affinity of the PTH of HA increased after HBP conjugation. The results, expressed in percent HA binding in Figure 5.5, indicated 70-80% mineral binding affinity of PTH conjugated to HBPs, with one exception. Conjugate 7-PTH showed about 55% of peptide binding, which was significantly lower than for all other HBP-PTH conjugates. Overall, all the conjugates showed significantly improved HA binding over non-conjugated PTH ($p < 0.05$).

Amount of PTH Immobilized on Bone Wafers. By measuring the relative amount of PTH bound to the bone surface (Figure 5.6), it was found that the conjugation of HBP molecules significantly increased the amount of PTH immobilized on bone wafers ($p<0.05$). The amount of adsorbed PTH on bone wafers was significantly lower than the PTH immobilized through HBPs. The length or lipophilicity of the HBP did not have a significant effect on the amount of PTH attached on bone wafers.

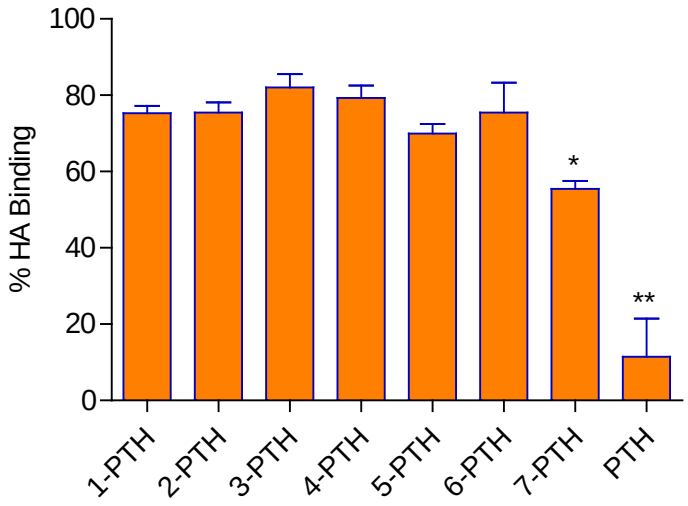

Figure 5.5. *In vitro* mineral affinity of HBP-PTH conjugates and PTH expressed in percent HA binding. The protein and protein conjugates were immobilized on HA. Immobilized protein was determined using the Micro BCA assay. Error bars denote standard deviations ($n \geq 3$). (* and ** indicate values that are significantly different from others $p < 0.05$).

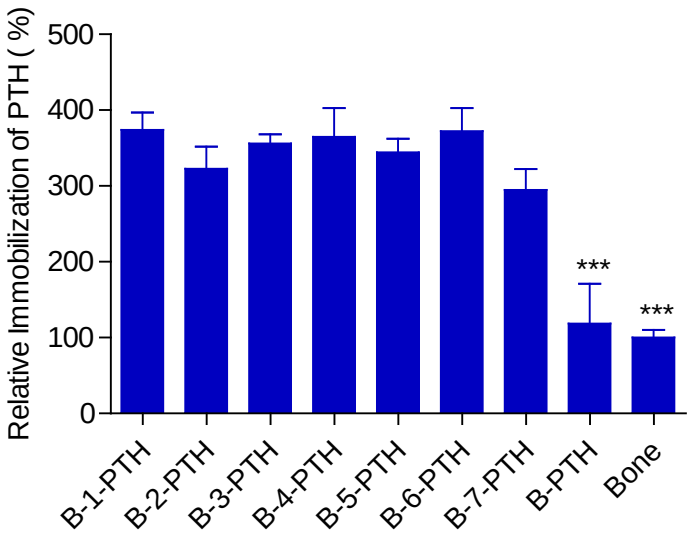

Figure 5.6. Quantification of PTH immobilized through HBP or PTH adsorbed on surfaces of bone wafers determined by the Micro BCA protein assay. PTH was immobilized on HA surfaces via seven different HBPs (**1**-**7**) (B-1-PTH through B-7-PTH) and by simple adsorption (B-PTH). Bone refers to the control experiment in the absence of any PTH or HBP-PTH. Error bars denote standard deviations ($n \geq 3$). (*** indicates the values are significantly different from others $p<0.05$).

Bioactivity of PTH Immobilized on Bone Wafers. Bioactivity of the immobilized PTH was determined by measuring the ability of the hormone fragment to stimulate the production of cAMP in pre-osteoblasts (MC3T3-E1 cells) (Figure 5.7). The amount of cAMP produced was normalized by the DNA content of the cell lysate. PTH immobilized through longer HBPs (**4**, **6**, and **7**) showed a significant increase in bioactivity compared to the adsorbed PTH, whereas PTH immobilized through shorter length HBPs (**1**, **2**, **3**, and **5**) did not show a significant increase in bioactivity ($p<0.05$). The adsorbed PTH demonstrated higher bioactivity than the control, where no PTH was added, but the effect was not statistically significant.

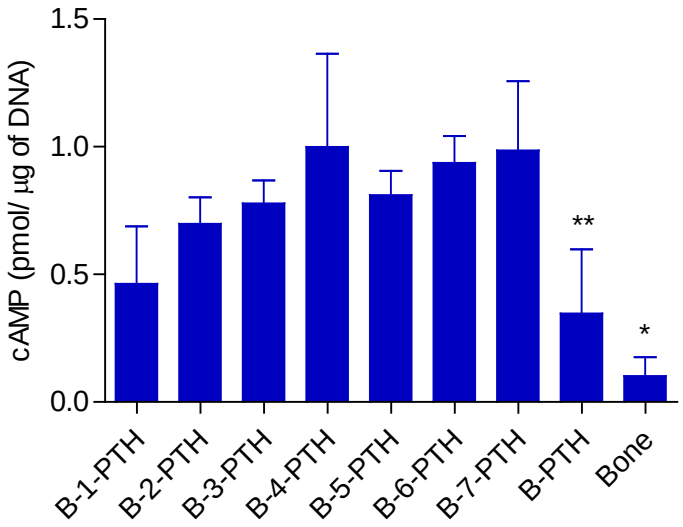

Figure 5.7. Intracellular cAMP content of MC3T3-E1 cells cultured on surfaces of bone wafers with immobilized or adsorbed PTH (1-34). PTH was immobilized via seven different HBPs (**1**-**7**) (B-1-PTH through B-7-PTH) and by simple adsorption (B-PTH). The amount of cAMP was normalized by the DNA content and the mass of the PTH present on the surface of the bone wafer. Error bars denote standard deviations ($n \geq 3$). (* indicates values that are significantly different from others except for PTH immobilized through HBP **1** and adsorbed PTH. ** indicates the values are significantly different from PTH immobilized through HBP **4**, **6**, and **7** $p<0.05$).

DISCUSSION

Targeted delivery of therapeutic agents to bone has been a subject of active investigation. Several methods have been explored, including use of D-aspartic acid octapeptide (*44*, *45*), polymalonic acid (*46*), tetracycline (*47, 48*), and BPs. Most of the reported systems explored the delivery of anti-catabolic agents that stop bone resorption but which do not promote bone formation. Anabolic molecules promote bone growth, and the majority are proteins and peptides. As such, these molecules have several types of functional groups, such as amines, carboxylates, thiols, and hydroxyls. Furthermore, each protein/peptide molecule likely has multiple copies of the same functional group. These commonly available functional groups can be useful for conjugation of the proteins with various drug delivery vehicles. Proteins can also be incorporated into polymeric scaffolds or micelles without any covalent bonding. Incorporation of anabolic molecules in drug delivery scaffolds might be good when materials are placed directly in the defect sites but not preferred for drug delivery through the systemic route. On the other hand, selective conjugation of protein/peptide molecules to a targeted delivery vehicle is challenging. It is critically important to retain the bioactivity of the protein/peptide after its conjugation and subsequent delivery to bone. A limited number of reports describe the delivery of anabolic protein biomolecule to bone tissue. In most of these reports, protein was modified through attachment of more than one targeting molecules, such as BPs, per protein molecule (*52, 130, 132, 168-170*).

We have explored the selective attachment of protein to a single molecule of bifunctional HBP, whose synthesis was discussed in Chapter Two (*176*). Because these

HBPs were reported to have enhanced affinity to bone mineral using a crystal growth inhibition assay and they are non-toxic to pre-osteoblasts (MC3T3-E1 cells) (*176*), they were deemed suitable candidate for delivery of biomolecules to bone mineral. HBPs have two phosphonates at one terminus causing affinity to bone mineral, while the other terminus, they have a hydrazine functionality, which can be conjugated to any aldehyde or ketone. In general, BPs are FDA-approved anti-resorptive agents and are being commonly prescribed for the treatment of bone diseases and cancer (*171*, *172*). Therefore, HBPs, which are derivatives of a widely prescribed drug, alendronate, should be suitable candidate to deliver biomolecules to bone tissue.

Alendronate has been sold by Merck under the brand name of Fosamax. Other commercially available BPs, such as risedronate, ibandronate, and zoledronate, are structurally similar to alendronate and HBPs except for their R^2 substituent. These BPs are effective anti-resorptive agents used in the treatment of various skeletal diseases. BPs are generally divided into two groups: BPs without nitrogen, or simple BPs, and N-containing BPs (N-BPs). N-BPs are more potent anti-resorptive agents than the simple BPs. Since HBPs are N-containing BPs and are structurally similar to alendronate, they could possess anti-resorptive properties. Therefore, we evaluated the toxicity and anti-resorptive properties of the HBPs on pre-osteoclasts (RAW 264.7 cells). The amount of caspase-3 produced by RAW 264.7 cells upon action of HBPs was measured to determine the extent of cell apoptosis. Apart from HBP **4**, all other HBPs induced no significant apoptosis or necrosis, thus demonstrating no anti-resorptive properties toward pre-osteoclasts. In general, nitrogen-containing BPs show higher drug potency (anti-resorptive activity) than BPs with no nitrogen. Alendronate, ibandronate, and

risendronate are the nitrogen containing BP showing high anti-resorptive properties. BPs interfere with the mevalonate biosynthetic pathway and affect cellular activity. In particular, they inhibit farnesyl diphosphate (FPP) synthase and stop biosynthesis of isoprenoid lipids, which are necessary for the prenylation of small GTPase signalling proteins. Discontinuation in cell signalling results in apoptosis of osteoclasts (*36, 177*). Although HBPs are structural derivatives of alendronate, they did not show any apoptotic activity, the exception being HBP **4**. This is not surprising because small structural changes can negatively affect drug activity. However, HBP **4** is the longest derivative of alendronate studied here, and it is possible that its terminal hydrazine might be able to reach the hydrophilic pocket of FPP synthase and inhibit it by forming additional hydrogen bonds in the FPP binding pocket. Presumably, therefore, HBP **4** showed pre-apoptotic affects.

In the present studies, PTH (1-34) was used as an anabolic agent. PTH (1-34) is the truncated version of PTH (1-84) with intact bone forming properties (*77*). In general, proteins with an N-terminal serine or threonine can be oxidized using sodium periodate under controlled conditions to obtain proteins with N-terminal aldehyde (*135, 173-175*). Since PTH (1-34) has a serine at its N-terminal, it was oxidized using sodium periodate to obtain an aldehyde, which was selectively conjugated to hydrazine of the HBPs through a hydrazone linkage. The obtained HBP-PTH conjugates were studied in terms of their *in vitro* toxicity and pro-apoptotic/anti-resorptive properties (Figures 5.3 and 5.4). The conjugates were found to be non-toxic to pre-osteoclastic and pre-osteoblastic cells. Therefore, it can be stated that HBPs and HBP-PTH conjugates could be used for further investigation of drug delivery.

Since HBPs demonstrate enhanced affinity to bone mineral, they should be able to deliver PTH to bone tissue. In other words, PTH should gain bone affinity after its conjugation to the HBPs. In general, it is reasonable to expect increased affinity when multiple BPs are attached to a single protein/peptide molecule. However, it was not known whether a single BP on PTH would substantially enhance binding relative to unconjugated PTH. HA binding of the HBP-PTH conjugates was found to be significantly higher than PTH. No significant effect of length or lipophilicity of HBPs was observed on the binding affinity of HBP-PTH conjugates except for 7-PTH. Conjugate 7-PTH was found to have significantly lower binding affinity than the remaining conjugates. However, the binding affinity of 7-HBP was found to be significantly higher than that of PTH ($p<0.05$). HBP **7** is the longest HBP with hydrophic spacer. It is possible that hydrophilic spacer interacts with PTH and makes the phosphonates functionalities of HBPs less available for mineral binding. Overall, all HBP-PTH conjugates had around 60 to 80% higher HA binding affinity over PTH. From these results it can be stated that the HBPs can be used to bind the conjugated PTH to bone tissue.

To determine the effect of the length or lipophilicity of the HBPs on the amount of PTH delivered to bone, HBP-PTH conjugates were mixed with bone wafers. The relative amount of the immobilized PTH on bone wafers through HBPs was found to be similar, which again proved the insignificant effect of length and lipophilicity of HBPs on the amount of protein delivered to bone. However, the amount of PTH immobilized through HBPs was significantly higher than adsorbed unconjugated PTH. These findings support the previously found increase in the bone affinity of PTH by HBP conjugation.

The ultimate purpose of delivering an anabolic biomolecule to bone through attachment of a single HBP molecule per anabolic molecule was to avoid a loss of bioactivity. To determine the bioactivity of the delivered PTH to bone, the PTH immobilized on bone wafers through HBPs was incubated with MC3T3-E1 cells (pre-osteoblasts), and the increase in the intracellular content of cAMP in the osteoblastic cells was measured. Overall, PTH delivered or immobilized through HBPs showed increased osteoblastic cell interactions compared to the adsorbed PTH and no PTH (control). In general, the effect of the immobilized (delivered) PTH on bone was mediated through the PTH/PTHrP (PTH related-protein) receptor of the cell. PTH/PTHrP is a G-protein coupled receptor, which binds to PTH at its N-terminal region (*178, 179*). Since the cell surface receptor binds to the N-terminal region of PTH, PTH immobilized through the longer HBPs might be expected to show higher bioactivity and vice versa. However, the bioactivity of the PTH immobilized through HBPs was not significantly affected by the length or lipophilicity of HBPs, which indicates that differences in the relative length of HBP are too small to alter the interactions between the immobilized PTH and receptor. In other words, HBPs are long enough to prevent interaction of the attached protein with the bone surface, or HBPs are not too long to prevent protein interactions with bone surface by folding of HBPs. In either case, protein might lose its bioactivity by interacting with bone surface. On the other hand, the N-terminus of the immobilized PTH, which is responsible for cell binding, appears to be accessible to the cell surface receptors, which is demonstrated by the production of cAMP. Overall, it can be stated that HBPs could deliver the attached protein to bone in a bioactive as well as accessible mode for improved cell interactions. It should be also noted that although PTH binds to its receptor

through its N-terminus, conjugation of HBPs at the N-terminus of PTH did not preclude peptide-receptor interaction.

CONCLUSIONS

Targeted delivery of therapeutic agents to bone reduces the drug toxicity and dosage frequency by distributing these agents with a more uniform effect at the bone surface. However, delivering therapeutic protein/peptide to bone is challenging because of their size and delicate nature. If the proteins are delivered to bone through a small delivery vehicle with minimum modification in the protein structure, the bioactivity and accessibility of the protein may be improved. The presented studies were intended to demonstrate the ability of improving the mineral affinity and delivery of the protein/peptide to bone through attachment of a single molecule of HBPs to the PTH to improve cell interactions at the bone surface. HBP **4** showed a significant drug potency (anti-resorptive/proapoptotic effects), similar to that of alendronate. PTH not only gained mineral binding affinity by its selective conjugation with HBPs, but conjugation also improved the cell interactions after its delivery to the bone surface; the observed effects were independent of the length and lipophilicity of the HBPs. Overall, the approach described for delivering PTH could be applicable to any therapeutic protein with an intrinsic N-terminal serine or threonine, and may improve cell/tissue responses for bone regeneration and/or faster recovery from a diseased state. It should be noted that even if a desired protein does not contain an intrinsic N-terminal serine or threonine, one could be introduced through conventional molecular biological methods.

CHAPTER SIX

CONCLUSIONS AND FUTURE RESEARCH

Skeletal diseases, bone injuries, and bone loss have a major impact on the worldwide population and economy. Although several therapeutic agents and treatments are available for addressing bone diseases, they are not being fully utilized because of their uptake at non-targeted sites and related side effects. Similarly, several biomaterials are being explored for the replacement of diseased or lost bone; however, their biocompatibility and their efficient interactions with the surrounding cells/tissue for bone regeneration have hardly been achieved. Active targeting with controlled delivery is an ideal approach for the treatment of skeletal diseases, while the site-specific immobilization of a bioactive protein on the bone implant material would be one of the most preferred ways to achieve biocompatibility and enhanced cell/tissue interactions. Because BPs are known to have high affinity to bone and are being widely used in treatment of various skeletal diseases, they are well-suited for drug targeting to bone as well as for bone tissue engineering applications. In this work, we have described the synthesis of bifunctional BPs and their utilization for the targeted delivery of therapeutic agents to bone as well as for oriented immobilization of bioactive proteins/peptides on bone implant materials.

Chapter Two and Three described the synthesis, characterization, and utilization of various bifunctional BPs for delivery of therapeutic agents. Crystal growth inhibition studies showed that the synthesized HBPs with spacers of varying length and lipophilicity

have high affinity to HA, while HBPs with shorter spacers bind stronger than alendronate to HA. Thus, the structural modifications improved the bone mineral affinities of BPs. HBPs were also evaluated for their non-cytotoxicity to the pre-osteoblast cells and by which they qualified for their *in vivo* applications. A model drug was conjugated to HBPs through hydrazone linkage, and its *in vitro* delivery to bone mineral was demonstrated at acidic pH. Overall, HBPs are non-toxic molecules with high affinity to bone mineral and could be used for targeted delivery of therapeutic agents to the sites of wound healing and bone resorption. Thus, the strategy of targeted delivery of drugs through HBP should improve the drug exposure to the diseased site and reduce the toxic effects due to their uptake at undesired sites.

Future work with respect to the work described in Chapters Two and Three should include the evaluation of binding affinities of HBPs in actual body fluids serum. This would indirectly elucidate the behavior of HBPs in the body. Furthermore, a small fluorescent molecule with the aldehyde functionality could be conjugated to HBPs through hydrazone linkage and delivered to mice or rats through an intravenous injection. Because of their bone affinity, HBPs would direct the attached fluorophore to bone sites, which could be analyzed by measurement of fluorescence. Moreover, the rate of release of fluorescent molecules could be detected.

Oriented immobilization of proteins is an important step in creating protein-based functional materials because it anchors the protein at a preferred location and enhances the usefulness of the protein for the desired application. However proteins are generally very complex molecules with various functional groups and it is critical to demonstrate a selective reaction of protein. Moreover, a small variation in the structure of protein could

result in the loss of bioactivity of the protein. Therefore, it is difficult to immobilize proteins with their bioactive and accessible state on the solid surface for specific biological actions.

Chapter Four has described a method to orient proteins, through HBPs, on HA surfaces, a widely used bone implant material. EGFP and β-lactamase, which have a serine and threonine at their N-terminus, respectively, were used as model proteins. They were treated with sodium periodate and immobilized on the HA surface that was modified with HBPs of varying length and lipophilicity. Thus, the selective oxidation of proteins with N-terminal serine or threonine could lead to a unique amino-terminal aldehyde functionality. Since hydrazine of HBPs selectively reacts with aldehydes and/or ketones at acidic pH where other nucleophilic functionalities of protein are nonreactive, a site-specific orientation of the proteins through HBPs is possible. The data demonstrate that the length or lipophilicity of HBPs had no significant effect on the amount of hydrazine functionalities as well as the amount of protein immobilized on HA surface. Moreover, HBP-immobilized protein showed improved bioactivity compared to the adsorbed protein. Since proteins can be engineered to introduce serine or threonine at their N-terminus for subsequent oxidation to get a single aldehyde, HBPs could be used for effective and bioactive immobilization of any protein. Therefore, the strategy of oriented immobilization of bioactive proteins presented in Chapter Four could be used in tissue engineering applications to improve the biocompatibility of implant materials. It will also provide an insight in various applications such as protein microarrays, biosensors, biotechnology, chemical manufacturing, nanotechnology, single molecule enzymology, and drug discovery.

The work described in Chapter Four can be further extended to bone growth proteins, such as bone morphogenetic proteins (BMPs). In general, bone fracture and bone loss are serious and growing concerns of society. The major challenges facing the treatment of bone loss are selective regeneration of bone tissue and controlling the bone regeneration at a desired site. BMPs are osteoinductive growth factors. They differentiate stem cells into osteoblasts and promote bone formation. However, they could form bone tissue anywhere in the body. Therefore, the use of the exogenous BMPs is highly regulated, challenging and costly. However, using the strategy presented in Chapter Four, BMPs could be immobilized on bone implant and studied for their improved bioactivity. Briefly, BMPs can be genetically modified to obtain N-terminal serine or threonine, followed by their selective oxidation and immobilization on ceramic implants. The bioactivity of the immobilized BMPs can be demonstrated by the addition of stem cells on implant surfaces followed by its incubation for a few days. The oriented immobilization of BMPs on ceramic implants will modulate the surrounding stem cell behavior for controlled bone regeneration. The bone formation could be analyzed by the alkaline phosphatase (ALP) activity and osteopontin mRNA expression.

There are several drugs available for osteoporosis, but most of the drugs (such as BPs) control bone resorption and do not promote bone formation. On the other hand, there are various therapeutic proteins/peptides, such as bone growth factors, PTH, etc., which could be used for bone formation. In general, delivery of bioactive therapeutic protein/peptide to bone is very difficult and hence use of therapeutic proteins in clinical settings is limited.

Chapter Five described a strategy to deliver the therapeutic protein/peptide using a single molecule of HBPs to improve the tissue/cell interactions at a bone surface. PTH (1-34), the only currently available anabolic agent for treatment of osteoporosis, was used as a model of bioactive macromolecule. PTH was selectively oxidized with periodate to obtain an N-terminal aldehyde that was then conjugated to HBPs of varying length and lipophilicity. The mineral binding study demonstrated that HBP conjugation improves the binding affinity of PTH independent of length and lipophilicity of the HBPs. PTH delivered through HBPs also showed the improved cell interactions. The approach presented in Chapter Five could be used for the delivery of therapeutic proteins/peptides to bone tissue and could potentially promote bone formation.

Chapter Five also investigated the cytotoxicity and the pro-apoptotic/anti-resorptive properties of HBPs and HBP-PTH conjugates with preosteoclastic cells (RAW 264.7). The results showed that HBP **4** has significant drug potency, while other HBPs have zero drug potency. Thus, small modifications in BP structure could alter the anti-resorptive properties of BP. Since BPs binds to FPP synthase causing inhibition of the resorptive function of osteoclasts, small changes in BP structure presumably alters the binding affinity of BP to FPP synthase and leads to a change in drug potency.

The research work presented in Chapter Five could be extended to demonstrate the *in vivo* delivery of protein in animal models (such as mice or rats). In brief, radio labeled PTH can be oxidized, conjugated to HBPs, followed by the intravenous injections of the HBP-PTH conjugates to mice. After a few hours of the injection, the mice can be analyzed for accumulation of PTH at skeletal sites. Furthermore, bioactivity of the delivered PTH can be measured by analyzing bone formation. This would require the

intermittent injections of higher amounts or infusion of low doses of the HBP-PTH conjugates. The bone formation could be analyzed after a few weeks. Scanning electron microscopy (SEM), FT-IR, X-ray Diffraction (XRD), and high-resolution X-ray computed tomography (micro-CT) could be used to determine the surface area, thickness or extent of mineralization of the mice bone.

In conclusion, various bifunctional HBPs with varying length and lipophilicity, were synthesized. HBPs were demonstrated to have high binding affinity to bone mineral and zero cytotoxicity. The drug potency of HBPs were also demonstrated by cell apoptosis, cell proliferation, and fluorescence microscopy and found that HBP **4** has higher drug potency than control. Furthermore, HBPs were successfully used for the targeted delivery of a model drug to bone. HBPs were utilized for oriented immobilization of proteins (EGFP and β-lactamase) on bone implants for improved bioactivity. Moreover, targeted delivery of bioactive peptide (PTH) to bone mineral was demonstrated *in vitro* using a single molecule of HBPs. Overall, novel HBPs were developed for various bone related applications. This research should provide further insight towards potential applications of bifunctional BPs towards the targeted delivery of therapeutic agents to bone and bone tissue engineering applications.

APPENDIX ONE

ANTICANCER DRUG POTENCY OF BIFUNCTIONAL BISPHOSPHONATES

Cancer is a debilitating disease that has a huge impact on world health and economy. It is the main reason of death in the United States, causing one in four deaths (*180*). Cancer is the uncontrolled growth of malignant cells in the body. The malignant cells divide, grow and form a malignant tumor by invading neighboring tissues/organs of the body. There are various types of cancers, such as prostate, colon, lung, breast, skin, etc. At the advanced stage, cancer can be spread to other parts of the body. Since the microenvironment of bone is suitable for tumor growth, cancer cells spread to bone tissue and develop bone metastases. Bone metastasis is a complex process, which could lead to osteolytic and/or osteoblastic lesions and causes many devastating events. Multiple myeloma, breast, lung, and prostate cancers are most likely to result in metastasis to bone (*181-183*). Therefore, along with anticancer therapies, treatment to prevent bone metastases is crucial.

In general, bone metastasis involves a series of steps: (a) angiogenesis in the primary tumor, (b) Invasion of malignant cells into circulation, (c) adhesion of malignant cells, (d) infiltration of malignant cells in the bone microenvironment, and (e) proliferation of malignant cells in bone. Bone metastasis could be avoided by controlling one of the above processes (*184*). Various therapies are being explored for the treatment of bone metastasis. Radiotherapy, chemotherapy, surgery, analgesics, and endocrine treatment are the conventional methods to treat cancer as well as skeletal complications

from bone metastasis. However, most of these treatments are not sufficient to control bone destruction or related complications by bone metastasis (*181*).

Recently, BPs have demonstrated a great potency in the treatment of malignant bone diseases by reducing the symptoms and complications related to bone malignancy. In addition to the antiresorptive property, BPs also possess antitumor properties against many cancer types. Especially nitrogen containing BPs, such as zoledronate, have shown anti-proliferative and apoptotic effects in cancer cells (*185-187*). Herein, we have explored the anticancer properties of the bifunctional HBPs, which were synthesized for targeted delivery of therapeutic agents to bone (described in Chapter Three). HBPs have nitrogen atoms in the form of amide and hydrazine functionalities at their R^2 substituent. Moreover, one of the HBPs showed apoptotic effects to preosteoclasts (described in Chapter Five). This has increased the possibility of HBPs to have anticancer properties. Therefore, we have explored the *in vitro* anticancer potencies of HBPs. In particular, HBPs were studied for breast, lung, and prostate cancers using MCF-7, H460, and PC-3 cells, respectively. Anticancer drug potencies of HBPs were demonstrated by measuring proliferative and apoptotic effects of HBPs on cancer cells.

EXPERIMENTAL SECTION

Materials. The breast cancer (MCF-7), lung cancer (H460), and human prostate carcinoma (PC-3) cell lines were obtained from American Type Culture Collection (ATCC, Rockville, MD). Roswell Park Memorial Institute 1640 (RPMI 1640), Dulbecco's Modified Eagle's Medium (DMEM), and fetal bovine serum (FBS) were

purchased from GIBCO-Invitrogen (Carlsbad, CA). The cell proliferation reagent WST-1 was purchased from Roche (Mannheim, Germany). Ac-DEVD-AFC was obtained from Enzo Life Sciences (Plymouth Meeting, PA). Aprotinin bovine, 3-[(3-cholamidopropyl)dimethylamino]-1-propanesulfonate (CHAPS), DL-dithiothreitol (DTT), etoposide, ethylenediaminetetraacetic acid disodium salt dehydrate (EDTA), glycerol, 4-(2-hydroxyethyl)piperazine-1-ethanesulfonic acid (HEPES), leupeptin hemisulfate salt, orthovanadate, phenylmethylsulfonylfluoride, potassium hydroxide, sodium acetate, sodium chloride, sodium hydroxide, sodium fluoride (NaF), sodium tris(hydroxymethyl)aminomethane hydrochloride (Tris-HCl), and Triton X-100 were purchased from Sigma-Aldrich (St. Louis, MO). Calcium chloride, hydrochloric acid, and potassium dihydrogen phosphate were obtained from EMD Chemicals (Gibbstown, NJ).

Hydrazine-Bisphosphonates (HBPs). HBPs (**1**-**7**) of various length and lipophilicity were synthesized according to the previously reported procedure (*81, 107, 134*) (Figure 2.1). All seven HBPs have terminal hydrazine and at least one amide group.

***In vitro* Activity of HBPs.** HBPs were explored for their proliferative and apoptotic effects using three different cancer cells (MCF-7, H-460, and PC-3). To study the *in vitro* proapoptotic activity of HBPs, MCF-7 and H460 cells were cultured in pre-warmed RPMI medium, while PC-3 cells were cultured in pre-warmed DMEM medium at 37 °C in a humidified atmosphere composed of 5% CO_2. Both the types of medium were supplemented with 10% FBS for the *in vitro* studies. The cells were seeded into 96-well plates at density of 5×10^3 cells/well for *in vitro* quantification of cell proliferation

and caspase-3 activity. One day after the cell seeding, the cultures were treated with various concentrations (10^{-6}, 10^{-5}, 10^{-4}, and/or 10^{-4} M) of HBPs. Cells without HBPs were used as a negative control, while cells treated with 10^{-6}, 10^{-5}, or 10^{-4} M of etoposide were used as positive controls. Cells were also treated with 10^{-8}, 10^{-7}, or 10^{-6} M of camptothecin for positive controls. The plates were incubated again for 24, 48, and 72 h before their use for further analysis. The experiments were conducted in triplicate and repeated at least three times to ascertain the reproducibility of the results.

Cell Proliferation Assay. The cell proliferation in presence of HBPs was determined using a colorimetric WST-1 assay. The assay was conducted after 24, 48, and 72 h of HBP treatment in accordance with the manufacturer's instructions. In brief, cultures in 96-well plates were incubated with 10 µL/well of cell proliferation reagent WST-1 at 37 °C for 60 min in a humidified atmosphere composed of 5% CO_2. The plate was cooled to RT, and the absorbance of the samples was measured at 450 nm on a plate reader.

Apoptosis Assay. Cell apoptosis was determined by measuring the intracellular caspase-3 activity. The cultures were lysed by 10 min of incubation in 50 µL of lysate buffer (20 mM Tris-HCl, pH 7.4, 150 mM NaCl, 1 mM EDTA, 10 mM NaF, 1 mM sodium orthovanadate, 5 µg/ml leupeptin, 0.14 U/ml aprotinin, 1 mM phenylmethylsulfonylfluoride, and 1% (v/v) Triton X-100), followed by 2 s of sonication. The cell lysate was treated with 50 µM Ac-DEVD-AFC in 50 mM HEPES buffer (pH 7.4, 100 mM NaCl, 0.1% CHAPS, 10 mM DTT, 1 mM EDTA, and 10% (v/v) glycerol)

at RT for 60 min in the dark. The caspase-3 activity was determined by measuring the fluorescence at λ_{em}=510 nm (λ_{ex}=485).

Statistical Analysis. Data are presented are mean ± standard deviation. A minimum of three replicates were used for each experiment. One-way analysis of variance (ANOVA) was conducted using GraphPad software (San Diego, CA). The results were considered significantly different when $p < 0.05$.

RESULTS AND DISCUSSION

Bone tissue is the most preferential site for cancer metastasis. Breast, lung, and prostate cancers, are the common cancers primarily transmitted to bone tissue and cause bone metastases. In the United States, about 300,000 - 400,000 people die from bone metastasis each year (*188*). In bone metastasis, overall osteoclastic bone resorption increases and bone mineral density reduces rapidly. It causes several symptoms, such as extreme pain, multiple skeletal fractures, spinal-cord compression, etc. Since BPs have been widely used in clinical settings for treatment of skeletal diseases, they are also being explored for the treatment of bone metastases (*189*). As such, BPs control the osteoclast-mediated bone resorption. Recent studies also suggested that BPs could influence the tumor growth by cell apoptosis or by inhibiting cell proliferation (*181, 182, 190*). In general, BPs could have direct or indirect antitumor effects in cancer. Direct apoptosis of breast, lung, and prostate cancer cells by BPs was demonstrated in a dose and time dependent manner (*191*). BPs also inhibit bone metastases by controlling the key steps

involved therein. Alendronate, clodronate, ibandronate, pamidronate, and zoledronic acid showed the dose-dependent inhibition of breast and prostate cancer cell adhesion to mineralized and non-mineralized bone matrices. The effect was not observed with normal cells (*192, 193*). In other words, BPs attached to the bone surface inhibit tumor cell adhesion and invasion, and control bone metastases. Zoledronic acid showed the inhibition of growth factor–stimulated proliferation of endothelial cells *in vitro*. It also demonstrated the dose-dependent inhibition of angiogenesis *in vivo* (*194*). Several direct or indirect antitumor effects of BPs have been discovered.

Overall, nitrogen containing BPs are more efficient anticancer agents. Since HBPs have inbuilt nitrogen and had never been explored for their anticancer activities, here we have studied the anticancer drug potency of HBPs. Widely used colorimetric WST-1 assay was demonstrated to determine the effect of HBPs on cell proliferation. Cell apoptosis by HBPs was determined by measuring the intracellular caspase-3 activity. Since breast, lung, and prostate cancers are mostly prone for bone metastases, MCF-7, H460 and PC-3 cells were chosen for this study. HBPs were tested at doses ranging from 10^{-6} to 10^{-3} M. Studies were performed for 24, 48, and 72 h, and assays were done after every 24 h.

Results of MCF-7 cell proliferation assays after 72 h of the addition of HBPs showed that the cell proliferation was significantly different for all four concentrations (1.0×10^{-6}, 1.0×10^{-5}, 1.0×10^{-4} M, and 1.0×10^{-3} M) of HBPs studied than for the control ($p < 0.05$). A dose dependent decrease of the survival of MCF-7 cells was observed (Figure 7.1). However, the results of the caspase-3 assay after 72 h of HBP addition showed no significant apoptosis at all four concentrations (1.0×10^{-6}, 1.0×10^{-5},

1.0×10^{-4}, and 1.0×10^{-3} M) of HBPs. A total of seven different analogues of HBPs of varying length and lipophilicity were studied. However, the cytotoxic affects of HBPs were found not to be dependent on the length or lipophilicity of HBPs. Overall, HBPs, at 10^{-3} M concentration, were cytotoxic to MCF-7 cells and reduced cell proliferation, but did not exhibit cell apoptosis.

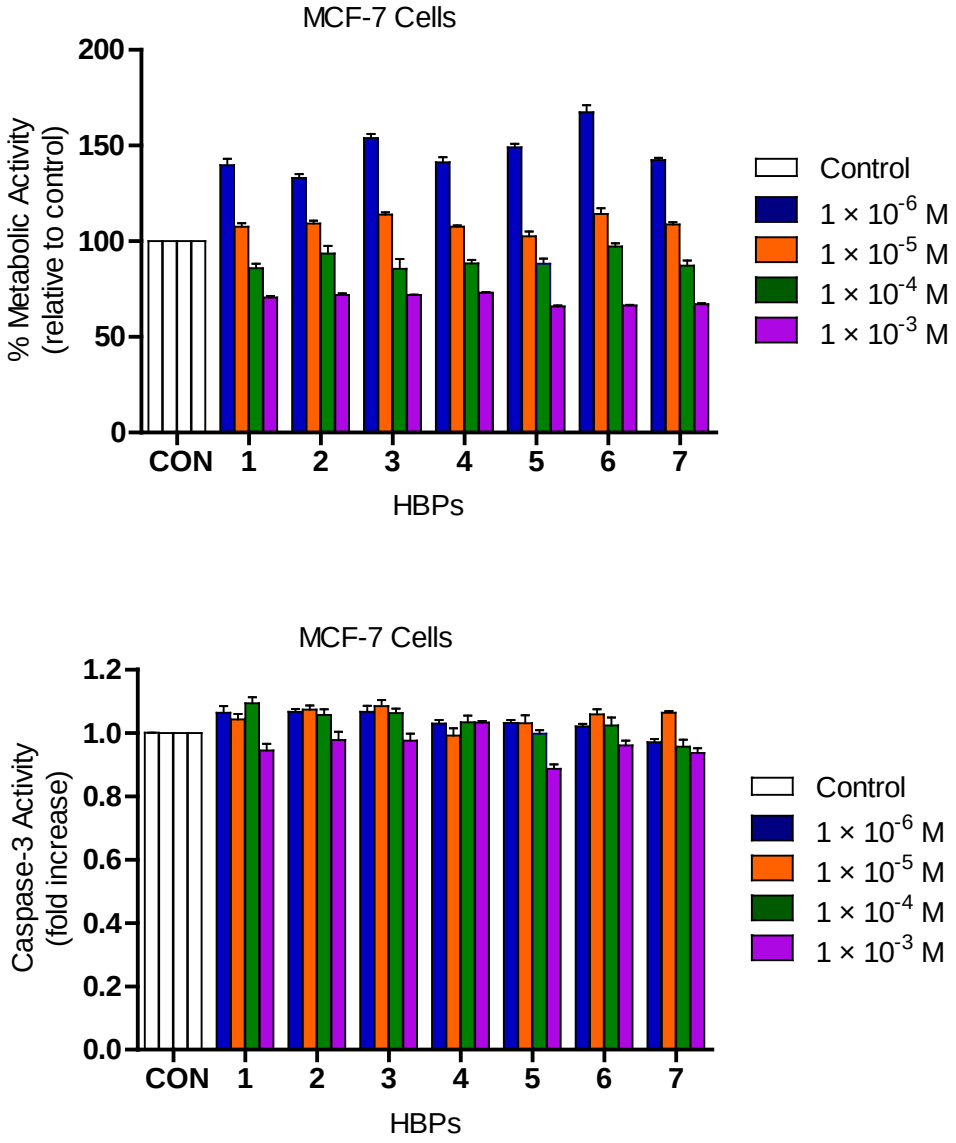

Figure 7.1. Percent metabolic activity and apoptosis of MCF-7 cells. For all experiments, the cell were measured after 72 h of incubation with no HBP (CON) and HBP **2**-**8** at different concentrations (1.0×10^{-6}, 1.0×10^{-5}, 1.0×10^{-4} M, and 1.0×10^{-3} M). Error bars denote standard deviations ($n \geq 3$).

In the case of lung cancer, cell proliferation and cell apoptosis was demonstrated at three different concentrations (1.0×10^{-6}, 1.0×10^{-5}, and 1.0×10^{-4} M) of HBPs. The results shown in Figure 7.2 indicate that the HBP-treated cells behave similar to the control. Overall, HBPs did not cause a cytotoxicity or apoptosis of H460 cells for 72 h. For prostate cancer, HBPs of four different concentrations (1.0×10^{-6}, 1.0×10^{-5}, 1.0×10^{-4}, and 1.0×10^{-3} M) were studied. It was observed that HBPs have no cytotoxic and apoptotic effects on PC-3 cells for 72 h. The results are shown in figure 7.3.

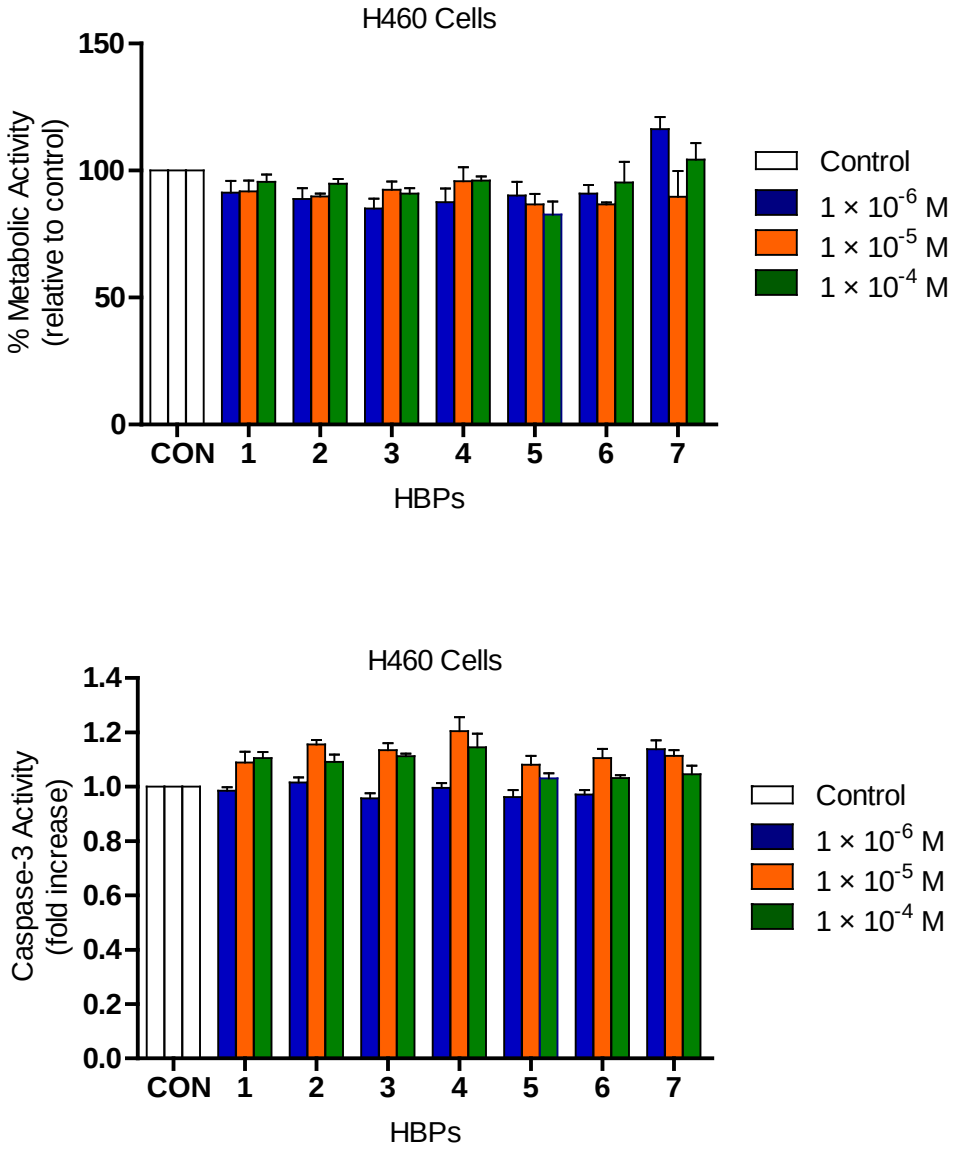

Figure 7.2. Percent metabolic activity and apoptosis of H460 cells. For all experiments, the cell were measured after 72 h of incubation with no HBP (CON) and HBP **2-8** at different concentrations (1.0×10^{-6}, 1.0×10^{-5}, and 1.0×10^{-4} M). Error bars denote standard deviations ($n \geq 3$).

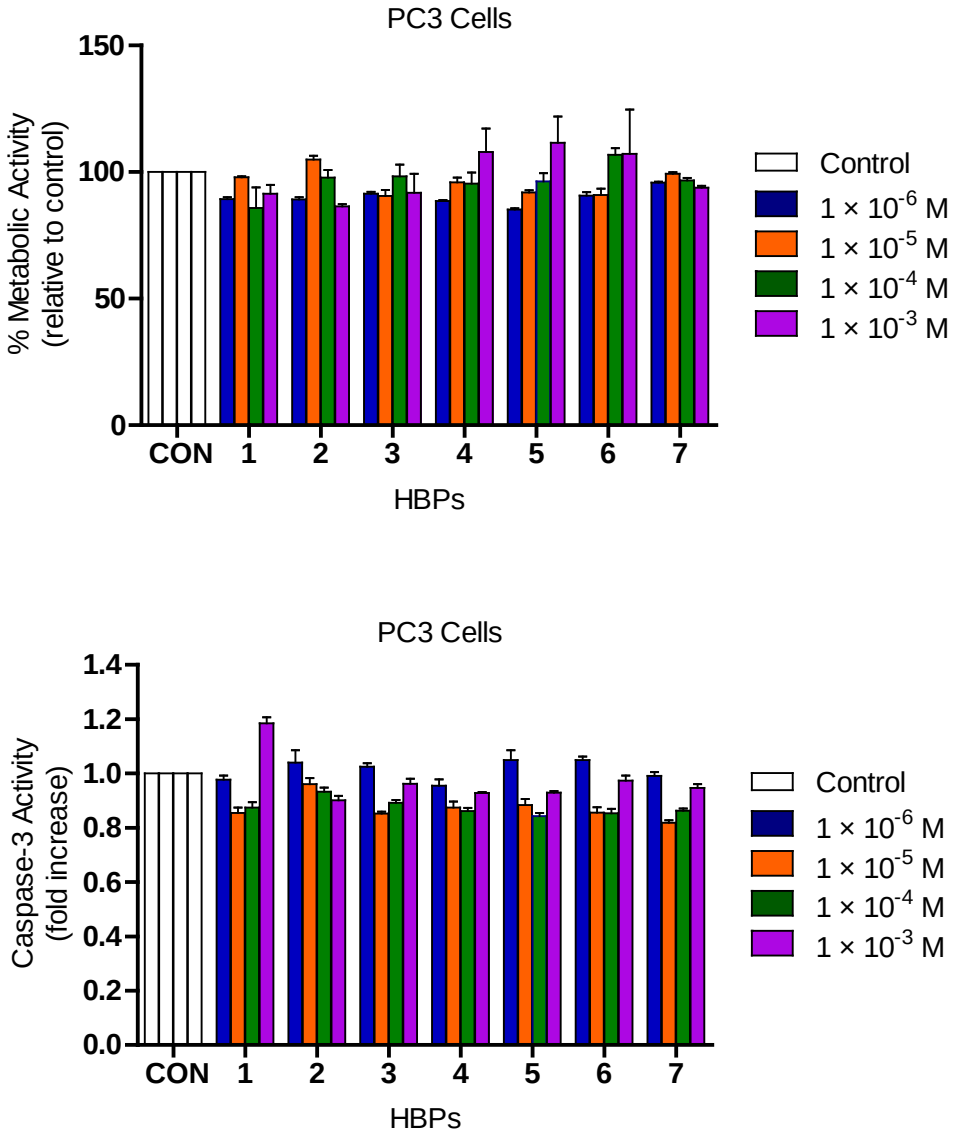

Figure 7.3. Percent metabolic activity and apoptosis of PC3 cells. For all experiments, the cell were measured after 72 h of incubation with no HBP (CON) and HBP **2**-**8** at different concentrations (1.0×10^{-6}, 1.0×10^{-5}, 1.0×10^{-4} M, and 1.0×10^{-3} M). Error bars denote standard deviations ($n \geq 3$).

Overall, our study confirmed that HBPs could have anticancer activity and it might vary with the type of cancer. The presented study did not concern the molecular mechanism of action of BPs to cancer cells. However, most of the nitrogen containing BPs interfere with the mavalonate pathway and inhibit cell functioning and cause cell death. Since HBPs have nitrogen in the form of hydrazine and amide functionality, presumably, they might have inhibited the mavalonate pathway and caused toxicity to MCF-7 cells. At the same time, other mechanisms of cell toxicity cannot be denied.

CONCLUSIONS

Skeletal tissue is the common metastatic site for various cancers. Breast, lung and prostate cancers are more invasive cancers and frequently cause bone metastases. BPs such as zolendronate are being used in the treatment of devastating cancers to control bone metastases. However, new BPs with higher anticancer drug potency need to be developed. The presented research is intended to demonstrate the anticancer drug potencies of the novel HBPs. All seven HBPs showed *in vitro* cytotoxic effects and no apoptotic effects to breast cancer cells. However, HBPs showed neither toxic nor apoptotic effects to lung and prostate cancer cells. Overall, anticancer drug potencies of HBPs vary with the type of cancer and therefore need to be studied for various other types of cancer cells.

REFERENCES

1. Ducy, P., Schinke, T., and Karsenty, G. (2000) The osteoblast: A sophisticated fibroblast under central surveillance, *Science 289*, 1501-1504.
2. Delahay, J. N. (2010) Basic science of bone and cartilage metabolism, In *Essentials of Orthopedic Surgery* (Wiesel, S. W., and Delahay, J. N., Eds.), pp 1-34, Springer New York.
3. Dawson-Hughes, B. (2010) Acid–base balance, bone, and muscle, In *Nutritional Influences on Bone Health* (Burckhardt, P., Dawson-Hughes, B., and Weaver, C., Eds.), pp 173-179, Springer London.
4. Safadi, F. F., Barbe, M. F., Abdelmagid, S. M., Rico, M. C., Aswad, R. A., Litvin, J., and Popoff, S. N. (2009) Bone structure, development and bone biology, In *Bone Pathology* (Khurana, J. S., Ed.), pp 1-50, Humana Press.
5. James, R., Deng, M., Laurencin, C., and Kumbar, S. (2011) Nanocomposites and bone regeneration, *Front. Mater. Sci. 5*, 342-357.
6. Harada, S., and Rodan, G. A. (2003) Control of osteoblast function and regulation of bone mass, *Nature 423*, 349-355.
7. Mitton, D., Roux, C., and Laugier, P. (2011) Bone overview, In *Bone Quantitative Ultrasound* (Laugier, P., and Haïat, G., Eds.), pp 1-28, Springer Netherlands.
8. Salo, J., Lehenkari, P., Mulari, M., Metsikkö, K., and Väänänen, H. K. (1997) Removal of osteoclast bone resorption products by transcytosis, *Science 276*, 270-273.

9. Binkley, N., Ramamurthy, R., and Krueger, D. (2010) Low vitamin D status: Definition, prevalence, consequences, and correction, *Endocrinol. Metab. Clin. N. Am. 39*, 287-301.

10. Stepensky, D., Kleinberg, L., and Hoffman, A. (2003) Bone as an effect compartment: Models for uptake and release of drugs, *Clin. Pharmacokinet. 42*, 863-881.

11. Rodan, G. A., and Martin, T. J. (2000) Therapeutic approaches to bone diseases, *Science 289*, 1508-1514.

12. Mantila Roosa, S., Hurd, A., Xu, H., Fuchs, R., and Warden, S. Age-related changes in proximal humerus bone health in healthy, white males, *Osteoporosis Int.*, 1-9.

13. Kiberstis, P., Smith, O., and Norman, C. (2000) Bone Health in The Balance, *Science 289*, 1497-.

14. Horowitz, M. C. (1993) Cytokines and estrogen in bone: Anti-osteoporotic effects, *Science 260*, 626-627.

15. Sunyer, T., Lewis, J., Collin-Osdoby, P., and Osdoby, P. (1999) Estrogen's bone-protective effects may involve differential IL-1 receptor regulation in human osteoclast-like cells, *J. Clin. Invest. 103*, 1409-1418.

16. Uludağ, H. (2002) Bisphosphonates as a foundation of drug delivery to bone, *Curr. Pharm. Des. 8*, 1929-1944.

17. Martin, R. M., and Correa, P. H. S. (2010) Bone quality and osteoporosis therapy, *Arq. Bras. Endocrinol. Metab. 54*, 186-199.

18. Vicente-Rodríguez, G., Ezquerra, J., Mesana, M., Fernández-Alvira, J., Rey-López, J., Casajus, J., and Moreno, L. (2008) Independent and combined effect of nutrition and exercise on bone mass development, *J. Bone Miner. Metab. 26*, 416-424.

19. Patel, S. (1996) Current and potential future drug treatments for osteoporosis, *Ann Rheum Dis 55*, 700-714.

20. Zhang, S., Gangal, G., and Uludağ, H. (2007) 'Magic bullets' for bone diseases: Progress in rational design of bone-seeking medicinal agents, *Chem. Soc. Rev. 36*, 507-531.

21. van Beek E., C. L., I. Que, S. Papapoulos. (1996) Dissociation of binding and antiresorptive properties of hydroxy bisphosphonates by substitition of the hydroxyl with an amino group, *J. Bone Miner. Res. 11*, 1492-1497.

22. Sunberg R. J., E. F. H., Mosher C. T., Roof C. F. (1991) Designing drugs for stronger bones *Chem. Tech. 21*, 305-309.

23. Lawson, M. A., Xia, Z., Barnett, B. L., Triffitt, J. T., Phipps, R. J., Dunford, J. E., Locklin, R. M., Ebetino, F. H., and Russell, R. G. G. (2010) Differences between bisphosphonates in binding affinities for hydroxyapatite, *J. Biomed. Mater. Res., Part B 92B*, 149-155.

24. Nancollas, G. H., Tang, R., Phipps, R. J., Henneman, Z., Gulde, S., Wu, W., Mangood, A., Russell, R. G. G., and Ebetino, F. H. (2006) Novel insights into actions of bisphosphonates on bone: Differences in interactions with hydroxyapatite, *Bone 38*, 617-627.

25. Lisic, E. C., Phillips, M., Ensor, D., Nash, K. L., Beets, A., and Knapp, F. F. (2001) Synthesis of a new bisphosphonic acid ligand (SEDP) and preparation of a 188Re-(Sn)SEDP bone seeking radiotracer, *Nucl. Med. Biol. 28*, 419-424.

26. Francis, M. D., and Valent, D. J. (2007) Historical perspectives on the clinical development of bisphosphonates in the treatment of bone diseases, *J. Musculoskelet. Neuronal. Interact. 7*, 2-8.

27. Green, J. R. (2004) Zoledronic acid: pharmacologic profile of a potent bisphosphonate, *J. Organomet. Chem. 690*, 2439-2448.

28. Rogers, M. J., Watts, D. J., and Russell, R. G. G. (1997) Overview of bisphosphonates, *Cancer 80 (Suppl.)*, 1652-1660.

29. Uludağ, H. (2002) Bisphosphonates as a foundation of drug delivery to bone, *Curr. Pharm. Des. 8*, 1929-1944.

30. Reszka, A. A., and Rodan, G. A. (2003) Mechanism of action of bisphosphonates, *Curr. Osteoporosis Rep. 1*, 45-52.

31. Vondracek, S. F., and Linnebur, S. A. (2009) Diagnosis and management of osteoporosis in the older senior, *Clin. Interventions Aging 4*, 121–136.

32. Polascik, T. J. (2009) Bisphosphonates in oncology: Evidence for the prevention of skeletal events in patients with bone metastases., *Drug Des., Dev. Ther. 3*, 27-40.

33. Lumachi, F., Brunello, A., Roma, A., and Basso, U. (2008) Medical treatment of malignancy-associated hypercalcemia, *Curr. Med. Chem. 15*, 415-421.

34. Thompson, K., and Rogers, M. (2007) The molecular mechanisms of action of bisphosphonates, *Clinic. Rev. Bone Miner. Metab. 5*, 130-144.

35. Russell, R. G. (2007) Bisphosphonates: Mode of action and pharmacology, *Pediatrics 119 Suppl 2,* S150-162.

36. Roelofs, A. J., Thompson, K., Gordon, S., and Rogers, M. J. (2006) Molecular mechanisms of action of bisphosphonates: Current status, *Clin. Cancer Res. 12*, 6222s-6230s.

37. Eriksen, E. (2010) Cellular mechanisms of bone remodeling, *Reviews in Endocrine & Metabolic Disorders 11*, 219-227.

38. Roelofs, A. J., Thompson, K., Gordon, S., and Rogers, M. J. (2006) Molecular Mechanisms of Action of Bisphosphonates: Current Status, *Clinical Cancer Research 12*, 6222s-6230s.

39. Fleisch, H. (1998) Bisphosphonates: Mechanisms of action, In *Advances in Organ Biology*, pp 835-850, Elsevier.

40. Reszka, A. A. (2010) Bisphosphonate Mechanisms of Action, In *Osteoporosis* (Adler, R. A., Ed.), pp 443-468, Humana Press.

41. Rodan, G. A. (1998) Mechanisms of action of bisphosphonates *Annu. Rev. Pharmacol. Toxicol. 38*, 375-388.

42. Halasy-Nagy, J. M., Rodan, G. A., and Reszka, A. A. (2001) Inhibition of bone resorption by alendronate and risedronate does not require osteoclast apoptosis, *Bone 29*, 553-559.

43. Bernecker, P. M. (2008) Therapeutic approaches and mechanisms of drug action, In *Radiology of Osteoporosis* (Grampp, S., Ed.), pp 53-68, Springer Berlin Heidelberg.

44. Wang, D., Miller, S. C., Shlyakhtenko, L. S., Portillo, A. M., Liu, X.-M., Papangkorn, K., Kopečková, P., Lyubchenko, Y., Higuchi, W. I., and Kopeček, J. (2007) Osteotropic peptide that differentiates functional domains of the skeleton, *Bioconjugate Chem. 18*, 1375-1378.

45. Wang, D., Sima, M., Mosley, R. L., Davda, J. P., Tietze, N., Miller, S. C., Gwilt, P. R., Kopečková, P., and Kopeček, J. (2006) Pharmacokinetic and biodistribution studies of a bone-targeting drug delivery system based on N-(2-Hydroxypropyl)methacrylamide copolymers, *Mol. Pharmaceutics 3*, 717-725.

46. Thompson, W. J., Thompson, D. D., Anderson, P. S., and Rodan, G. A. (1989) Polymalonic acids as boneaffinity agents, *EP 0341961*.

47. Orme, M. W., and Labroo, V. M. (1994) Synthesis of [beta]-estradiol-3-benzoate-17-(succinyl-12A-tetracycline): A potential bone-seeking estrogen, *Bioorg. Med. Chem. Lett. 4*, 1375-1380.

48. Zheng, H., and Weng, L. (1997) Bone resorption inhibition/osteogenesis promotion pharmaceutical composition, *US 5,698,542*.

49. Herczegh, P., Buxton, T. B., McPherson, J. C. I., Kovács-Kulyassa, Á., Brewer, P. D., Sztaricskai, F., Stroebel, G. G., Plowman, K. M., Farcasiu, D., and Hartmann, J. F. (2002) Osteoadsorptive bisphosphonate derivatives of fluoroquinolone antibacterials, *J. Med. Chem. 45*, 2338-2341.

50. Årstad, E., Hoff, P., Skattebøl, L., Skretting, A., and Breistøl, K. (2003) Studies on the synthesis and biological properties of non-carrier-added [125I and 131I]-labeled arylalkylidenebisphosphonates: Potent bone-seekers for diagnosis and therapy of malignant osseous lesions, *J. Med. Chem. 46*, 3021-3032.

51. Ehrick, R. S., Capaccio, M., Puleo, D. A., and Bachas, L. G. (2007) Ligand-modified aminobisphosphonate for linking proteins to hydroxyapatite and bone surface, *Bioconjugate Chem. 19*, 315-321.

52. Doschak, M. R., Kucharski, C. M., Wright, J. E. I., Zernicke, R. F., and Uludağ, H. (2009) Improved bone delivery of osteoprotegerin by bisphosphonate conjugation in a rat model of osteoarthritis, *Mol. Pharmaceut. 6*, 634-640.

53. Le Goff, B., and Heymann, D. (2011) Pharmacodynamics of bisphosphonates in arthritis, *Expert Rev. Clin. Pharmacol. 4*, 633-641.

54. Henrotin, Y. (2012) Osteoarthritis year 2011 in review: Biochemical markers of osteoarthritis: an overview of research and initiatives, *Osteoarthr. Cartilage (DOI:10.1016/j.joca.2012.01.008).*

55. Felson, D. T., Lawrence, R. C., Dieppe, P. A., Hirsch, R., Helmick, C. G., Jordan, J. M., Kington, R. S., Lane, N. E., Nevitt, M. C., Zhang, Y., Sowers, M., McAlindon, T., Spector, T. D., Poole, A. R., Yanovski, S. Z., Ateshian, G., Sharma, L., Buckwalter, J. A., Brandt, K. D., and Fries, J. F. (2000) Osteoarthritis: New insights. Part 1: The disease and its risk factors, *Ann. Intern. Med. 133*, 635-646.

56. Jang, H.-W., Kang, J.-K., Lee, K., Lee, Y.-S., and Park, P.-K. (2011) A retrospective study on related factors affecting the survival rate of dental implants, *J. Adv. Prosthodont. 3*, 204-215.

57. Duan, K., and Wang, R. (2006) Surface modifications of bone implants through wet chemistry, *J. Mater. Chem. 16*, 2309-2321.

58. Tomford, W. W. (2000) Bone allografts: Past, present and future, *Cell and Tissue Banking 1*, 105-109.

59. Vandrovcova, M., and Baeakova, L. (2011) Adhesion, growth and differentiation of osteoblasts on surfaceModified materials developed for bone implants *Physiol. Res. 60*, 403-417.

60. Steinemann, S. G. (1998) Titanium — the material of choice?, *Periodontology 2000 17*, 7-21.

61. Vagaska, B., Bacakova, L., Flova, E., and Balik, K. (2010) Osteogenic cells on bio-inspired materials for bone tissue engineering *Physiol. Res. 59*, 309-322.

62. Hench, L. L. (1975) Prosthetic implant materials, *Annu. Rev. Mater. Sci. 5*, 279-300.

63. Langer, R., and Vacanti, J. (1993) Tissue engineering, *Science 260*, 920-926.

64. Yuan, Y., Chesnutt, B. M., Wright, L., Haggard, W. O., and Bumgardner, J. D. (2008) Mechanical property, degradation rate, and bone cell growth of chitosan coated titanium influenced by degree of deacetylation of chitosan, *J. Biomed. Mater. Res., Part B 86B*, 245-252.

65. Dohan Ehrenfest, D. M., Coelho, P. G., Kang, B.-S., Sul, Y.-T., and Albrektsson, T. (2010) Classification of osseointegrated implant surfaces: Materials, chemistry and topography, *Trends Biotechnol. 28*, 198-206.

66. Wazen, R. M., Lefebvre, L.-P., Baril, E., and Nanci, A. (2010) Initial evaluation of bone ingrowth into a novel porous titanium coating, *J. Biomed. Mater. Res., Part B 94B*, 64-71.

67. Richert, L., Variola, F., Rosei, F., Wuest, J. D., and Nanci, A. (2010) Adsorption of proteins on nanoporous Ti surfaces, *Surf. Sci. 604*, 1445-1451.

68. Martin, H. J., Schulz, K. H., Bumgardner, J. D., and Walters, K. B. (2007) XPS study on the use of 3-aminopropyltriethoxysilane to bond chitosan to a titanium surface, *Langmuir 23*, 6645-6651.

69. Variola, F., Brunski, J. B., Orsini, G., Tambasco de Oliveira, P., Wazen, R., and Nanci, A. (2011) Nanoscale surface modifications of medically relevant metals: state-of-the art and perspectives, *Nanoscale 3*, 335-353.

70. Ito, Y. (2008) Covalently immobilized biosignal molecule materials for tissue engineering, *Soft Matter 4*, 46-56.

71. Morra, M. (2006) Biochemical modification of titanium surfaces: Peptides and ECM proteins, *Eur. Cell. Mater. 12*, 1-15.

72. Gittens, S. A., Bansal, G., Zernicke, R. F., and Uludağ, H. (2005) Designing proteins for bone targeting, *Adv. Drug Deliver. Rev. 57*, 1011-1036.

73. Pan, H., Kopečková, P., Wang, D., Yang, J., Miller, S., and Kopeček, J. (2006) Water-soluble HPMA copolymer—prostaglandin E1 conjugates containing a cathepsin K sensitive spacer, *J. Drug Target. 14*, 425-435.

74. Rusmini, F., Zhong, Z., and Feijen, J. (2007) Protein immobilization strategies for protein biochips, *Biomacromolecules 8*, 1775-1789.

75. Lin, P.-C., Weinrich, D., and Waldmann, H. (2010) Protein biochips: Oriented surface immobilization of proteins, *Macromol. Chem. Phys. 211*, 136-144.

76. Rao, S. V., Anderson, K. W., and Bachas, L. G. (1998) Oriented immobilization of proteins, *Microchim. Acta 128*, 127-143.

77. Sibai, T., Morgan, E., and Einhorn, T. (2011) Anabolic agents and bone quality, *Clin. Orthop. Relat. Res. 469*, 2215-2224.

78. Trivedi, R., Goswami, R., and Chattopadhyay, N. (2010) Investigational anabolic therapies for osteoporosis, *Expert Opin. Invest. Drugs 19*, 995-1005.

79. Fleisch, H. (2002) The role of bisphosphonates in breast cancer: Development of bisphosphonates, *Breast Cancer Res. 4*, 30 - 34.

80. Fleisch, H., Russell, R., Bisaz, S., Casey, P., and Muhlbauer, R. (1968) The influence of pyrophsophate analogues (diphosphonates) on the precipitation and dissolution of calcium phosphate in vitro and in vivo, *Calcif. Tissue Res. 2(suppl)*, 10 - 10a.

81. Kieczykowski, G. R., Jobson, R. B., Melillo, D. G., Reinhold, D. F., Grenda, V. J., and Shinkai, I. (1995) Preparation of (4-amino-1-hydroxybutylidene)bisphosphonic acid sodium salt, MK-217 (alendronate sodium). An improved procedure for the preparation of 1-hydroxy-1,1-bisphosphonic acids, *J. Org. Chem. 60*, 8310-8312.

82. Lecouvey, M., and Leroux, Y. (2000) Synthesis of 1-hydroxy-1,1-bisphosphonates, *Heteroat. Chem. 11*, 556-561.

83. McConnell, R. L., and Coover, H. W. (1956) Preparation of 1-Hydroxyalkylidenediphosphonates, *J. Am. Chem. Soc. 78*, 4450-4452.

84. Fitch, S. J., and Moedritzer, K. (1962) N.m.r. Study of the P-C(OH)-P to P-C-O-P Rearrangement: Tetraethyl 1-Hydroxyalkylidenediphosphonates, *J. Am. Chem. Soc. 84*, 1876-1879.

85. Karaman, R., Goldblum, A., Breuer, E., and Leader, H. (1989) Acylphosphonic acids and methyl hydrogen acylphosphonates: physical and chemical properties and theoretical calculations, *J. Chem. Soc., Perkin Trans. 1*, 765-774.

86. Lecouvey, M., Mallard, I., Bailly, T., Burgada, R., and Leroux, Y. (2001) A mild and efficient one-pot synthesis of 1-hydroxymethylene-1,1-bisphosphonic acids. Preparation of new tripod ligands, *Tetrahedron Lett. 42*, 8475-8478.

87. Dhawan, B., and Redmore, D. (1984) o-Hydroxyaryl diphosphonic acids, *J. Org. Chem. 49*, 4018-4021.

88. Pascale Even, Erwann Guenin, Mounya Benramdame, Patricia Quidu, Manouni, D. E., and Lecouvey, M. (2004) Synthesis of new ligands derived from polyphosphonates partial esters, *Lett. Org. Chem. 1*, 75-77.

89. Hirabayashi, H., Takahashi, T., Fujisaki, J., Masunaga, T., Sato, S., Hiroi, J., Tokunaga, Y., Kimura, S., and Hata, T. (2001) Bone-specific delivery and sustained release of diclofenac, a non-steroidal anti-inflammatory drug, via bisphosphonic prodrug based on the osteotropic drug delivery system (ODDS), *J. Control. Release 70*, 183-191.

90. Gil, L., Han, Y., Opas, E. E., Rodan, G. A., Ruel, R., Seedor, J. G., Tyler, P. C., and Young, R. N. (1999) Prostaglandin E2-bisphosphonate conjugates: Potential agents for treatment of osteoporosis, *Bioorg. Med. Chem. 7*, 901-919.

91. Ora, M., Lönnberg, T., Florea-Wang, D., Zinnen, S., Karpeisky, A., and Lönnberg, H. (2008) Bisphosphonate derivatives of nucleoside antimetabolites: Hydrolytic stability and hydroxyapatite adsorption of 5′-β,γ-methylene and 5′-β,γ-

(1-hydroxyethylidene) triphosphates of 5-fluorouridine and ara-cytidine, *J. Org. Chem. 73*, 4123-4130.

92. El-Mabhouh, A., Angelov, C., McEwan, A., Jia, G., and Mercer, J. (2004) Preclinical investigations of drug and radionuclide conjugates of bisphosphonates for the treatment of metastatic bone cancer, *Cancer Biother. Radiopharm. 19*, 627-640.

93. Wang, J. B., Yang, C. H., Yan, X. M., Wu, X. H., and Xie, Y. Y. (2005) Novel bone-targeted agents for treatment of osteoporosis, *Chin. Chem. Lett. 16*, 859-862.

94. Blower, P. (2006) Towards molecular imaging and treatment of disease with radionuclides: The role of inorganic chemistry, *Dalton Trans.*, 1705-1711.

95. Ogawa, K., Mukai, T., Inoue, Y., Ono, M., and Saji, H. (2006) Development of a novel 99mTc-chelate-conjugated bisphosphonate with high affinity for bone as a bone scintigraphic agent, *J. Nucl. Med. 47*, 2042-2047.

96. Torres Martin de Rosales, R., Finucane, C., Foster, J., Mather, S. J., and Blower, P. J. (2010) 188Re(CO)3-dipicolylamine-alendronate: A new bisphosphonate conjugate for the radiotherapy of bone metastases, *Bioconjugate Chem. 21*, 811-815.

97. Zaheer, A., Lenkinski, R. E., Mahmood, A., Jones, A. G., Cantley, L. C., and Frangioni, J. V. (2001) In vivo near-infrared fluorescence imaging of osteoblastic activity, *Nat. Biotechnol. 19*, 1148-1154.

98. van Beek, E. R., Lowik, C., Que, I., and Papapoulos, S. (1996) Dissociation of binding and antiresorptive properties of hydroxy bisphosphonates by substitition of the hydroxyl with an amino group, *J. Bone Miner. Res. 11*, 1492-1497.

99. Sunberg, R. J., Ebetino, F. H., Mosher, C. T., and Roof, C. F. (1991) Designing drugs for stronger bones, *Chemtech 21*, 305-309.

100. Pack, D. W., Hoffman, A. S., Pun, S., and Stayton, P. S. (2005) Design and development of polymers for gene delivery, *Nat Rev Drug Discov 4*, 581-593.

101. Schneider, L., Korber, A., Grabbe, S., and Dissemond, J. (2007) Influence of pH on wound-healing: A new perspective for wound-therapy?, *Arch. Dermatol. Res. 298*, 413-420.

102. Teitelbaum, S. L. (2000) Bone resorption by osteoclasts, *Science 289*, 1504-1508.

103. Xu, S., Krämer, M., and Haag, R. (2006) pH-Responsive dendritic core-shell architectures as amphiphilic nanocarriers for polar drugs, *J. Drug Target. 14*, 367-374.

104. Kale, A. A., and Torchilin, V. P. (2007) Design, synthesis, and characterization of pH-sensitive PEG−PE conjugates for stimuli-sensitive pharmaceutical nanocarriers: The effect of substitutes at the hydrazone linkage on the pH stability of PEG−PE conjugates, *Bioconjugate Chem. 18*, 363-370.

105. Sawant, R. M., Hurley, J. P., Salmaso, S., Kale, A., Tolcheva, E., Levchenko, T. S., and Torchilin, V. P. (2006) "SMART" drug delivery systems: Double-targeted pH-responsive pharmaceutical nanocarriers, *Bioconjugate Chem. 17*, 943-949.

106. Pritchard, E. M., Dennis, P. B., Omenetto, F., Naik, R. R., and Kaplan, D. L. (2012) Physical and chemical aspects of stabilization of compounds in silk, *Biopolymers (DOI: 10.1002/bip.22026)*.

107. Chebbi, I., Migianu-Griffoni, E., Sainte-Catherine, O., Lecouvey, M., and Seksek, O. (2010) In vitro assessment of liposomal neridronate on MDA-MB-231 human breast cancer cells, *Int. J. Pharm. 383*, 116-122.

108. Braslau, R., Anderson, M. O., Rivera, F., Jimenez, A., Haddad, T., and Axon, J. R. (2002) Acyl hydrazines as precursors to acyl radicals, *Tetrahedron 58*, 5513-5523.

109. Nicholson, D. A., and Vaughn, H. (1971) A general method of preparation of tetramethyl alkyl-1-hydroxy-a,l-diphosphonate, *J. Org. Chem. 36*, 3843-3845.

110. Langer, R. (2001) Drug delivery: Drugs on target, *Science 293*, 58-59.

111. Goltzman, D. (2002) Discoveries, drugs and skeletal disorders, *Nat. Rev. Drug Discovery 1*, 784-796.

112. Deal, C. (2009) Future therapeutic targets in osteoporosis, *Curr. Opin. Rheumatol. 21*, 380-385.

113. Chapurlat, R. D., and Delmas, P. D. (2006) Drug insight: Bisphosphonates for postmenopausal osteoporosis, *Nat. Clin. Pract. Endocrinol. Metab. 2*, 211-219.

114. Peppas, N. A. (2004) Intelligent therapeutics: Biomimetic systems and nanotechnology in drug delivery, *Adv. Drug Delivery Rev. 56*, 1529-1531.

115. Peppas, N. A. (2006) Vecteurs de médicaments innovants et « intelligents » : leurs applications pharmaceutiques, *Ann. Pharm. Fr. 64*, 260-275.

116. Langer, R., and Peppas, N. A. (2003) Advances in biomaterials, drug delivery, and bionanotechnology, *AIChE J. 49*, 2990-3006.

117. Oh, Y.-K., Senter, P. D., and Song, S.-C. (2009) Intelligent drug delivery systems, *Bioconjugate Chem. 20*, 1813-1815.

118. MacEwan, S. R., and Chilkoti, A. (2010) Elastin-like polypeptides: Biomedical applications of tunable biopolymers, *Pept. Sci. 94*, 60-77.

119. Betre, H., Liu, W., Zalutsky, M. R., Chilkoti, A., Kraus, V. B., and Setton, L. A. (2006) A thermally responsive biopolymer for intra-articular drug delivery, *J. Control. Release 115*, 175-182.

120. Rodan, G. A., and Fleisch, H. A. (1996) Bisphosphonates: Mechanisms of action, *J. Clin. Invest. 97*, 2692-2696.

121. Koutsoukos, P., Amjad, Z., Tomson, M. B., and Nancollas, G. H. (1980) Crystallization of calcium phosphates. A constant composition study, *J. Am. Chem. Soc. 102*, 1553-1557.

122. Fleisch, H. (1998) Bisphosphonates: Mechanisms of action, *Endocr. Rev. 19*, 80 - 100.

123. Segal, E., Pan, H., Ofek, P., Udagawa, T., Kopečková, P., Kopeček, J., and Satchi-Fainaro, R. (2009) Targeting angiogenesis-dependent calcified neoplasms using combined polymer therapeutics, *PloS ONE 4*, e5233.

124. Prommer, E. E. (2009) Toxicity of bisphosphonates, *J. Palliat. Med. 12*, 1661-1665.

125. Lazebnik, Y. A., Kaufmann, S. H., Desnoyers, S., Poirier, G. G., and Earnshaw, W. C. (1994) Cleavage of poly(ADP-ribose) polymerase by a proteinase with properties like ICE, *Nature 371*, 346-347.

126. Wong, L. S., Khan, F., and Micklefield, J. (2009) Selective covalent protein immobilization: Strategies and applications, *Chem. Rev. 109*, 4025-4053.

127. Tetala, K. K. R., and Beek, T. A. V. (2010) Bioaffinity chromatography on monolithic supports, *J. Sep. Sci. 33*, 422-438.

128. Saleemuddin, M. (1999) Bioaffinity based immobilization of enzymes, In *Thermal Biosensors, Bioactivity, Bioaffinitty* (Bhatia, P., Danielsson, B., Gemeiner, P., Grabley, S., Lammers, F., Mukhopadhyay, A., Ramanathan, K., Saleemuddin, M., Scheper, T., Stefuca, V., Thiericke, R., and Xie, B., Eds.), pp 203-226, Springer Berlin / Heidelberg.

129. Köhn, M. (2009) Immobilization strategies for small molecule, peptide and protein microarrays, *J. Pept. Sci. 15*, 393-397.

130. Uludağ, H., Kousinioris, N., Gao, T., and Kantoci, D. (2000) Bisphosphonate conjugation to proteins as a means to impart bone affinity, *Biotechnol. Prog. 16*, 258-267.

131. Uludağ, H., and Yang, J. (2002) Targeting systemically administered proteins to bone by bisphosphonate conjugation, *Biotechnol. Prog. 18*, 604-611.

132. Gittens, S. A., Matyas, J. R., Zernicke, R. F., and Uludağ, H. (2003) Imparting bone affinity to glycoproteins through the conjugation of bisphosphonates, *Pharm. Res. 20*, 978-987.

133. Costa, L., and Major, P. P. (2009) Effect of bisphosphonates on pain and quality of life in patients with bone metastases, *Nat. Clin. Pract. Oncol. 6*, 163-174.

134. Yewle, J. N., Puleo, D. A., and Bachas, L. G. (2011) Enhanced affinity bifunctional bisphosphonates for targeted delivery of therapeutic agents to bone, *Bioconjugate Chem. 22*, 2496-2506.

135. Mikolajczyk, S. D., Meyer, D. L., Starling, J. J., Law, K. L., Rose, K., Dufour, B., and Offord, R. E. (1994) High yield, site-specific coupling of N-terminally modified β-lactamase to a proteolytically derived single-sulfhydryl murine Fab', *Bioconjugate Chem. 5*, 636-646.

136. Sharon, J. L., and Puleo, D. A. (2008) The use of N-terminal immobilization of PTH(1-34) on PLGA to enhance bioactivity, *Biomaterials 29*, 3137-3142.

137. Puleo, D. A., Kissling, R. A., and Sheu, M. S. (2002) A technique to immobilize bioactive proteins, including bone morphogenetic protein-4 (BMP-4), on titanium alloy, *Biomaterials 23*, 2079-2087.

138. Puleo, D. A. (1997) Retention of enzymatic activity immobilized on silanized Co-Cr-Mo and Ti-6Al-4V, *J. Biomed. Mater. Res. Part A 37*, 222-228.

139. Huang, W., Wang, J., Bhattacharyya, D., and Bachas, L. G. (1997) Improving the activity of immobilized subtilisin by site-specific attachment to surfaces, *Anal. Chem. 69*, 4601-4607.

140. Fields, R., and Dixon, H. B. F. (1968) A spectrophotometric method for the microdetermination of periodate, *Biochem. J. 108*, 883-887.

141. Wolke, J., de Blieck-Hogervorst, J., Dhert, W., Klein, C., and de Groot, K. (1992) Studies on the thermal spraying of apatite bioceramics, *J. Therm. Spray Technol. 1*, 75-82.

142. Bouyer, E., Gitzhofer, F., and Boulos, M. (1997) The suspension plasma spraying of bioceramics by induction plasma, *JOM-J. Min. Met. Mat. S. 49*, 58-62.

143. Søballe, K. (1993) Hydroxyapatite ceramic coating for bone implant fixation, *Acta Orthop. Scand. Suppl. 255*, 1-58.

144. Greenfield, R. S., Kaneko, T., Daues, A., Edson, M. A., Fitzgerald, K. A., Olech, L. J., Grattan, J. A., Spitalny, G. L., and Braslawsky, G. R. (1990) Evaluation in vitro of adriamycin immunoconjugates synthesized using an acid-sensitive hydrazone linker, *Cancer Res. 50*, 6600-6607.

145. Raddatz, S., Mueller-Ibeler, J., Kluge, J., Wäß, L., Burdinski, G., Havens, J. R., Onofrey, T. J., Wang, D., and Schweitzer, M. (2002) Hydrazide oligonucleotides: New chemical modification for chip array attachment and conjugation, *Nucleic Acids Res. 30*, 4793-4802.

146. Antsypovich, S. I., and Von Kiedrowski, G. (2005) A novel versatile phosphoramidite building block for the synthesis of 5′- and 3′-hydrazide modified oligonucleotides, *Nucleos. Nucleot. Nucl. 24*, 211-226.

147. Thermo scientific pierce (2009) crosslinking technical handbook. .

148. Watanabe, J., and Ishihara, K. (2007) Multiple protein-immobilized phospholipid polymer nanoparticles: Effect of spacer length on residual enzymatic activity and molecular diagnosis, *Nanobiotechnology 3*, 76-82.

149. Cao, T., Wang, A., Liang, X., Tang, H., Auner, G. W., Salley, S. O., and Ng, K. Y. S. (2007) Investigation of spacer length effect on immobilized Escherichia coli pili-antibody molecular recognition by AFM, *Biotechnol. Bioeng. 98*, 1109-1122.

150. Nouaimi, M., Möschel, K., and Bisswanger, H. (2001) Immobilization of trypsin on polyester fleece via different spacers, *Enzyme Microb. Technol. 29*, 567-574.

151. Brogan, K. L., and Schoenfisch, M. H. (2005) Influence of antibody immobilization strategy on molecular recognition force microscopy measurements, *Langmuir 21*, 3054-3060.

152. Lee, W.-H., Loo, C.-Y., Van, K. L., Zavgorodniy, A. V., and Rohanizadeh, R. (2011) Modulating protein adsorption onto hydroxyapatite particles using different amino acid treatments, *J. R. Soc. Interface (DOI: 10.1098/rsif.2011.0586)*

153. Marina J, G. (1984) The interaction of proteins with hydroxyapatite: II. Role of acidic and basic groups, *Anal. Biochem. 136*, 433-439.

154. Seeberg, A. H., Tolxdorff-Neutzling, R. M., and Wiedemann, B. (1983) Chromosomal beta-lactamases of Enterobacter cloacae are responsible for resistance to third-generation cephalosporins, *Antimicrob. Agents Chemother. 23*, 918-925.

155. Cabana, H., Alexandre, C., Agathos, S. N., and Jones, J. P. (2009) Immobilization of laccase from the white rot fungus Coriolopsis polyzona and use of the immobilized biocatalyst for the continuous elimination of endocrine disrupting chemicals, *Bioresour. Technol. 100*, 3447-3458.

156. Wang, J., Bhattacharyya, D., and Bachas, L. G. (2001) Orientation specific immobilization of organophosphorus hydrolase on magnetic particles through gene fusion, *Biomacromolecules 2*, 700-705.

157. Cao, L. (2006) Covalent Enzyme Immobilization, In *Carrier-bound Immobilized Enzymes*, pp 169-316, Wiley-VCH Verlag GmbH & Co. KGaA.

158. De Maio, A., El-Masry, M. M., De Luca, P., Grano, V., Rossi, S., Pagliuca, N., Gaeta, F. S., Portaccio, M., and Mita, D. G. (2003) Influence of the spacer length on the activity of enzymes immobilised on nylon/polyGMA membranes - Part 2: Non-isothermal conditions, *J. Mol. Catal. B: Enzym. 21*, 253-265.

159. Serda, R. E., Godin, B., Blanco, E., Chiappini, C., and Ferrari, M. (2011) Multi-stage delivery nano-particle systems for therapeutic applications, *Biochimica et Biophysica Acta (BBA) - General Subjects 1810*, 317-329.

160. Borm, P. J. A., and Müller-Schulte, D. (2006) Nanoparticles in drug delivery and environmental exposure: same size, same risks?, *Nanomedicine 1*, 235-249.

161. Cho, K., Wang, X., Nie, S., Chen, Z., and Shin, D. M. (2008) Therapeutic nanoparticles for drug delivery in cancer, *Clin. Cancer Res. 14*, 1310-1316.

162. Nishiyama, N., and Kataoka, K. (2006) Current state, achievements, and future prospects of polymeric micelles as nanocarriers for drug and gene delivery, *Pharmacol. Ther. 112*, 630-648.

163. Malam, Y., Loizidou, M., and Seifalian, A. M. (2009) Liposomes and nanoparticles: nanosized vehicles for drug delivery in cancer, *Trends Pharmacol. Sci. 30*, 592-599.

164. Al-Jamal, W. T., and Kostarelos, K. (2011) Liposomes: From a clinically established drug delivery system to a nanoparticle platform for theranostic nanomedicine, *Acc. Chem. Res. 44*, 1094-1104.

165. Xinming, L., Yingde, C., Lloyd, A. W., Mikhalovsky, S. V., Sandeman, S. R., Howel, C. A., and Liewen, L. (2008) Polymeric hydrogels for novel contact lens-based ophthalmic drug delivery systems: A review, *Contact Lens and Anterior Eye 31*, 57-64.

166. Hoare, T. R., and Kohane, D. S. (2008) Hydrogels in drug delivery: Progress and challenges, *Polymer 49*, 1993-2007.

167. Fischer, J., Kolk, A., Wolfart, S., Pautke, C., Warnke, P. H., Plank, C., and Smeets, R. (2011) Future of local bone regeneration – Protein versus gene therapy, *J. Cranio. Maxill. Surg. 39*, 54-64.

168. Wright, J. E. I., Gittens, S. A., Bansal, G., Kitov, P. I., Sindrey, D., Kucharski, C., and Uludag, H. (2006) A comparison of mineral affinity of bisphosphonate-protein conjugates constructed with disulfide and thioether linkages, *Biomaterials 27*, 769-784.

169. Gittens, S. A., Bagnall, K., Matyas, J. R., Löbenberg, R., and Uludağ, H. (2004) Imparting bone mineral affinity to osteogenic proteins through heparin-bisphosphonate conjugates, *J. Control. Release 98*, 255-268.

170. Bansal, G., Wright, J. E. I., Zhang, S., Zernicke, R. F., and Uludağ, H. (2005) Imparting mineral affinity to proteins with thiol–labile disulfide linkages, *J. Biomed. Mater. Res. Part A 74A*, 618-628.

171. Russell, R. G. G. (2011) Bisphosphonates: The first 40 years, *Bone 49*, 2-19.

172. Coleman, R. E., and McCloskey, E. V. (2011) Bisphosphonates in oncology, *Bone 49*, 71-76.

173. Wolfe, C. A. C., and Hage, D. S. (1995) Studies on the rate and control of antibody oxidation by periodate, *Anal. Biochem. 231*, 123-130.

174. Geoghegan, K. F., and Stroh, J. G. (1992) Site-directed conjugation of nonpeptide groups to peptides and proteins via periodate oxidation of a 2-amino alcohol. Application to modification at N-terminal serine, *Bioconjugate Chem. 3*, 138-146.

175. Gaertner, H. F., and Offord, R. E. (1996) Site-specific attachment of functionalized poly(ethylene glycol) to the amino terminus of proteins, *Bioconjugate Chem. 7*, 38-44.

176. Yewle, J. N., Puleo, D., and Bachas, L. G. (2011) Enhanced affinity bifunctional bisphosphonates for targeted delivery of therapeutic agents to bone, *Bioconjugate Chem. (DOI: 10.1021/bc2003132).*

177. Green, J., and Clézardin, P. (2010) The molecular basis of bisphosphonate activity: A preclinical perspective, *Semin. Oncol. 37*, S3-S11.

178. Barden, J. A., and Kemp, B. E. (1993) NMR solution structure of human parathyroid hormone(1-34), *Biochemistry 32*, 7126-7132.

179. Jin, L., Briggs, S. L., Chandrasekhar, S., Chirgadze, N. Y., Clawson, D. K., Schevitz, R. W., Smiley, D. L., Tashjian, A. H., and Zhang, F. (2000) Crystal structure of human parathyroid hormone 1–34 at 0.9-Å resolution, *J. Biol. Chem. 275*, 27238-27244.

180. Siegel, R., Ward, E., Brawley, O., and Jemal, A. (2011) Cancer statistics, 2011, *CA Cancer J. Clin. 61*, 212-236.

181. Theresa A, G. (2008) Antitumor effects of bisphosphonates: Promising preclinical evidence, *Cancer Treat. Rev. 34, Supplement 1*, S19-S24.

182. Mystakidou, K., Katsouda, E., Stathopoulou, E., and Vlahos, L. (2005) Approaches to managing bone metastases from breast cancer: The role of bisphosphonates, *Cancer Treatment Reviews 31*, 303-311.

183. Mundy, G. R. (2002) Metastasis to bone: Causes, consequences and therapeutic opportunities, *Nat. Rev. Cancer 2*, 584-593.

184. Hanahan, D., and Weinberg, Robert A. (2011) Hallmarks of cancer: The next generation, *Cell 144*, 646-674.

185. Tassone, P., Tagliaferri, P., Viscomi, C., Palmieri, C., Caraglia, M., D'Alessandro, A., Galea, E., Goel, A., Abbruzzese, A., Boland, C. R., and Venuta, S. (2003) Zoledronic acid induces antiproliferative and apoptotic effects in human pancreatic cancer cells in vitro, *Br. J. Cancer 88*, 1971.

186. Corey, E., Brown, L. G., Quinn, J. E., Poot, M., Roudier, M. P., Higano, C. S., and Vessella, R. L. (2003) Zoledronic acid exhibits inhibitory effects on osteoblastic and osteolytic metastases of prostate cancer, *Clin. Cancer Res. 9*, 295-306.

187. Lyseng-Williamson, K. A. (2008) Zoledronic acid: A review of its use in breast cancer, *Drugs 68*, 2661-2682

188. Roodman, G. D. (2009) Pathophysiology of bone metastases, In *Bone Metastases* (Kardamakis, D., Vassiliou, V., and Chow, E., Eds.), pp 31-50, Springer Netherlands.

189. Sturge, J., Caley, M. P., and Waxman, J. (2011) Bone metastasis in prostate cancer: Emerging therapeutic strategies, *Nat. Rev. Clin. Oncol. 8*, 357-368.

190. Derenne, S., Amiot, M., Barillé, S., Collette, M., Robillard, N., Berthaud, P., Harousseau, J.-L. U. C., and Bataille, R. (1999) Zoledronate is a potent inhibitor of myeloma cell growth and secretion of IL-6 and MMP-1 by the tumoral environment, *J. Bone Miner. Res. 14*, 2048-2056.

191. Green, J. R. (2004) Bisphosphonates: Preclinical Review, *The Oncologist 9*, 3-13.

192. Boissier, S., Magnetto, S., Frappart, L., Cuzin, B., Ebetino, F. H., Delmas, P. D., and Clezardin, P. (1997) Bisphosphonates inhibit prostate and breast carcinoma cell adhesion to unmineralized and mineralized bone extracellular matrices, *Cancer Res. 57*, 3890-3894.

193. Boissier, S., Ferreras, M., Peyruchaud, O., Magnetto, S., Ebetino, F. H., Colombel, M., Delmas, P., Delaissé, J.-M., and Clézardin, P. (2000) Bisphosphonates inhibit breast and prostate carcinoma cell invasion, an early event in the formation of bone metastases, *Cancer Res. 60*, 2949-2954.

194. Croucher, P. I., De Raeve, H., Perry, M. J., Hijzen, A., Shipman, C. M., Lippitt, J., Green, J., Van Marck, E., Van Camp, B., and Vanderkerken, K. (2003) Zoledronic acid treatment of 5T2MM-bearing mice inhibits the development of myeloma bone disease: Evidence for decreased osteolysis, tumor burden and angiogenesis, and increased Survival, *J. Bone Miner. Res. 18*, 482-492.

VITA

Jivan Namdeo Yewle was born on February 12, 1980 in Otur, Pune, India. He attended the A.W. College at the University of Pune, India, where he graduated among the top of the class with a Bachelor of Science, in May 2000. He completed a Master's in Organic Chemistry with First Class from the Department of Chemistry at the University of Pune, India, in May 2002. From June 2002 to July 2005, he worked in Research and Development in well-known pharmaceutical companies (Dr. Reddy's Lab, Hyderabad; Glenmark Pharmaceuticals, Mumbai; and AJ Organica, Pune) in India. He joined the Department of Chemistry at the University of Kentucky, USA in August 2005 as a PhD candidate.

HONORS AND AWARDS

- Recipient of University of Kentucky Research Challenge Trust Fund Fellowship, 2010-2011
- 1st prize, Oral research presentation competition at Kentucky Academy of Science (KAS) 95th annual meeting, Morehead, KY, 2009
- Recipient of University of Kentucky Research Challenge Trust Fund Fellowship, 2007-2009
- 1st prize, Oral research presentation competition at Kentucky Academy of Science (KAS) 93rd annual meeting, Louisville, KY, 2007
- Recipient of University of Pune Eklavya Scholarship, 2000-2002

PUBLICATIONS

- J.N. Yewle, D.A. Puleo, and L.G. Bachas, "Enhanced Affinity Bifunctional Bisphosphonates for Targeted Delivery of Therapeutic Agents to Bone", *Bioconjugate Chemistry*, **2011**, *22*, 2496-2506.
- J.N. Yewle, Y. Wei, D.A. Puleo, S. Daunert, and L.G. Bachas, "Oriented Immobilization of Proteins on the Surface of Hydroxyapatite Implants Using Bisphosphonates as a Linker", submitted.
- J.N. Yewle, D.A. Puleo, and L.G. Bachas, "Bifunctional Bisphosphonates for Delivering PTH (1-34) to Bone Mineral with Enhanced Bioactivity", to be submitted.
- J.N. Yewle, and L.G. Bachas, "Review: Bisphosphonate Conjugates for Bone diseases", in preparation for *Bioconjugate Chemistry*.

CONFERENCE PRESENTATIONS

Jivan has presented papers and posters at several national and regional meetings including National Meetings of the American Chemical Society (ACS) (Boston, 2010; Washington, 2009; Salt Lake City, 2009; New Orleans, 2008).